A STUDY OF THE METABOLIC DEVELOPMENT OF THE NUCLEUS TRACTUS SOLITARIUS IN NORMOTENSIVE AND HYPERTENSIVE RATS

TERESA LOUISE KRUKOFF

A STUDY OF THE METABOLIC DEVELOPMENT IN THE NUCLEUS TRACTUS SOLITARIUS IN NORMOTENSIVE AND HYPERTENSIVE RATS

by

© Teresa Louise Krukoff, B.Sc., M.Sc.

A Thesis submitted in partial fulfillment
of the requirements for the degree of
Doctor of Philosophy

Faculty of Medicine
Memorial University of Newfoundland
September 1982

St. John's Newfoundland

ABSTRACT

The nucleus tractus solitarius, a nuclear column in the medulla oblongata, plays an important role in cardiovascular regulation. In particular, the subnuclei nucleus commissuralis (NC) and nucleus medialis (NM) have been implicated to be the sites of this regulation. The ontogeny of the metabolic requirements in these subnuclei was studied in the postnatal Wistar-Kyoto rat (WKY) using the ^{3}H-2-deoxy-D-glucose (^{3}H-2DG) autoradiography technique. The metabolic development of the same subnuclei was then studied in the spontaneously hypertensive rat (SHR) in which a state of elevated blood pressure is genetically triggered to determine if the metabolic requirements within the NC and NM are altered during the development of hypertension.

It was found that the metabolic requirements in the NC and NM of the WKY were not constant between 2 and 12 weeks of age. A high level of metabolic activity at 2 and 8 weeks was contrasted by a lower level at 4 and 12 weeks. The same trends of metabolic requirements found in the normotensive rats were found in the SHRs; however, the relative metabolic activity in the NC of 2 and 4 week SHRs was significantly higher than in the normotensive rat.

To extend the developmental studies and to examine the possibility that structural differences in the NC and NM between the two strains were responsible for the

differences observed in the metabolic requirements in the NC of young hypertensive rats, the exchange vessel densities and neuronal densities in the two subnuclei were quantitated.

No differences in exchange vessel densities were found in the NC and NM between 4- and 12-week-old rats, between the NC and NM at either age, or between WKYs and SHRs.

Neuronal densities in the NM were generally higher than in the NC of both WKYs and SHRs. Densities in the two subnuclei of WKYs decreased linearly as the rats matured. In the SHRs as compared to the WKYs, the densities of neurons were significantly higher in the NM and NC, beginning at 4 and 8 weeks, respectively.

Therefore it has been found that the metabolic activity in the NC and NM of WKYs and SHRs is not constant between 2 and 12 weeks of age. Significantly higher energy requirements were found in the NC of prehypertensive SHRs which were not related to differences in exchange vessel or neuronal densities.

ACKNOWLEDGEMENTS

I sincerely thank my supervisor, Dr. T.M. Scott, for the guidance and instruction which he gave me during the course of this investigation. I am also endebted to Dr. D. Bieger for his interest and thought-provoking advice.

Assistance from the Medical Audio-visual Services and Ms. J. Foote was appreciated. Thank-you also to my friends who helped to make life fun.

I would like to express my loving thanks to my parents for the confidence and support which they have always given me.

Financial assistance from the Faculty of Graduate Studies and the Faculty of Medicine was greatly appreciated. This study was financed in part by a Sigma Xi Grant-in-Aid-of-Research.

TABLE OF CONTENTS

LIST OF TABLES

LIST OF FIGURES

INTRODUCTION

The central and peripheral nervous systems are responsible for the short-term regulation of arterial blood pressure (79). This regulation is achieved by changes in peripheral resistance by means of vasoconstriction or vasodilation at the arteriole level in the vasculature and/or alterations in cardiac output. The pressure is kept from rising or falling to extremes from minute to minute by circulatory reflexes, one of the most important of which is the baroreceptor reflex. The baroreceptor reflex functions by way of an arc, whereby visceral information concerning blood pressure changes reaches the CNS and, after modulation from higher brain centres, efferent information reaches the effector organs directly. These organs in turn make the necessary changes that result in blood pressure modifications. A second component of the baroreceptor reflex is thought to be one where appropriate information is relayed from the CNS back to the periphery by way of the spinal cord (153).

The multisynaptic baroreceptor reflex arc has its first synapse in the nucleus tractus solitarius (NTS) of the medulla oblongata (14, 109, 166, 208). Fibres of the secondary neurons in the NTS terminate in various brainstem nuclei and reach, either directly or indirectly, higher regions of the brain. The loop of the baroreceptor reflex arc is completed when efferent, modulatory information from

the CNS reaches the periphery so that adjustments can be made in response to the original stimulus.

Because of its important location in the baroreceptor reflex arc, the NTS has become the focus of attention in a large number of studies concerned with cardiovascular regulation. It has been strongly suggested that parts of the NTS itself play a role in the regulation of blood pressure. In spite of its importance in the control of blood pressure, very little emphasis has been placed on the study of the postnatal development of the NTS to date. Since this type of information would give a better insight into the mechanisms by which the NTS exerts its influence in cardiovascular regulation, the ontogeny of metabolic requirements in the specific subnuclei of the rat NTS which are thought to be involved in blood pressure control was investigated. It was then asked how, if at all, the development of the NTS subnuclei would be altered in a model where a state of elevated blood pressure is genetically triggered. Thus the ontogeny of metabolic requirements in the NTS subnuclei of the spontaneously hypertensive rat (SHR) was studied.

Developmental studies of neuronal densities and exchange vessel capacities in the NTS subnuclei were undertaken in order to add to the general knowledge about the development of these subnuclei as well as to determine whether possible ontogenic differences in metabolic requirements between WKYs and SHRs might be due to changes

in one or both of these parameters.

HISTORICAL REVIEW

1. Architecture of the nucleus tractus solitarius

1.1. Introduction

The NTS is consistently present in the medulla of all mammals. It provides the first central relay for most primary sensory axons of the facial (VII), glossopharyngeal (IX), and vagal (X) cranial nerves in a rostro-caudal organization (14, 40, 109, 166, 208). Since cardiovascular information travels via IX and X and since these nerves project to the caudal two-thirds of the NTS, it is this particular area of the NTS which will be described.

1.2. Cellular components

Various investigators have assigned different names to the subdivisions of the NTS so that the nomenclature used to describe the same components of the solitary complex varies considerably. The original classification into medial and lateral divisions (23, 208) has been generally replaced by more complex divisions of its cytoarchitecture (103, 121, 123). Loewy and Burton (123), in an attempt to standardize the nomenclature of NTS subnuclei, have reclassified the caudal two-thirds of the NTS (of the cat) according to the following scheme which has been adopted for the purposes of the present study.

At the level of the area postrema, several subnuclei

can be recognized. The ventrolateral nucleus (SVL) contains clusters of large neurons lying ventrolateral to the solitary tract, although most of the neurons are medium-sized. This subnucleus can be easily recognized to a level just caudal to the obex and, although it is probably present at even more caudal levels, the absence of the large neurons makes it difficult to distinguish its exact location.

The intermediate nucleus (NInt) contains medium-sized neurons which lie medial to the SVL and just lateral to the dorsal motor nucleus of the vagus nerve (DMN) and the hypoglossal nucleus (XII). At this latter level, this subnucleus has been called the parahypoglossal nucleus (25, 203).

The medial nucleus (NM), containing small round and fusiform cells, is located on the medial aspect of the tract. It extends ventrally to the dorsal border of DMN. A part of this nucleus has been called the lateral nucleus by several investigators (14, 11, 208). Chiba and Kato (34) found only one type of neuron in this subnucleus. The neurons were 15 to 20 μm in diameter; they were oval or triangular in shape, with pale nuclei and prominent nucleoli. Most synapses were of the axo-dendritic type, although the axo-somatic type was also found.

At the level of the area postrema, the parvocellular nucleus (NSpc) covers the medial aspect of the NM (123). Part of the NSpc has been called the subnucleus gelatinosus

(102, 121). It contains a large number of glial cells and very small neurons which contain little Nissl substance. More caudally, the nucleus commissuralis (NC) lies medial to NM. The NC is continuous from one side to the other over the dorsal surface of the central canal. Except for more fusiform cells, NC is similar to NM in cell content. Chiba and Doba (32, 33) have characterized the content of NC as being small neurons of 10 μm in diameter interspersed among myelinated nerve fibre bundles. They also described thick dendritic profiles, astrocytic processes filled with thin filaments, and synapses of the axo-axonic and axo-dendritic types.

1.3. Neurogenesis in the Lower Medulla

The neurons of the lower medulla are primarily formed between gestational days 11 and 16 (E11, E16) in the rat (7, 145). In general, neurogenesis in the motor nuclei occurs between E11 and E13, with a peak occurring on E12 (7, 145); for example, in XII and the DMN 80% of the neuronal population is acquired on that day (145). Neurogenesis in the sensory relay nuclei of the lower medulla, including the NTS, takes place slightly later than in the motor nuclei, with the peak of neuron formation occurring on E13. In addition, the generation of the total neuronal population in the sensory relay nuclei occurs over a more extended period of time (E12-E15) (7, 145). Thus neurons in the rat brainstem are formed according to the

general pattern of neurogenesis where sensory nuclei form more slowly and after the motor nuclei of that vicinity (96).

1.4. Blood supply

The medulla, pons, mesencephalon, and cerebellum receive their blood supplies from the vertebral basilar system; the basilar artery is the unpaired ventral artery formed by the union of the paired vertebral arteries at about the level of the caudal margin of the pons. More specifically, the medulla and pons are supplied by the anterior and posterior spinal arteries, and by branches of the vertebral, basilar, and posterior inferior cerebellar arteries (with a possible contribution from the anterior inferior cerebellar arteries). The NTS receives its blood supply from the anterior spinal arteries (209).

The arteries of the brain send small branches into the pia-arachnoid. The penetrating vessels are rarely larger than 70 μm and are generally less than 50 μm in diameter (4, 177). Anastomoses are common among larger vessels on the surface of the brain, but in the deep parts, such anastomoses are limited to vessels that are less than 20 to 30 μm in diameter (4, 177). Capillaries anastomose freely so as to constitute a three-dimensional network throughout the nervous system (225).

The veins of the nervous system, which do not usually accompany arteries closely, drain into a system of sinuses

enclosed in the dura mater. The large veins draining the choroid plexus of the fourth ventricle, most of the pons, and the upper medulla empty into the sigmoid sinus or the superior or inferior petrosal sinuses. The veins draining the caudal parts of the medulla empty into the anterior and posterior spinal veins (225).

In general, the main arterial supply of the brain reaches it from the ventral aspect, whereas the more extensive venous drainage tends to be dorsal (225).

Blood vessels may be specially organized in some areas of the brain. King (111) has shown that the blood vessels in the lateral reticular formation of the medulla run in sheets according to the orientation of certain cranial nerve rootlets. He suggests that the sheets of vessels could provide, or reflect, the anatomical substrate that controls not only the gross connections of the reticular formation, but the detailed topography as well.

2. The baroreceptor reflex arc and the role of the NTS in the control of blood pressure

2.1. Introduction

Many early reports dealing with the central nervous control of the circulation begin with the description of a "medullary cardiovascular centre". It was believed that cardiovascular control is exerted by, and integrated in, this special centre which is tonically active. The centre was thought to be the primary site of the neural outputs

which controlled vasoconstriction in all regions of the body (79). All afferent inputs would act via the centre; for example, the baroreceptor input could only produce its effects by exciting the neurons of the inhibitory region or by directly inhibiting the neurons of the excitatory region (90).

The participation of neurons at many levels of the CNS in cardiovascular control and the multipurpose roles played by the neurons of any particular area have led investigators to discard the concept of a single medullary control centre. Rather, the model of organization of central cardiovascular regulation which is now accepted (154) suggests an "integrated participation of all levels of the CNS" with inputs from all afferent systems, a central interconnecting system, and efferent projections from different levels in the CNS to the final common pathway.

Integration of all levels of input and output is necessary for the process of cardiovascular regulation. For the purpose of simplication, however, the various components of the baroreceptor reflex arc will be presented as separate entities.

2.2. Primary baroreceptor neurons

The cell bodies of the primary baroreceptor neurons which conduct information to the lower brainstem are located in the nodose, or inferior ganglion. The

information is relayed to the nodose ganglion from the baroreceptors in the carotid sinus, aortic arch and other large systemic vessels, and cardiac structures via the carotid sinus nerve and the depressor nerve, the "buffer" nerves (151).

The baroreceptors are sensitive to stretch and therefore are capable of sensing changes in blood pressure (79). It appears that the aortic arch and carotid sinus baroreceptors do not function in an equivalent manner (88). The aortic arch component of the reflex, for example, appears to function primarily as an antihypertensive mechanism, whereas the carotid sinus baroreceptors operate primarily in hypotensive situations in the dog and cat (9, 155). In addition, the carotid sinus baroreceptors have been found to be more sensitive to pulse pressure changes in the dog (8).

Baroreceptors in the carotid sinus give rise to both myelinated (A-fibre) and unmyelinated (C-fibre) afferents (68). The former have low thresholds and are active at normal blood pressures while the latter often have quite high thresholds and operate at hypertensive pressure levels (1, 68, 146). Bolter & Ledsome (20) have found that low threshold carotid sinus baroreceptors (leading to presumptive A-fibres) are generally not susceptible to sympathetic modulation. It is likely that these afferent fibres have endings closely associated with smooth muscle cells. They have concluded that the profound baroreflex

effects of sympathetic nerve stimulation must be due to the direct influence of catecholamines on the high threshold unmyelinated C fibres. Thus, the differnt reflex efferent patterns induced by myelinated and unmyelinated baroreceptor afferents may be of significance for cardiovascular control in hypertension (146).

The buffer nerves carry both baroreceptor and chemoreceptor information from the periphery to the CNS, but there appear to be species differences in anatomical location and physiological responses of the two. For example, the rat aortic depressor nerve has been found to carry baroreceptor information almost exclusively (175), while in the cat and dog, the same nerve carries both baroreceptor and chemoreceptor information (38, 39, 49, 50, 61).

In general, the termination of fibres from VII, IX, and X in the NTS follows a rostro-caudal pattern. That is, axons from VII extend to a more rostral extent than those of IX which, in turn, extend more rostrally than X (14, 40, 109, 166, 208). The fibres of the primary baroreceptor neurons travel amongst other fibres of the glossopharyngeal (IX) and vagus (X) nerves and reach the medulla laterally at a level close to the obex. The fibres pass through the spinal nucleus and tract of the trigeminal nerve (6, 11, 14, 70, 208), and reach the NTS via a dorsal and ventral route, although only the ventral fibres appear to be necessary in the baroreceptor reflex (54). The fibres then

turn caudally and the majority of them terminate caudal to the rostral pole of XII (208). In the pigeon, the projection of IX to the NTS is primarily confined to the area directly surrounding the solitary tract while that of X is much denser in the NM and NSpc of the ipsilateral, and to a lesser degree, the contralateral NTS (14). The same findings had earlier been made in the rat (208), although terminations from IX and X were not distinguished as belonging specifically to one nerve or the other. In the cat (103) projections from the nodose ganglion to the NTS were studied with horseradish peroxidase (HRP) (retrograde transport) and radioactive amino acids (anterograde transport). In both cases, the NM was most intensely labelled, labelling was bilateral. After HRP application, the NC was also heavily labelled; labelling was bilateral but was more prominent on the contralateral side. Moderate ipsilateral HRP labelling was found in the dorsal, dorsolateral, intermediate, ventrolateral, and ventral subnuclei. After the application of radioactive amino acids, heavy bilateral labelling was found in the intermediate subnucleus in addition to the NM. Moderate labelling was found in the NC, dorsal, dorsolateral, VL, and ventral nuclei. Recently, it has been suggested by means of intracellular recording and iontophoretic application of HRP (47) during blood pressure changes that second order baroreceptor neurons in the cat are located only in close vicinity to the medial border of the solitary

tract near the level of the obex.

2.3. The "cardiovascular" NTS

2.3.1. Afferents

The number of studies demonstrating primary afferents which project to the NTS (other than from the baroreceptors) has been relatively small. The amygdala, in particular the central nucleus, has been shown to project to the NM and NSpc of the cat (93), to the NSpc in the rostral NTS of the monkey (160), and to the NTS/DMN border between 3.5 mm rostral and 3.5 mm caudal to the obex in the rabbit (182). Direct projections from the bed nucleus of the stria terminalis and the substantia innominata to the NTS/DMN border in the rabbit were also described (182). However, HRP injections in the latter study did not localize the exact target of these projections as being the NTS or the DMN. A later study (169) suggests that the target is, in fact, the DMN, and not the NTS.

A direct projection from the hypothalamus, including the paraventricular nucleus, to the NM and NSpc of the NTS of rats, cats, and monkeys has been described (174). Again, however, injection sites were large so that precise localization of projections could not be made.

Basbaum et al. (12) demonstrated a direct projection from the nucleus raphe magnus located ventrally in the midline of the rostral medulla to the NSpc and NInt at a level just rostral to the area postrema in the cat.

In a recent study, Ross, Ruggiero, and Reis (169) studied the afferents to the middle third of the rat NTS more systematically using retrograde HRP transport. The injection site included the areas dorsal, dorsomedial, and dorsolateral to the solitary tract. Medullary afferents to these regions of the NTS were found to originate from the nucleus ambiguus, nucleus raphe pallidus and magnus, and an area in the ventrolateral rostral reticular formation corresponding to the C1 catecholamine area. In the cerebellum, afferents to the NTS arose from the fastigial nucleus, in the pons, from the nucleus reticularis parvocellularis, the ventral reticular formation, a group of neurons from the same area as the A5 catecholamine group, the Kolliker-Fuse nucleus, and a group of neurons from the same area as the A7 catecholamine group. An extensive projection from the paraventricular nucleus of the hypothalamus was found. The insular cortex also projected to the NTS.

2.3.2. The nucleus

The caudal two-thirds of the NTS plays a primary role in the cardiovascular reflex arc. Lesions of this area of the NTS cause acute hypertension in rats, cats, and dogs (54, 55, 62) while electrical stimulation of the same area results in hypotension and bradycardia (54-56). Both species demonstrate large and immediate postoperative elevation of arterial pressure which lasts for several

hours. In the rat, bilateral lesions of the caudal NTS lead to hypertension, followed by myocardial failure, pulmonary edema, and death (165). The cat, unlike the rat, survives the initial period of hypertension. The blood pressure thereafter is no longer consistently elevated and periods of labile hypertension occur instead (165). In the dog (26) bilateral NTS lesions at the level of the obex result in the immediate increase in blood pressure which remains elevated and which demonstrates no fluctuations due to environmental factors. These studies suggest that there may be species differences in the location of the baroreceptor terminals in the NTS.

The destruction of adrenergic nerve terminals by 6-hydroxydopamine (6-OHDA; 2,4,5-trihydroxyphenethylamine) has been well documented. The action of 6-OHDA in the brain of experimental animals has been largely interpreted to suggest that central adrenergic mechanisms influence cardiovascular regulation to a very large extent (see reviews, 30 and 80). For example, intraventricular injection of 6-OHDA was found to prevent the development of various forms of experimental hypertension, but was ineffective in established hypertension (69). These results suggested that the effect of 6-OHDA is probably due to the destruction of central noradrenergic and/or dopaminergic structures which are involved in the initiation of hypertension, but which appeared to be of no importance for the maintenance of established hypertension.

Working directly within the NTS, Healy et al. (85) injected 6-OHDA into the intermediate NM. They found that selective destruction of catecholamine nerve terminals in the intermediate NM caused significant and persistent bradycardia without changes in blood pressure. On the other hand, it had been found previously (30) that 6-OHDA lesions of the NM at a more caudal level (ie. at the obex) or lesions of parts of NC interfered with blood pressure regulation. Healy et al. (85) therefore concluded that the baroreceptor reflex arc is likely sensitive to impulses from noradrenaline axons entering the more rostral intermediate NM. They suggested that catecholamine terminals in this area could act through an interneuron, or that catecholamine terminals influence the adjacent DMN directly, thereby inhibiting the neurons of the DMN that generate vagal bradycardia.

2.3.3. Efferent connections of the "cardiovascular" NTS

Humphrey (94) recorded evoked potentials from the paramedian nucleus of the reticular formation during stimulation of the carotid sinus nerve. These responses were attributed to the relay of the afferent input via the NTS. In the same way, potentials of long latencies have been recorded from the nucleus parvocellularis, nucleus gigantocellularis, and the lateral reticular nucleus during stimulation of the carotid sinus, glossopharyngeal, aortic depressor and superior laryngeal nerves (18). Because of

their latencies these responses have been interpreted to be due to activation of polysynaptic pathways, presumably including a synapse in the NTS.

After placement of a lesion in the intermediate NTS, degeneration of axons has been observed in the DMN, the intercalated nucleus, the different subdivisions of the NTS, the lateral reticular nucleus, the nucleus gigantocellularis, and the nucleus ambiguus (116, 133,151, 217). The fact that degenerating fibres were found within other parts of the NTS may imply a multisynaptic organization within the NTS, as has been suggested by the electrophysiological studies of Humphrey (94) and Miura & Reis (134).

Early studies reported that spinal projections from the cat NTS originate primarily from the area surrounding the solitary tract (64, 65, 208). These axons were thought to carry respiratory information. NTS neurons receiving arterial baroreceptor input also send axons to the spinal cord. Loewy & Burton (123) found that solitariospinal projections arise primarily from the NInt and SVL, although the NC also sends a small number of fibres to the spinal cord. The fibres project bilaterally, but primarily to the contralateral side, and travel in the medial part of the ventrolateral funiculus of the cervical spinal cord. (It became more difficult to identify the fibres in lower spinal cord levels.) The bilaterally projecting fibres terminate in three areas of the spinal cord: (1) the

region of the phrenic motor neurons, (2) the thoracic ventral horn, and (3) the intermediolateral cell column at thoracic, $lumbar_{1-4}$, and $sacral_2$ levels. Using the retrograde HRP labelling technique, Kneisley, Biber, and LaVail (112) also found that, after cervical injections of HRP in the monkey, labelled cells were seen bilaterally in the ventral and ventrolateral parts of the NTS. With respect to specific organization, Satoh et al. (176) reported that, in rats, the distribution of labelled cells in the NC shifted more caudally as the HRP injection site in the spinal cord moved more caudally. Blessing et al. (19) expanded these findings to show that the spinal projections of rabbit NTS are organized in a clear-cut viscerotopic fashion, such that lumbar segments of the spinal cord are innervated by the caudal NC, while thoracic segments are innervated by the ventrolateral and intermediate subnuclei of the NTS. The exact proportions of these which carries baroreceptor information is not known but termination location of these fibres suggests that this proportion is relatively high (115).

Various nuclei of the reticular formation in the medulla have been shown to project directly to the intermediolateral nucleus of the spinal cord (87). The terminations of secondary neurons from the NTS on various nuclei of the reticular formation in the medulla may suggest that baroreceptor reflexes could also reach the spinal cord by a multisynaptic pathway: via the

NTS-reticular formation-intermediolateral nucleus of the spinal cord (151).

Early neuroanatomical evidence indicated that the NTS relays cardiovascular afferent information to the hypothalamus through intermediate connections in the brain stem reticular formation (6, 41, 134, 138); recent studies have reported direct projections from the NTS to the hypothalamus (31, 36, 37, 167, 173) as well. Electrophysiologically, Ciriello & Calaresu (37) showed that the cell bodies of the ascending projections to the hypothalamus are located primarily in the NInt and VL. Other prosencephalic structures to which the NTS appears to project are the central nucleus of the amygdala, the bed nucleus of the stria terminalis, the medial preoptic area, and the periventricular nucleus of the thalamus (167). The significance of these latter projections in terms of cardiovascular regulation will be discussed subsequently.

2.4. Higher modulatory centres

The cardiovascular reflex arc is influenced by neuronal inputs from higher centres in the brain. For example, hypertension produced by NTS lesions has been found to be dependent on the integrity of structures lying above the medulla (62). Midcollicular decerebration will abort the development of hypertension which would have resulted from NTS lesions or abort the lesion-caused hypertension which was already established. In general,

the sympathetic neural response to disturbances in the environment of the organism is dependent on the integrity of forebrain and/or hypothalamic mechanisms (114). The existence of the higher modulatory mechanisms for the cardiovascular reflexes has been demonstrated in a number of electrophysiological studies, and neuroanatomical observations have made possible the localization of the cells, of the pathways, and of the descending neuronal pathways.

The hypothalamus has been implicated as a possible site of origin of the higher cardiovascular mechanisms. Electrical stimulation of the anterior hypothalamus and the preoptic area elicits bradycardia and hypotension (212, 213) and inhibits the baroreceptor reflexes (89, 129), whereas bilateral lesions of the anterior hypothalamus produce arterial hypertension (140). Stimulation of the posterior hypothalamus causes a rise in blood pressure (162); stimulation of the posteromedial hypothalamus causes increased blood pressure, tachycardia, and inhibition of reflex vagal bradycardia (207).

The direct projections from the NTS to the paraventricular, dorsomedial, and arcuate nuclei of the hypothalamus (37, 167, 173) provide anatomical evidence for the existence of a pathway originating in cardiovascular receptors and, through the hypothalamus, mediating the release of hormones as suggested by Share & Levy (187, 188). These investigators found that activation of

baroreceptor and chemoreceptor afferent fibres alters the release of antidiuretic hormone by the paraventricular nucleus neurons under conditions of increased blood volume.

The electrophysiological information regarding descending pathways from the hypothalamus suggests that hypothalamic pressor responses are mediated by two separate pathways. One activates sympathetic fibres with a long latency and is inhibited by increased arterial pressure. The other activates the same fibres with a shorter latency and is not inhibited by increased arterial pressure (72). A direct pathway from the hypothalamus to the spinal cord has also been described (174, 196).

As mentioned earlier, other prosencephalic structures to which the NTS projects directly are the central nucleus of the amygdala, the bed nucleus of the stria terminalis, the medial preoptic area, and the periventricular nucleus of the thalamus (167). These direct pathways may be the means by which cardiovascular afferent information is relayed to these structures. The importance of the region of the bed of the stria terminalis in the regulation of cardiovascular reflexes has been demonstrated by experiments in which combined lesions of the anterior hypothalamus, including the region of the bed nucleus, and of the medullary depressor area abolished the baroreceptor reflex, whereas a lesion of the depressor area alone did not (91). Fibres run from the bed nucleus to the amygdala which is also proposed to be a neuronal region influencing

cardiovascular responses (91). The observation that injection of noradrenaline into the bed nucleus induces a fall in blood pressure and heart rate (205) also is suggestive of a role played by the bed nucleus of the stria terminalis in the baroreceptor control mechanisms. With regard to the amygdala, it has been found that alterations in blood pressure and cardiac frequency can be elicited by localized stimulation of the central nucleus (93, 135).

As stated by Ricardo and Koh (167), the existence of the above described direct projections by no means implies that the more circuitous routes recognized earlier play a minor functional role. The direct projections could, in fact, be interpreted as only one extreme in a group of conduction lines, and "although it is likely that the direct and polysynaptic components of the system function in concert in many physiological situations, they need not be of identical significance even when sharing the same origin and distribution." (167).

The locus coeruleus (LC) and its neighboring area may also influence cardiovascular mechanisms. Electrical stimulation of this region elicits changes in arterial pressure (29, 214) and modulates cardiovascular activity (104, 105, 215). The LC sends descending projections to the medulla; the fibres and their neurons are noradrenergic (35, 48, 124, 210). The noradreneric nerve endings of the posterior hypothalamus originate from the cell bodies located in the LC (124). Electrical stimulation of the LC

elicits a pressor response which is diminished after destruction of the posterior hypothalamus (162). These data support the hypothesis that one of the functions of the noradrenergic cell bodies in the LC and their ascending fibres may be the regulation of arterial blood pressure.

Several investigators have suggested that the LC receives projections from the NTS (28, 106, 172, 216) but such projections were not found by either Loewy & Burton (123) or Ricardo & Koh (167).

Crawley et al (43), in their study on the LC, concluded that, while the anatomical region of the LC appears to activate the sympathetic nervous system when it is stimulated, the functional presence of the LC cells may not be essential for sympathetic nervous system activation.

Finally, discrete areas of the ventrolateral medulla, rostral to the obex, have been shown to play a role in cardiovascular regulation. In 1962, Chai & Wang (29) demonstrated that electrical stimulation of the ventrolateral medulla in the cat elicits an increase in arterial pressure. Dampney & Moon (53) found the same effect in the rabbit ventrolateral medulla; the centre of the ventrolateral pressor area was found to be located at the level of the rostral pole of the inferior olive. On the other hand, bilateral lesions of the ventrolateral pressor area of the cat (78) and rabbit (53) result in a large fall in resting arterial pressure. The fall in blood pressure following these lesions is unlikely to be due to

interruption of descending pathways from higher centres since complete pontomedullary transection has little effect on the resting arterial pressure (52). It was determined (51) that the cell bodies themselves are sympatho-excitatory. In addition, it was found (19, 77) that these neurons project directly to thoracic and lumbar segments of the spinal cord. Thus it appears that the pathway originating from the ventrolateral medullary neurons provides a tonic input to the spinal sympathetic outflow which in turn maintains resting arterial pressure (51).

Dampney (51) determined that there are two separate groups of cell bodies which project to the ventrolateral pressor area: (1) within the medial nucleus of the NTS, and (2) within the parabrachial nucleus of the pons. The significance of these two areas in the control of blood pressure has already been discussed.

The precise function of the ventrolateral neurons in cardiovascular regulation remains to be determined. Neither stimulation nor destruction of these cells significantly affects heart rate (53); thus is appears that these neurons regulate only sympathetic vasomotor outflow. It has been suggested (53) that the neurons respond to their chemical environment, either directly or through inputs from central chemosensitive neurons, and that changes in tissue p_{O_2}, p_{CO_2}, or pH cause them to discharge.

2.5. Summary

It is generally accepted that the NTS is the primary relay station in the baroreceptor reflex arc and that secondary projections from the NTS appear to be rather diverse so that connections are made with other medullary nuclei as well as with the hypothalamus and other prosencephalic structures. Modulatory input to the baroreceptor reflex from higher centres is known to exist, but there is a debate about the exact sources, extent, and nature of the input. Several studies have suggested that the NTS, besides being a relay station for the baroreceptor reflex, also exerts a modulatory influence over cardiovascular regulation. For example, the presence of axo-axonic synapses, the presumed anatomical substrate for presynaptic inhibition, in the NC of the NTS suggests that the NC is the primary site where regulation of the baroreceptor reflex occurs through presynaptic inhibition (32, 33). The possibility of cardiovascular regulation exerted by the NTS is, therefore, an open and controversial question.

3. The spontaneously hypertensive rat

The spontaneously hypertensive rat (SHR) was first introduced in 1963 by Okamoto and Aoki (149). The SHR was produced by selective inbreeding of Wistar-Kyoto rats that resulted in the development of hypertension in 100% of the progeny. Since then, the SHR has been used extensively in

the study of human essential hypertension.

SHRs reach the hypertensive level as early as 5 weeks of age; by 7 or 8 weeks the rats are hypertensive without exception, and by 12 weeks, the hypertension is well established (150). Inheritance of the hypertension is presumed to be polygenic although the number of genes involved is probably relatively small (206). The hypertension is transmitted equally by males and females but blood pressure in females is lower than in males throughout their life span (148). The SHRs are prone to infections, especially chronic respiratory disease; their life span is significantly lower than that of normotensive rats (206).

The primary advantage in using the SHR as a model for elevated blood pressure is that neither surgical manipulation nor administration of drugs is required for the development of elevated blood pressure.

4. Brain Metabolism

4.1. Glucose

4.1.1. Introduction

Approximately 90% of the brain's energy comes from the metabolism of glucose (92, 130, 193). The brain is dependent on a constant supply of glucose from the blood since its carbohydrate stores can provide only a few minutes of energy. Glucose crosses the blood-brain

barrier, diffuses through the extracellular space, and is finally transported through nerve and glial cell membranes. That glucose transport across the blood-brain barrier is achieved by means of facilitated diffusion was first suggested by Crone (44, 45), and thereafter verified by many others.

Glucose transport through the blood-brain barrier is stereospecific (46, 224); closely related carbohydrates are competitively transported by the same carrier mechanism according to the following rank order of affinity: a-D-glucose > 2-deoxy-D-glucose ≳ 3-O-methyl-D-glucose ≳ B-D-glucose > D-mannose ≳ D-galactose > D-xylose > L-glucose = D-fructose (17, 24, 119, 152). The transport across the barrier occurs at nearly the same rate in the direction from blood to brain as it does from brain to blood. The net transport occurs in the direction of the concentration gradient, which normally is in the direction of blood to brain (45, 152, 202).

4.1.2. Factors which affect glucose metabolism

a. Activity--regulation of glucose consumption

The capacity for transporting glucose across the blood-brain barrier, in the direction of blood to brain, is two to three times greater than the phosphorylation rate. Therefore, under normal conditions the transport of glucose across the blood-brain barrier has no regulatory function on glucose metabolism (126). Rather, the regulation must

be accomplished by the metabolic activity of the nervous tissue (125).

That increased functional states in neural tissues require larger glucose supplies has been convincingly demonstrated by the use of radioactively labelled 2-deoxy-D-glucose (see subsequent section). In turn, it has been shown (95, 118) that increased cerebral activity causes an increased blood flow in the respective brain areas. Two processes might be expected to facilitate this increased blood flow:

(1) Increased linear blood flow

An increase above normal values of the linear flow rate causes only a minor increase in the glucose transport rate across the blood-brain barrier, since the glucose concentration in the brain capillaries increases only slightly. The reason for this very modest increase is that the glucose permeability in the blood-brain barrier in relation to flow is such that glucose passage over the barrier is diffusion limited. A tripling of the linear flow rate has been shown to cause only a 15% increase in the glucose transport (125). Therefore only a moderate increase in the glucose transport across the blood-brain barrier can be achieved by an increase of the flow rate above normal values.

(2) Recruitment of capillaries

The recruitment of capillaries provides a much greater possibility of an increase in glucose transport than that

permitted by increased linear flow. Gjedde and Rasmussen, 1980 (73) have suggested that there is, in brain, a set of "reserve" capillaries that are recruited according to need. A decreased metabolic rate in pentobarbital-anesthetized rat brains was explained by a decrease in the number of perfused capillaries. Bolwig et al. (21, 22) have shown that the increase in blood flow seen at the conclusion of epileptic convulsions is produced by recruitment of capillaries rather than by increased linear flow. The increased cerebral blood flow found in N_2O-anesthetized rats, compared with pentobarbital-anesthetized rats (144, 152) has also been attributed to capillary recruitment. Miller et al. (132) showed that hypercapnic rats given electroconsulsive shock treatment demonstrated an increased cerebral blood flow, once again explained by an increased number of perfused capillaries in the brain. Thus, although capillary recruitment may not be the only mechanism by which glucose transport to the brain is increased, it appears to be the major such mechanism.

b. Anesthesia

Glucose consumption in the CNS can be substantially altered by anesthesia. Most barbiturates lower oxygen consumption in the brain (143, 157, 202, 218). Pentobarbital has been found to have a dose dependent effect on cerebral glucose and lactate levels and to depress glucose utilization (42, 83). While pentobarbital

has essentially no effect on blood-brain barrier glucose transport kinetics (142), it does decrease blood flow to the brain (22, 73). Goldman and Sapirstein (76) found that the greater the perfusion was in any part of the brain, the more was its flow depressed by pentobarbital anesthesia.

4.2. 2-Deoxy-D-glucose

4.2.1. Introduction

The first demonstration that radioactive 2-deoxy-D-glucose (2DG) could be used to localize regional functional activity in the nervous system was made by Kennedy et al. (107). 2DG, the structural analog of glucose, differs from glucose only by lacking an oxygen on the second carbon atom. According to Sokoloff et al. (202), the 2DG is transported into brain cells by the normal glucose transport system and is then phosphorylated to 2DG-6-phosphate by the same hexokinase that phosphorylates glucose. However, unlike glucose-6-phosphate, 2DG-6-phosphate cannot be metabolized further due to the lack of a hydroxyl group on its second carbon atom. Furthermore, brain glucose-phosphatase activity has been found to be very low in mammalian brain (126, 159, 202). Thus, after administration of a bolus of ^{3}H- or ^{14}C-2DG, ^{3}H- or ^{14}C-2DG-6-phosphate accumulates in the brain and the regional variation in uptake can be used to quantify local cerebral glucose utilization autoradiographically (199, 200).

4.2.2. Theory

The application of the 2DG model to the quantification of local cerebral utilization is dependent on the validity of several assumptions and/or conditions (198, 202). These are:

1) A steady state for glucose (ie. a constant plasma glucose concentration and a constant rate of tissue glucose consumption) is maintained throughout the experimental procedure.

2) There are homogeneous tissue compartments within which the precursor concentrations of 2DG are uniform and exchange directly with the plasma.

3) 2DG is present in tracer amounts. It has been calculated that the maximum allowable 2DG concentration is 2.5 μmoles/kg body weight in the rat (201).

If the above conditions are met, the relationships of glucose, 2DG and their metabolites within the tissue can be mathematically defined and an operational equation derived (201). The equation can be generally stated as follows:

$$\text{Rate of reaction} = \frac{\text{labeled product formed in interval of time, 0 to T}}{\text{isotope effect correction factor} \times \text{integrated specific activity of precursor}}$$

Thus rates of enzyme-catalyzed reactions are determined

from measurements made with the radioactive tracer. The numerator represents the amount of radioactive product formed in a given time and is equal to the combined concentrations of ^{14}C-DG and ^{14}C-DG-6-phosphate in the tissue at time T (measured by autoradiography) less the amount of free unmetabolized ^{14}C-DG still remaining in the tissue. The denominator represents the integrated specific activity of the precursor pool times a factor, the lumped constant, which is equivalent to a correction factor for an isotope effect (198). The former contains a term which takes into account the lag in the equilibrium of the tissue precursor pool with the plasma.

Sokoloff and his colleagues (107, 108, 198, 202) have determined that the time interval between the injection of 2DG and the sacrifice of the experimental animal should be 45 minutes with a minimum of 30 minutes and a maximum of 60 minutes. From the values of the rate constants determined in normal animals and the usual time course of the clearance of the 2DG from the arterial plasma following a single pulse at time 0, an interval of 45 minutes is adequate for these terms to become sufficiently small that considerable latitude in inaccuracies of the rate constants is permissible without appreciably increased error in the estimates of local glucose consumption (152). In addition, although low, glucose-6-phosphatase activity is not zero, and the 2DG-6-phosphate in the brain is not retained indefinitely. The effects of the enzyme activity become

noticeable at 60 minutes, and are substantial at 90 minutes. Once again, therefore, it was recommended that the experimental period be limited to 45 minutes.

4.2.3. Techniques of autoradiography

a. ^{3}H versus ^{14}C

The 2DG technique was developed using the ^{14}C-labeled compound and X-ray film to obtain the final autoradiograms (107, 108, 198, 200, 202). A bolus of ^{14}C-2DG was administered to the experimental animal; after 45 to 60 minutes, the animal was sacificed and the brain was removed and frozen. Sections were cut in a cryostat and either freeze-dried or mounted on a slide or coverslip and dried on a hot-plate. These sections were then apposed to X-ray film and stored in the dark for the appropriate exposure time prior to autoradiographic processing. Since then, this particular method has been widely used (2, 5, 10, 59, 75, 84, 97, 101, 171, 184, 185, 189, 190, 194, 195) when macroscopic visualization of metabolism within the brain structures has been required. However, due to the high energy beta-particle emissions from ^{14}C and the subsequent necessity to use relatively insensitive X-ray film, resolution of a microscopic order was not attainable. As a result, many investigators have used ^{3}H-labeled 2DG for their autoradiographic studies of metabolic changes in the brain (3, 59, 63, 67, 122, 158, 171, 184, 189, 191, 204). The advantages of using ^{3}H-2DG are as follows:

1) Low energy beta particles are emitted from the source. It follows that thinner autoradiographic film (including nuclear track emulsion) can be used. Because the liquid nuclear track emulsions, for example, are of a much finer grain, autoradiographic resolution can be increased manyfold.

2) Variations in source (ie. section) thickness have no effect on optical density of autoradiographic grains (3). Because of the less energetic beta emissions from ^{3}H, the self-absorption of tissue for ^{3}H beta particles is sufficient to absorb virtually all of the radiation from layers more than 5 μm away from the emulsion (66). Thus, errors caused by microtome imprecision (which are important when ^{14}C-2DG is used) are eliminated.

b. Methods developed for ^{3}H-2DG autoradiography

2-DG-6-phosphate, the metabolite of 2DG which becomes trapped within cells, is water-soluble. Thus the histological technique used for ^{3}H-2DG autoradiography must be one specially designed for diffusible substances (168). Recently, several variations of this type of technique have been reported in the literature. Several groups have demonstrated good isotope localization in tissues processed for plastic embedding and emulsion autoradiography (13, 57, 186). Advantages of the approach (57) are: the isotope cannot diffuse out of the plastic into the emulsion, the histological quality is excellent, and the method is

suitable to electron microscopy. The technique has been successfully used to study small isolated tissues such as the retina, but plastic embedding is impractical when many serial sections from larger brains are required. In an attempt to overcome this drawback Durham et al (63) have used paraffin-embedding after stabilizing carbohydrates "in situ" so that many sections can be cut quickly and easily.

Thaw-mounting techniques have become the most commonly used techniques for ^{3}H-2DG autoradiography. Sharp (190) applied frozen sections of fresh brain directly on frozen emulsion-coated slides under a safelight. Sections remained frozen during the exposure period, thus eliminating the water phase through which diffusion could occur. The primary problem encountered with the latter technique was one of adequate adhesion of the sections to the slides. To overcome this drawback, Pilgrim and Wagner (158) ensured better contact of tissue and emulsion by touching the back of each slide with a finger. The moment of thawing was determined and the slide was refrozen immediately thereafter. Once again, sections were kept frozen (-30°C) during the exposure period.

Recently Lippe et al. (122) and Steward and Smith (204) described the use of a similar technique with the exception that, after sections were thaw-mounted onto room temperature slides, they were allowed to air-dry prior to storage for exposure. With this procedure, autoradiograms were obtained which were of comparable quality of

resolution to sections mounted on cold slides provided that sections were thin (about 5μm) (204).

4.2.4. Functional activity, energy requirements, and 2DG

The development of the 2DG technique for the "in vivo" determination of glucose consumption by Sokoloff and his colleagues has provided a non-invasive method to study cerebral patterns of glucose utilization during different functional states. Using this technique, investigators have obtained pictorial representations of regional cerebral glucose utilization resulting from various changes in cerebral functional activity. Examples of local metabolic changes have been reported in the cerebral cortex (170), the olfactory system (10, 97, 189, 190), the visual system (2, 13, 59, 181, 211, 221), the vestibular system (189), the motor (75) and premotor (128) cortices, the hippocampus (137, 204), the hypoglossal nucleus (194), and the substantia nigra-forebrain system (171, 184, 185); neural connections of the gastrointestinal system (101) and sexual organs in rats (5) have also been studied with the aid of this technique. These studies have clearly demonstrated that there is a close relationship between functional activity in the brain and energy metabolism. For example, two groups of investigators (181, 211) have recently shown that orientation columns in the cat visual cortex, which are known from physiological studies to demonstrate increased activity during visual stimulation,

are clearly revealed with the ^{14}C-2DG technique. That is, areas of greater activity showed a greater uptake of ^{14}C-2DG.

If such a relationship exists, some energy-consuming physical and/or chemical process should be associated with neural functional activity (201). It appears that electrical activity is the physical process which is most involved with functional activity and that energy is required to restore ionic gradients to their resting levels (201). It would be expected that more energy would be required to restore ionic gradients when there exists an increased frequency of action potentials (and therefore greater ionic fluxes). This observation has, in fact, been made by Yarowsky et al. (223). They found that in the superior cervical ganglion a direct linear relationship exists between the frequency of the electrical spike input and the rate of glucose utilization. It has been estimated that more than 40% of the brain's energy consumption is used for the maintenance and restoration of ionic gradients and membrane potentials (219).

The above findings suggest that the Na^+, K^+-ATPase system is of major importance in the coupling of glucose utilization to functional activity (201). In support of this hypothesis, Mata et al. (127) found that electrical stimulation of cultured rat pituitary led to increased glucose utilization that was blocked by ouabain, an inhibitor of Na^+, K^+-ATPase. It has been suggested (201)

that the increased glucose utilization observed by Mata et al. (127) reflected mainly the metabolic activity of the axonal terminals. Schwartz and coworkers (184, 185), in their studies of dopaminergic pathways, have also shown a greater sensitivity of axonal terminals and/or synaptic elements than that of perikarya to metabolic activation. Diamond (60) has demonstrated a high-affinity transport of DG in synaptosomes. Therefore, these studies suggest that the changes in brain glucose utilization which occur in response to altered functional activity and which are demonstrated by the 2DG technique in fact mainly represent alterations in the metabolic activity of synaptic terminals triggered by changes in Na^+, K^+-ATPase activity (201).

A recent study using cerebral cortex slices, on the other hand, suggests that glucose utilization shows no dependence on Na^+-K^+-ATPase or upon extracellular K^+, Mg^{++}, or Cl^-, but may be dependent upon mitochondrial energy (74).

4.2.5. Summary

It can be concluded from the literature that:
(1) by using trace amount of radioactively-labelled 2DG, glucose utilization in the CNS in response to different functional states can be determined since it has been demonstrated that functional activity in specific components of the CNS is (as in other tissues) closely coupled to the local rate of energy metabolism.

(2) for high resolution quantification of glucose utilization, ^{3}H rather than ^{14}C is the preferred label for 2DG.

MATERIALS AND METHODS

1. Maintenance of colonies

Both Wistar-Kyoto (WKY) rats and spontaneously hypertensive rats (SHRs) were maintained at the Animal Care facility at the Faculty of Medicine, Memorial University of Newfoundland. The SHR strain was originally obtained from the NIH laboratories and the WKY strain from the Charles River Lakeview laboratories (N.Y.). The strains were maintained by brother-sister matings. Offspring were weaned at 4 weeks of age. Animals over 4 weeks of age were housed three to a cage in a 12 hour light/dark lighting schedule. The animals were given access to unlimited water and Purina rat chow.

2. Blood pressure measurements

Systolic and diastolic blood pressures were measured in the femoral arteries of rats anesthetized with 35 to 40 mg/kg sodium pentobarbital i.p. Cannulas pulled from PE-90 tubing were connected to a P23AA pressure transducer and pen recordings were made on a Beckman R411 Dynograph recorder. Blood pressures measurements were made on male WKYs and SHRs at ages 4, 8, and 12 weeks. Data were analyzed with a Student's t test.

3. Study of the relative metabolism in the NTS

3.1. Unlabelled 2-deoxyglucose controls

Non-radioactive 2DG was administered to rats of ages comparable to those to be used in the ^{3}H-2DG studies (ie. 4, 8, and 12 weeks) to determine whether the compound itself affects blood pressure over the time periods of interest.

Animals were anesthetized with 35 to 40 mg/kg sodium pentobarbital. The left femoral arteries were cannulated so that the blood pressures of the rats could be monitored over the experimental period. At time zero, 0.5 mg/kg 2DG, dissolved in saline (see appendix 1.1), was injected intraperitoneally into the experimental animal. Blood pressure was recorded at this time, at 10 minute intervals, and after 45 minutes. At the end of the recording period, the animal was sacrificed with an overdose of sodium pentobarbital.

3.2. Sham controls

A sham control study was carried out in which four 13-week male WKYs were given an intraperitoneal injection of saline in volumes comparable to those used in the unlabelled 2DG control study. Blood pressures were once again monitored at time zero and after 45 minutes.

3.3. ^{3}H-2-deoxy-D-glucose

a. Male SHR and WKY rats were studied at ages 2, 4, 8, and

12 weeks, 4 animals per group. While the four animals in any particular age group or strain were studied within a week of each other, different age agroups or strains were studied at random with respect to time of year. Animals were given intraperitoneal injections of ^{3}H-2DG (obtained from New England Nuclear, Boston, Ma.) at a dosage of 200 μCi/100 gm body weight (see appendix 1.2).

b. The rats, conscious and unrestrained, were allowed to survive for 45 minutes and were then anesthetized with ether. The chests were opened and the rats were perfused through the left ventricle with:

i. 100 ml/kg of 0.1M phosphate buffer

ii. 200 ml/kg of 2% glutaraldehyde in 0.05M phosphate buffer.

c. The brains were removed and trimmed so that the fore- and midbrains were excluded. Using minced liver as a mounting medium, the brainstem blocks were positioned upon the cryostat chucks. Freezing was accomplished by submerging the chuck and liver but not the brain tissue into hexane that had been cooled in liquid N_2. This procedure allowed the brain to freeze more gradually than if it had been submerged. (Since very rapid freezing causes freezing artefacts to be formed in the tissue, it is to be avoided.) When the entire tissue block was frozen, it was transferred to a cryostat set at -20° to -22° C and allowed to equilibrate for at least one hour.

d. Six μm-thick sections were cut on the cryostat in the

dark with the aid of a safelamp (filter OC). Sections at 25 to 35 µm intervals were thaw-mounted (one to each slide) onto dry emulsion-coated slides (see section 2.3.5). Rapid drying of the sections was ensured by the use of a small fan which directed room air over the surface of the sections.

e. The slides with their sections were placed into light-tight slide boxes along with a small amount of Drierite which would ensure that the slides remained dry over the exposure period. Slide boxes were stored at 4°C for one to two months, depending on the exposure time required for each set of slides.

3.4. Blank autoradiography controls

In order to assess the effects of physical and chemical factors on the autoradiograms, non-radioactive sections were subjected to the steps of autoradiogram preparation described in the previous section.

A 12-week male WKY rat was anesthetized with ether and perfused as described. The brainstem was removed and frozen, and 6 µm-thick sections were cut on the cryostat. Sections were thaw-mounted, four to a slide, onto dry emulsion-coated slides. Slides were placed into light-tight slide boxes along with a small amount of Drierite, and stored at 4°C for two months.

3.5. Autoradiography

3.5.1. Emulsion

Kodak NTB-2 nuclear track emulsion was heated to 45^{o}C in a water bath so that liquefaction occurred. The emulsion was then diluted 1:1 with distilled water. The amount of emulsion used depended upon the number of slides to be dipped.

If many slides (more than 10) were to be dipped, the dipping jar containing the diluted emulsion was kept in the water bath to prevent cooling. Slides were dipped once and excess emulsion was wiped off the back of the slides. The slides were air-dried in the vertical position for at least one-half hour. Upon drying, the slides were placed in a light-tight slide box in the presence of a drying agent (Drierite) and stored until required.

3.5.2. Processing

i. Slides ready for processing were placed in alternate slots of a slide staining rack. It was found that this type of placement was necessary to allow adequate circulation of the photographic solutions around the emulsion.

ii. Slides were developed in Microdol-X developer (at room temperature) for 8 minutes.

iii. Slides were rinsed in distilled water.

iv. Fixation of the slides in Kodak rapid fixer was carried out for 4 minutes.

v. Slides were then washed in tap water for 30 minutes.

vi. Autoradiograms were post-fixed in 4% formalin for 10 minutes, and washed for one-half hour in tap water.

vii. After a final rinse in distilled water, sections were stained in 1% cresyl violet for 2 to 5 minutes until the desired intensity of Nissl stain was achieved. The slides were rinsed in distilled water and differentiated in 95% alcohol. Dehydration in absolute alcohol was followed by clearing in xylene; coverslips were mounted over the sections using Permount.

3.6. Delineation of NTS subnuclei

In order to define the nucleus commissuralis (NC) and nucleus medialis (NM) of the NTS, Nissl stained sections (with cresyl violet) from representative levels in the brainstem were studied. Borders of the subnuclei were placed according to surrounding structural landmarks and cell characteristics of the subnuclei.

3.6.1. NC boundaries

The caudalmost level used was one immediately rostral to the decussation of the pyramids where the rootlets of XII have begun to appear (figure 1). At this level the NC is continuous over the midline, the dorsal column nuclei are prominent, and the DMN has appeared. The area postrema (AP) is not present at this level.

The rostral border of the NC was placed at a level

about 50 µm caudal to the level where the AP bisects the NTS (figure 1). Thus the NC is still continuous over the midline. The dorsal column nuclei have moved laterally and the external cuneate nucleus has begun to appear near the dorsolateral surface of the brainstem.

In transverse section, the medial border was placed at the midline of the NC. The dorsal border was formed by the dorsal column nuclei, the ventral border by the dorsal border of the DMN. The lateral border was formed by the tractus solitarius and, more ventrally, by a line drawn from the lateral border of the DMN dorsally to the tract (figure 2).

3.6.2. NM boundaries

The caudal border of the NM was placed at a level just rostral to where the AP bisects the NTS. The fourth ventricle has not yet opened at this level (figure 1).

The rostralmost level used in these studies was one just caudal to the level where the NTS begins to move laterally from the walls of the open fourth ventricle. The dorsal column nuclei are no longer present, the external cuneate nucleus is prominent, and XII has diminished in size at this level.

The NM contains small, rather densely packed neurons and is located on the medial aspect of the tract. Its medial border is formed by the presence of the NSpc which in turn contains very small neurons containing little Nissl

Figure 1: Line drawings of transverse sections through the medulla oblongata to show the levels between which the subnuclei NC and NM were studied. Section A is most caudal and section D is most rostral. Sections between levels A and B were used to study the NC, sections between C and D were used to study the NM. (NC = nucleus commissuralis; NM = nucleus medialis; DMN = dorsal motor nucleus of the vagus; XII = hypoglossal nucleus; C and G = dorsal column nuclei cuneatus and gracilis; EC = external cuneate nucleus).

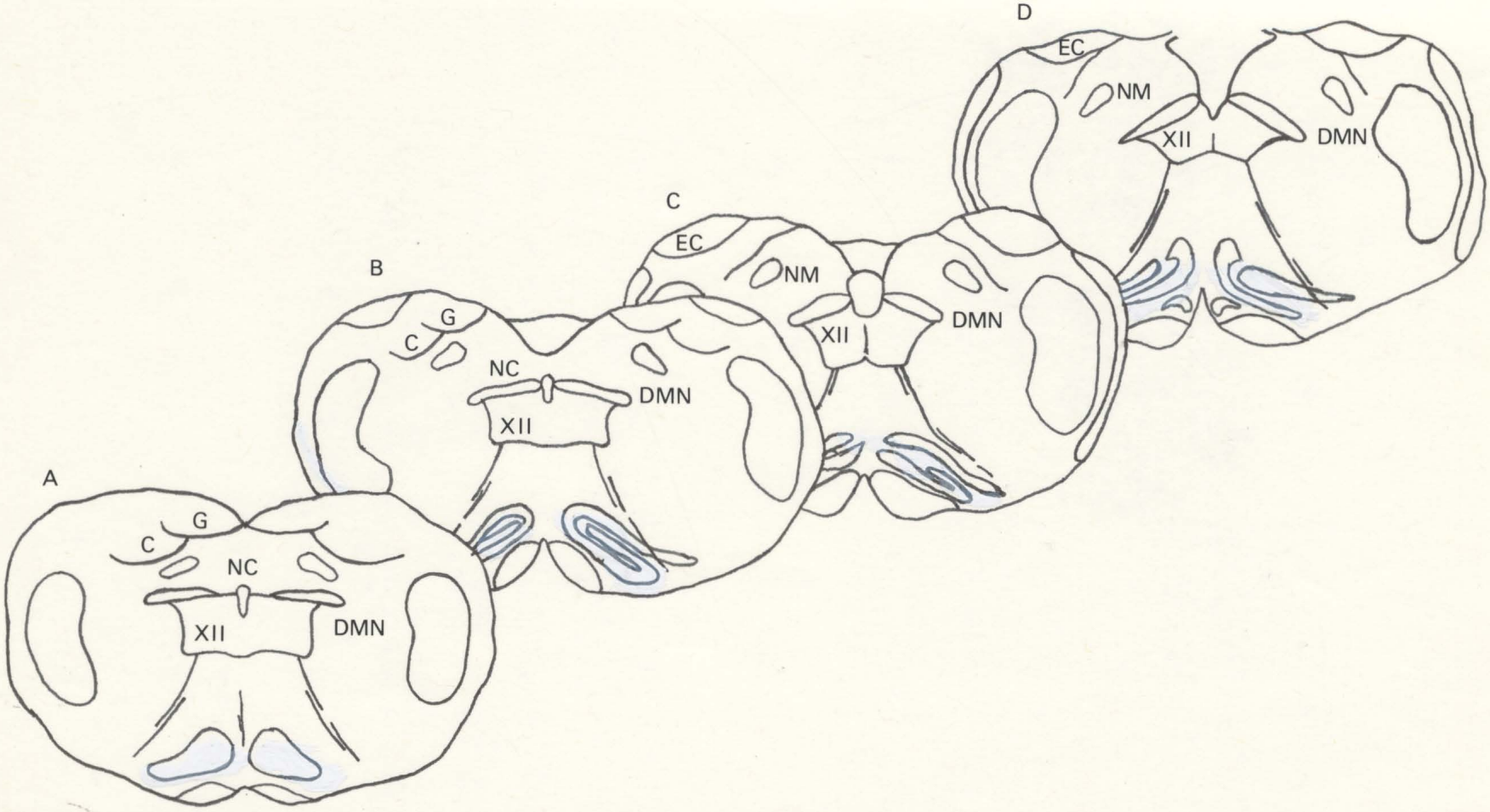
A
G
C
NC
XII
DMN
B
G
C
NC
XII
DMN
C
EC
NM
XII
DMN
D
EC
NM
XII
DMN

Figure 2: Transverse section of rat brainstem to show extent of nucleus commissuralis (NC) studied. Cresyl fast violet. (x100).

Figure 3: Transverse section of rat brainstem to show extent of nucleus medialis (NM) studied. Cresyl fast violet. (x100).

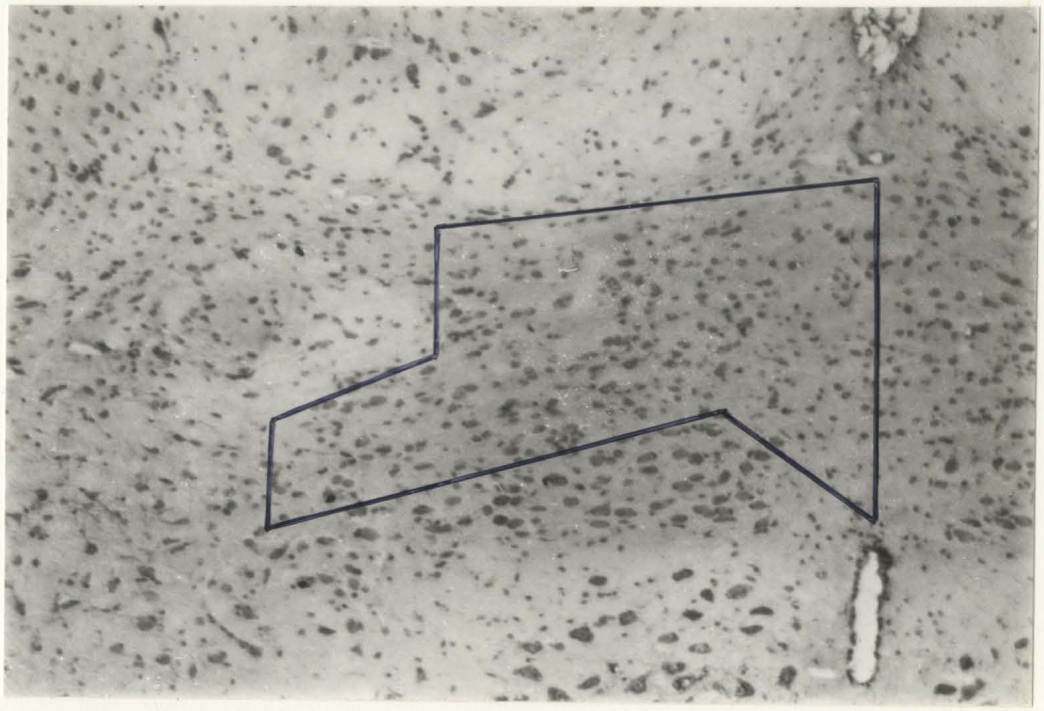

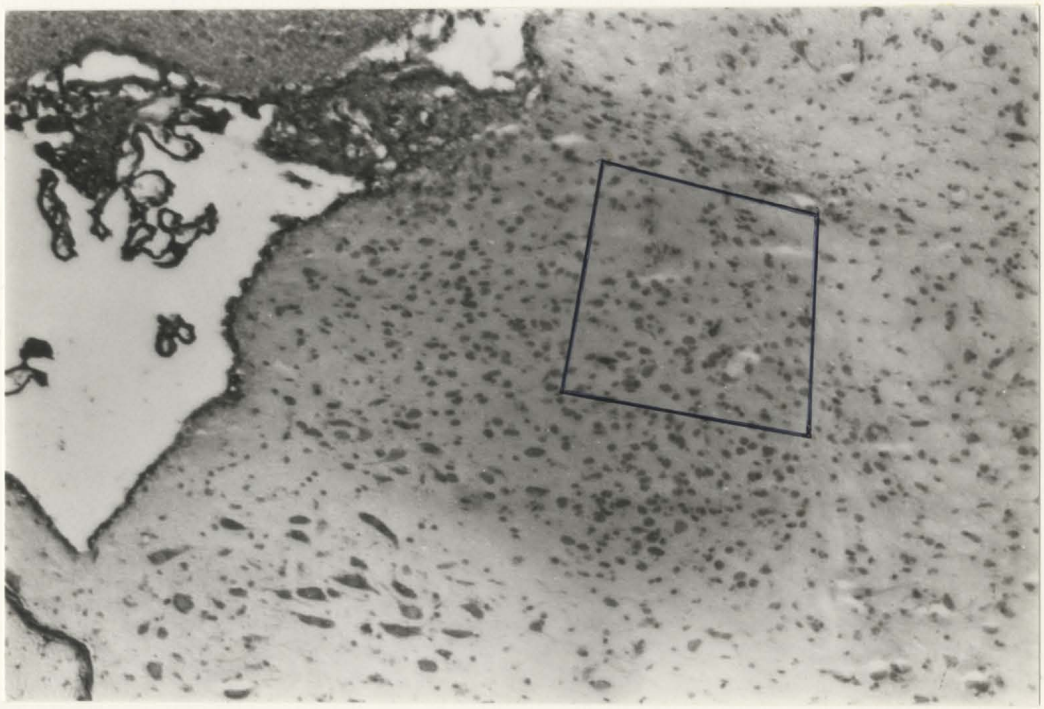

substance. Therefore, the distinction between NM and NSpc was easily made. The ventral border of NM is formed by the dorsal border of DMN (figure 3).

3.7. Analysis of autoradiograms

Measurement of relative metabolic activity in the NC and NM of the NTS was made by quantifying the ^{3}H-2DG uptake into the tissues. This uptake was quantified by counting silver grains from photographs of the autoradiograms or directly from the autoradiograms themselves, as described below.

It was necessary to determine the appropriate sizes of boxes to be used to generate representative counts of silver grains from photographs of XII (used in a correction factor described below) and NC since boxes of too small dimensions would introduce an error due to inherent variations in standard deviations. Therefore, ten counts were made from boxes at each of the various dimensions. The standard deviations from the counts at each box size were then plotted against the dimensions of the boxes as is shown in figures 4 and 5. The points at which the standard deviations no longer increased indicated the minimum necessary dimensions of the boxes which were used for counts in XII and NC. Thus, 2 x 2 cm^2 and 3.5 x 3.5 cm^2 boxes were used for XII and NC, respectively.

In order to eliminate variations in the grain counts which would be due to variations inherent to

Figure 4: Determination of the appropriate box dimensions to be used to generate representative counts of silver grains from photographs of the hypoglossal nucleus. Standard deviations were plotted versus size of boxes (cm^2). Each curve represents a different set of data. The standard deviations stabilized at 4 cm^2; therefore, boxes of 2 x 2 cm^2 were used.

Figure 5: Determination of the appropriate box dimensions to be used to generate representative counts of silver grains from photographs of the nucleus commissuralis. Standard deviations were plotted versus size of boxes (cm^2). Each curve represents a different set of data. The standard deviations stabilized at 12.25 cm^2; therefore, boxes of 3.5 x 3.5 cm^2 were used.

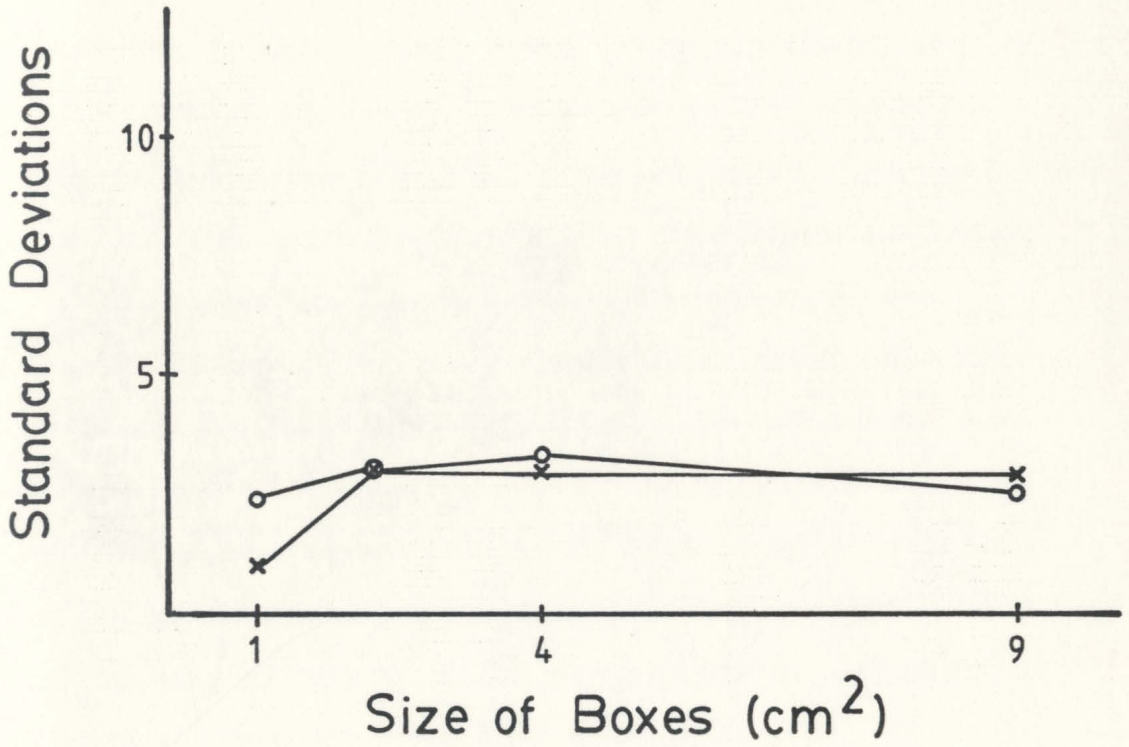
Standard Deviations
10
5
1
4
9
Size of Boxes (cm²)

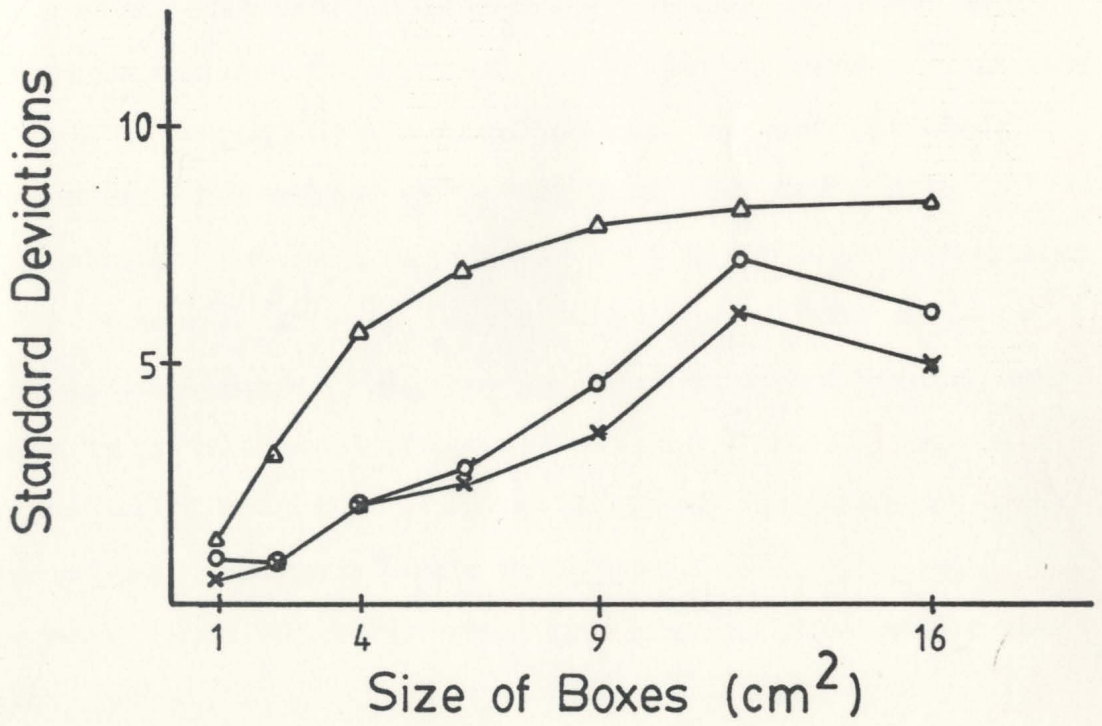
Standard Deviations
10
5
1
4
9
16
Size of Boxes (cm²)

autoradiography (eg. thickness of emulsion, slight differences in development times or temperatures, etc.), XII was used as an internal standard against which the counts from the NTS subnuclei were corrected. For both the NC and NM, the corresponding XII on the ipsilateral side was photographed at the ventrolateral aspect of the nucleus. Counts of grains representing ^{3}H-2DG were made from the final print (x830). Representative counts were made from the photograph by counting the grains within 2 x 2 cm^2 boxes that were drawn on an acetate sheet and laid over the photograph. Six such counts were made (see fig. 6). The mean of the 6 values was calculated and used as the internal standard for that section.

3.7.1. NC

Since the area encompassed by the NC is relatively large, a montage of one-half of the NC was constructed from 4 to 6 photographs; the magnification of each photograph was x830. The number of photographs required per NC depended on the level of the section since more photographs were necessary at more rostral levels where the NC is relatively larger. Representative counts for each NC were made by counting the grains within 3.5 x 3.5 cm^2 boxes drawn on an acetate sheet and laid over the montage. Two counts per photograph were made (see fig. 6) so that between 8 and 12 counts were made per NC. The counts were totalled and averaged to the equivalent of 10 counts so

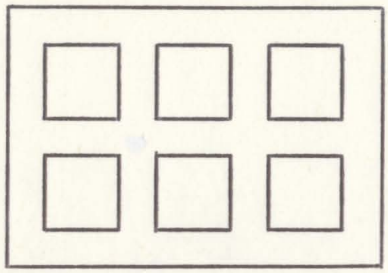

A

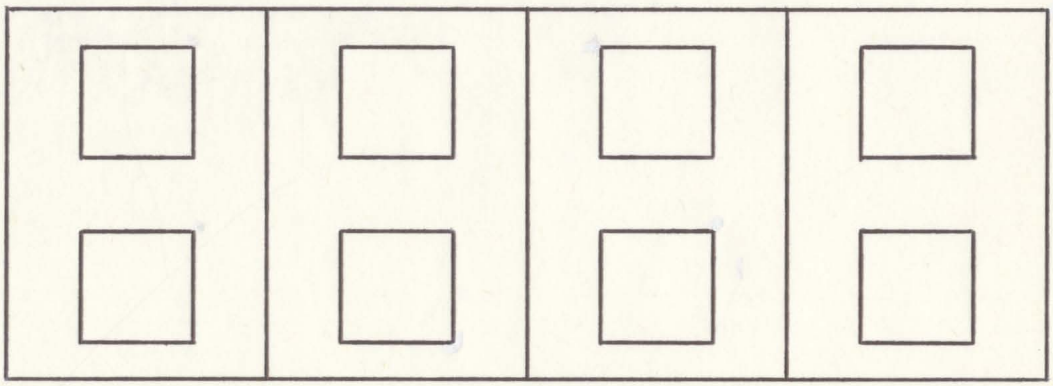

B

Figure 6 A,B: Diagrams to illustrate placement of boxes over photographs in order to generate representative counts of silver grains in experimental autoradiograms.

A. Six boxes (2 x 2 cm^2) were placed over photographs (x830) of XII in the positions shown in the diagram.

B. Montages of the NC were made from photographs, x830. Boxes (3.5 x 3.5 cm^2) were placed, two on a photograph, in the positions shown in the diagram.

that comparisons between sections and animals could be made.

3.7.2. NM

Grain counts of the NM were made directly from the autoradiograms since the area of the NM is relatively small. Using a camera focussing eyepiece and a x40 objective, the grains within two 35 mm rectangles in the eyepiece were counted on one side of the section and totalled. Approximately 50% of the NM was included in the two rectangles.

3.7.3. Final calculation of relative metabolic activity

Eight sections each of the NC and NM were analyzed in each animal as outlined above. The internal standards calculated from each of the corresponding XII's were averaged and used in a correction factor for each NC and NM count according to the following equation:

$$N = \frac{\text{Individual XII count per section}}{\text{Mean of XII counts for that animal}} \times \text{Individual NTS Counts (NC or NM)}$$

Thus factors unrelated to the uptake of ^{3}H-2DG into the NTS were eliminated from the final values for relative metabolic activity.

The mean of the 8 corrected values for the uptake of ^{3}H-2DG into the NC or NM in one animal was calculated and

used to represent the relative metabolic activity for that subnucleus in that animal.

4. Neuronal Density Study

The sections from which neuronal cell counts were made were the same sections as those used in the measurement of metabolic activity in the NTS using ^{3}H-2DG. Therefore, for the preparation of these tissue sections, see section 3.3. Counts were made in WKYs and SHRs at 2, 4, 8, and 12 weeks of age (4 animals per group).

The NC and NM subnuclei from one-half of the NTS were projected onto centimeter graph paper with a Leitz drawing tube (x86). Boundaries of the subnuclei were drawn and the location of neurons, identified by Nissl staining, was recorded on the graph paper. Neurons were then counted and expressed as the number of neurons per cm which is equivalent to "n" neurons/3.6 x 10^{3} μm^{2}. Eight such counts were made per subnucleus per animal. The mean of the 8 counts was calculated and expressed as the neuronal density of that subnucleus for that animal. Finally, the neuronal density of the subnuclei for the animals within a group was calculated by finding the mean value of the individual values per animal.

5. Blood Vessel Study

Male WKYs and SHRs at 4 and 12 weeks of age (4 animals per group) were anesthetized with ether. The chests were

opened and the rats were perfused through the left ventricle with one-half strength Karnovsky fixative (see appendix 2.1). Brains were removed and trimmed; brainstems were placed into fresh fixative. After one-half to one hour the brainstems were sliced into approximately 0.5 mm slices with a razor blade at the level of the NTS. The slices were replaced into fixative for one additional hour. After fixation, the brain slices were processed and embedded in Araldite (see appendix 2.2). One-half micron sections were cut on an LKB Huxley ultra-microtome. The sections were mounted onto glass slides and stained with toluidine blue. Only those sections which demonstrated patent blood vessels devoid of blood were used in the subsequent analysis.

The NC and NM subnuclei from one-half of the NTS were projected onto centimeter graph paper with a Leitz drawing tube (x166). For each of the subnuclei in each animal, two sections were analyzed, one from the caudal half of the subnucleus and the other from the rostral half. In each case, the blood vessels from an area of 5.4×10^4 μm^2 were drawn as seen. Blood vessels of 10 μm or less in diameter were then counted for each section. No attempt was made to distinguish between capillaries or venules.

RESULTS

1. Rat colonies

1.1. Blood pressures

The mean arterial pressures (MAPs) of the WKY and SHR colonies from which experimental animals were used are plotted in figure 7. Blood pressure measurements were made on male rats at 4, 8, and 12 weeks of age.

At 4 weeks, there was no significant difference between the MAPs of WKYs and SHRs (85 ± 7 mm Hg and 83 ± 2 mm Hg, respectively). At both 8 and 12 weeks, however, the MAPs of the SHRs were significantly higher than those of the WKYs. At 8 weeks, the MAPs were 92 ± 6 mm Hg and 111 ± 7 mm Hg for WKYs and SHRs, respectively. At 12 weeks, MAPs were 98 ± 7 mm Hg and 124 ± 16 mm Hg for WKYs and SHRs, respectively.

1.2. Weights

The mean weights of WKYs and SHRs at 2, 4, 8, and 12 weeks of age are plotted in figure 8.

There was no significant difference between the weights of the two strains at any of the ages studied. The greatest increase in weight in both strains occurred between 4 and 8 weeks. For example, 4 week WKYs weighing 50 ± 16 gm increased to a weight of 166 ± 24 gm by 8 weeks. WKYs and SHRs at 12 weeks of age attained weights of 185 ± 28 gm and 201 ± 53 gm, respectively.

Figure 7: Mean arterial pressures (MAPs) (mm Hg) in Wistar-Kyoto (WKY) (white bars) and spontaneously hypertensive rats (SHR) (stippled bars) at 4, 8 and 12 weeks of age. Number of animals used: 4 weeks, WKY = 5, SHR = 5; 8 weeks, WKY = 9, SHR = 7; 12 weeks, WKY = 6, SHR = 11. (xx = significant difference; $p < 0.05$).

Figure 8: Mean weights (gm) of Wistar-Kyoto (WKY) (white bars) and spontaneously hypertensive rats (SHR) (stippled bars) at 2, 4, 8, and 12 weeks of age. Number of animals used: 2 weeks, WKY = 18; SHR = 14; 4 weeks, WKY = 22; SHR = 12; 8 weeks, WKY = 11, SHR = 11; 12 weeks, WKY = 11, SHR = 11.

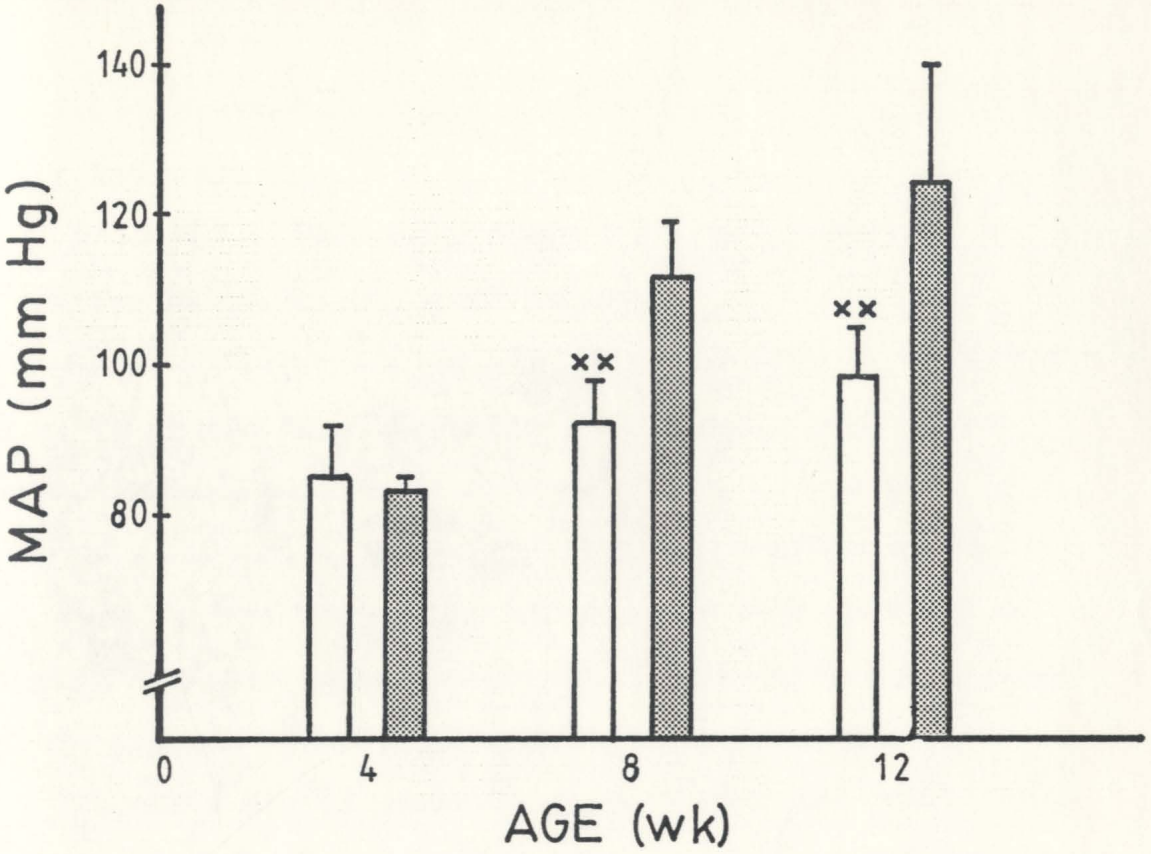
140
120
100
80
MAP (mm Hg)
××
××
0
4
8
12
AGE (wk)

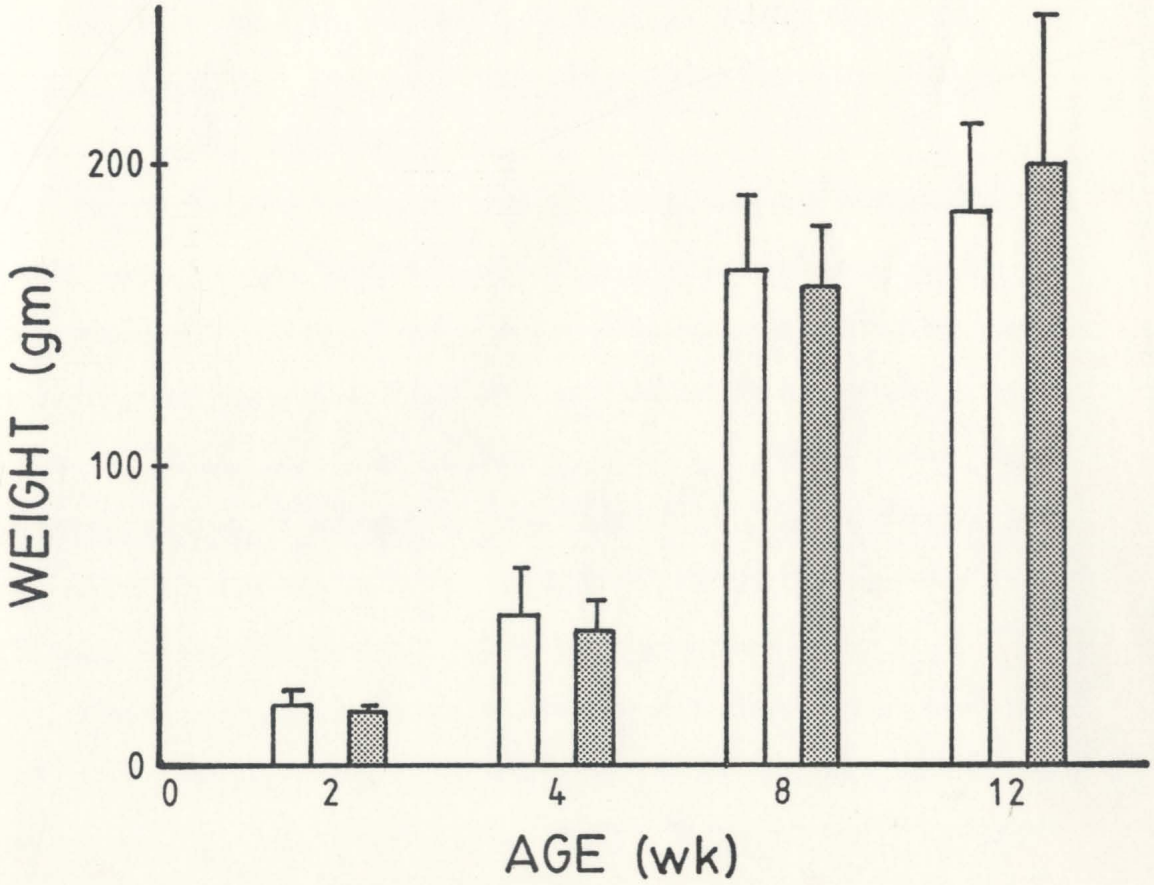
200
100
0
WEIGHT (gm)
0
2
4
8
12
AGE (wk)

2. Study of the metabolism in NC and NM

2.1. 2DG controls

In order to determine whether the 2DG component of H-2DG has an effect on blood pressure, pentobarbital-anesthetized male WKYs and SHRs at 4, 8, and 12 weeks of age were administered unlabelled 2DG; blood pressures were recorded at time zero, at 10 minutes intervals, and again after 45 minutes. Results are shown in table 1. The changes in MAP between time zero and 45 minutes are given for each group of animals in the top part of the table.

In the 4 and 12 weeks rats (both WKYs and SHRs) blood pressure had shifted after 45 minutes to a point lower than that at time zero. In the 8 week rats (both WKYs and SHRs), the blood pressure was at a level slightly higher than the level at time zero.

To determine whether the blood pressure changes would occur even in the absence of 2DG, a sham control study was carried out. Five 13 week male WKYs were treated as before except that physiological saline was administered in the place of 2DG. The change in MAP for the group after 45 minutes was -6 ± 12 mm Hg (see table 1). As a comparison, the mean of the MAP drift for all animals which received 2DG was also calculated (-1 ± 13 mm Hg).

Thus there was no significant difference between the MAP shift found after 2DG administration in any of the age groups or in the total shift of all animals and the shift

Table 1: Results of control study for 2-deoxyglucose (2DG) showing the mean change in mean arterial pressure (MAP) between time zero and 45 minutes after administration of 2DG in pentobarbital-anesthetized WKYs and SHRs of 4, 8, and 12 weeks of age. The mean change for all of the animals combined and the mean in a group of WKYs which was administered physiological saline in the place of 2DG are shown in the lower part of the table.

	Mean Change in MAP (mm Hg)		
	4 week	8 week	12 week
WKY	-9 ± 3 (n=5)	+1 ± 11 (n=9)	-2 ± 5 (n=7)
SHR	-3 ± 6 (n=5)	+6 ± 11 (n=7)	-3 ± 14 (n=4)
Total	+1 ± 13 n=37)		
Sham	-6 ± 12 (n=5)		

found when saline alone was administered (Student's t test).

2.2. Blank autoradiographical controls

Since no isotope was used in this control study, artifacts caused by the autoradiographical technique itself, either physical or chemical, were determined.

When silver grains were present over the control sections, they were observed in the following areas (see figures 9 to 11):

1) along the periphery of the sections,

2) in tears of the tissue which had been formed during sectioning,

3) in the central canal of the brainstem, although the density of grains in the central canal was less than that in the tears across the sections,

4) in areas where adhesion was poor,

5) in the AP

6) over some large neurons such as in XII,

The presence of silver grains appeared to depend on the drying process of the section on the slide. Of the four sections mounted per slide those sections which had their drying process interrupted several times and thus had longer drying periods showed more artifact grains than those which had no (or only one) interruption in their drying process.

Figures 9 to 11: Blank autoradiographical controls used to demonstrate accumulation of artifact silver grains due to stress forces when no isotope was present. Cresyl fast violet.

Figure 9: Artifact grains formed along the periphery of the sections and in tears of the tissue formed during sectioning. (x100)

Figure 10: Artifact grains formed in the area postrema (AP), seen in the left portion of this photograph. (x664).

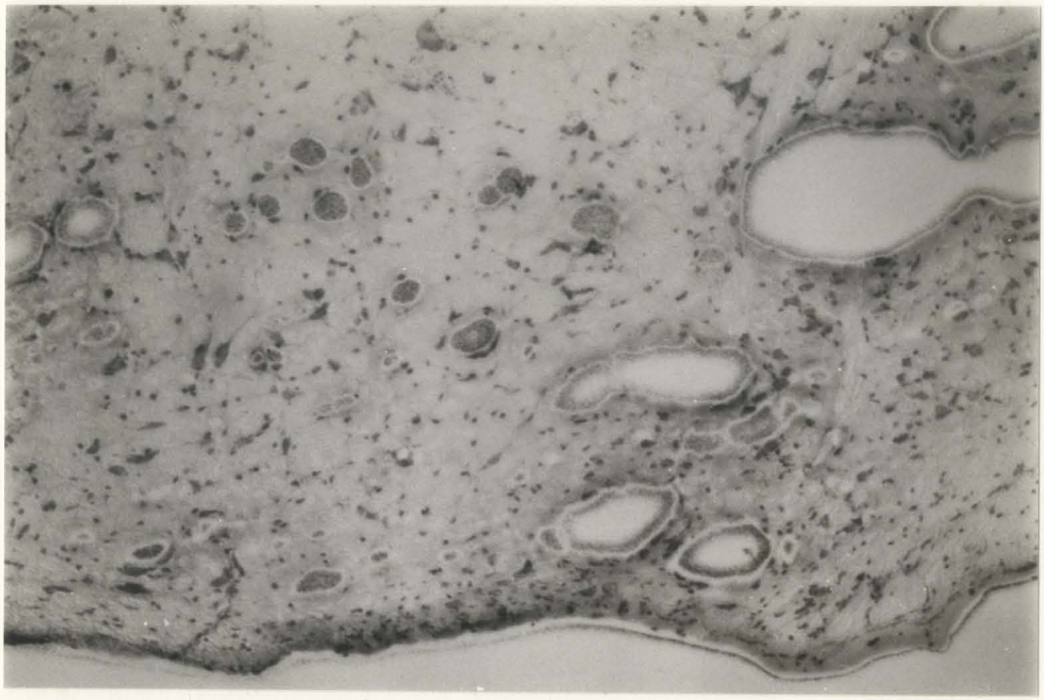

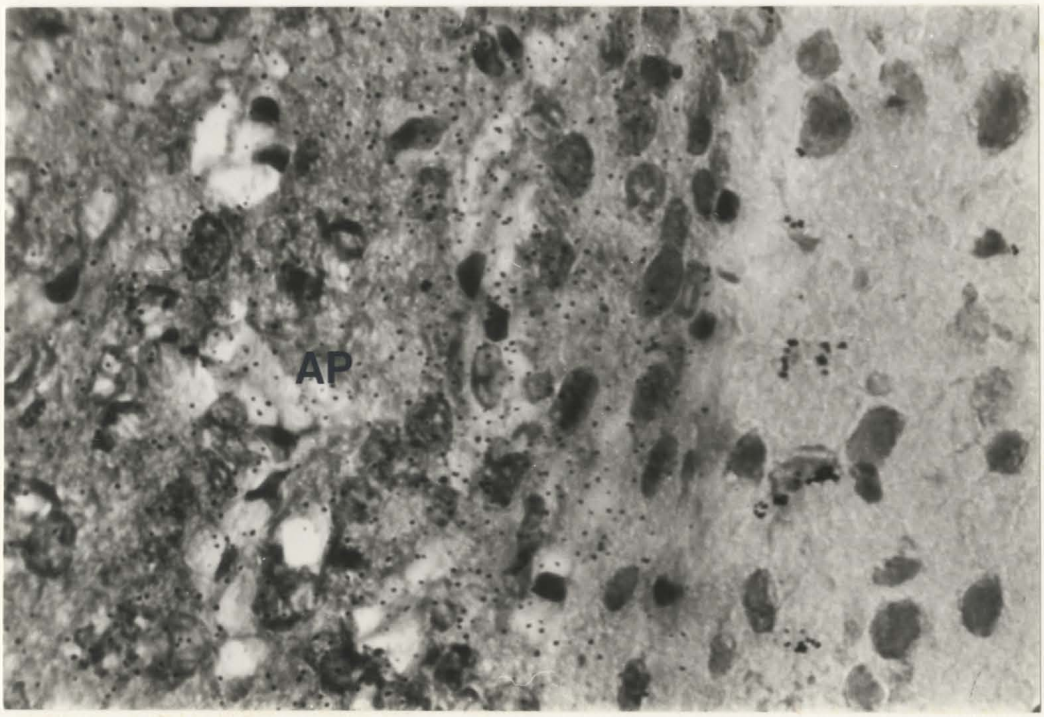
AP

Figure 11: Artifact silver grains formed over large neurons when drying of the thaw-mounted sections was prolonged. Note absence of artifact grains over fibre tracts.

A. Neurons in the central reticular formation. (x664).

B. Neurons in the hypoglossal nucleus. (x664).

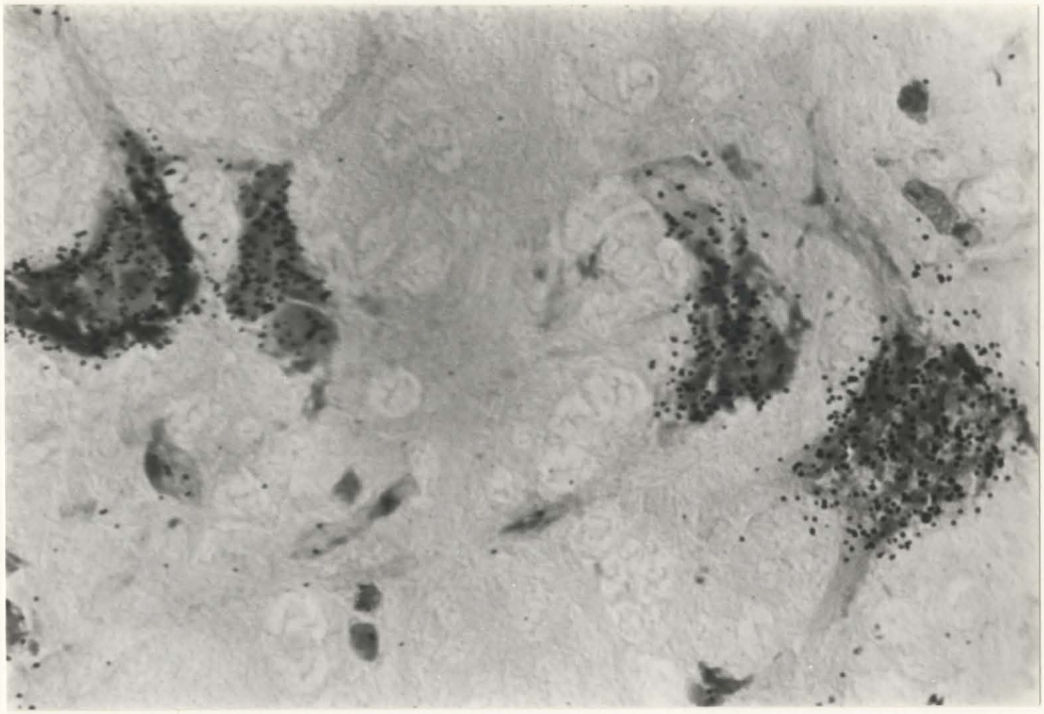

A

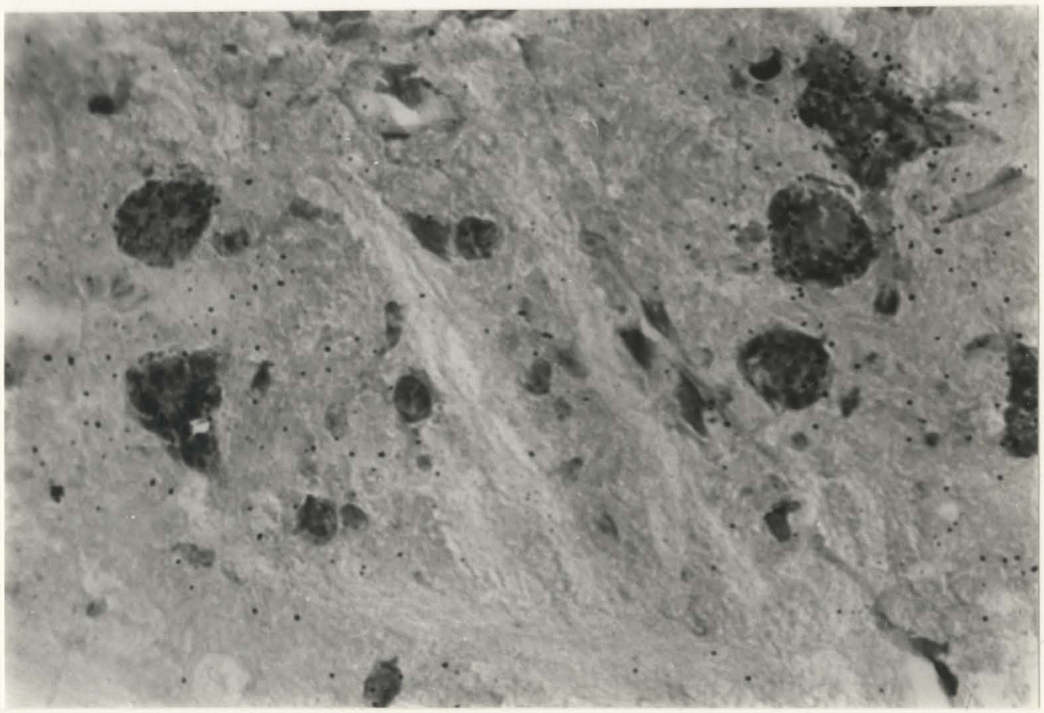

B

In general, if no accumulation of grains over cell bodies was present in these blank controls, grain density in other parts of the section, with the exception of tears and edges of the section, was very low.

Artifact grains over the NTS were always very small in in number whereas they were more numerous over XII when drying of that section was interrupted two or three times. Fibre tracts showed no artifact grain accumulation (see fig.11). Background silver grains off the sections were insignificant.

2.3. General uptake of ^{3}H-2DG in experimental sections

2.3.1. Animals 4 weeks of age and older

Uptake of ^{3}H-2DG into the brainstems of rats 4 weeks of age and older was not uniform in a transverse plane. Certain areas such XII and the inferior olive demonstrated higher uptake levels than the surrounding areas. The NTS and DMN consistently showed a lower level of ^{3}H-2DG uptake than their surrounding areas. A sharp border formed by silver grains was always seen between XII and NTS/DMN (fig. 12, A and B).

Fibre tracts such as the rootlets of XII and internal arcuate fibres were clearly delineated by silver grains (fig. 13, A and B). This specific localization of ^{3}H-2DG was more prominent in 8 and 12 week animals than in 4 week animals. Localization of ^{3}H-2DG was not observed to be higher in cell perikarya than in the surrounding neuropil.

Figure 12: Autoradiograms to demonstrate the sharp border formed by silver grains between XII and NTS/DMN in experimental slides. (XII = hypoglossal nucleus; NTS = nucleus tractus solitarius; DMN = dorsal motor nucleus of the vagus nerve; top of micrograph = dorsal; bottom of micrograph = ventral).

A. Light-field micrograph. Cresyl fast violet, x664

B. Dark-field micrograph, x344

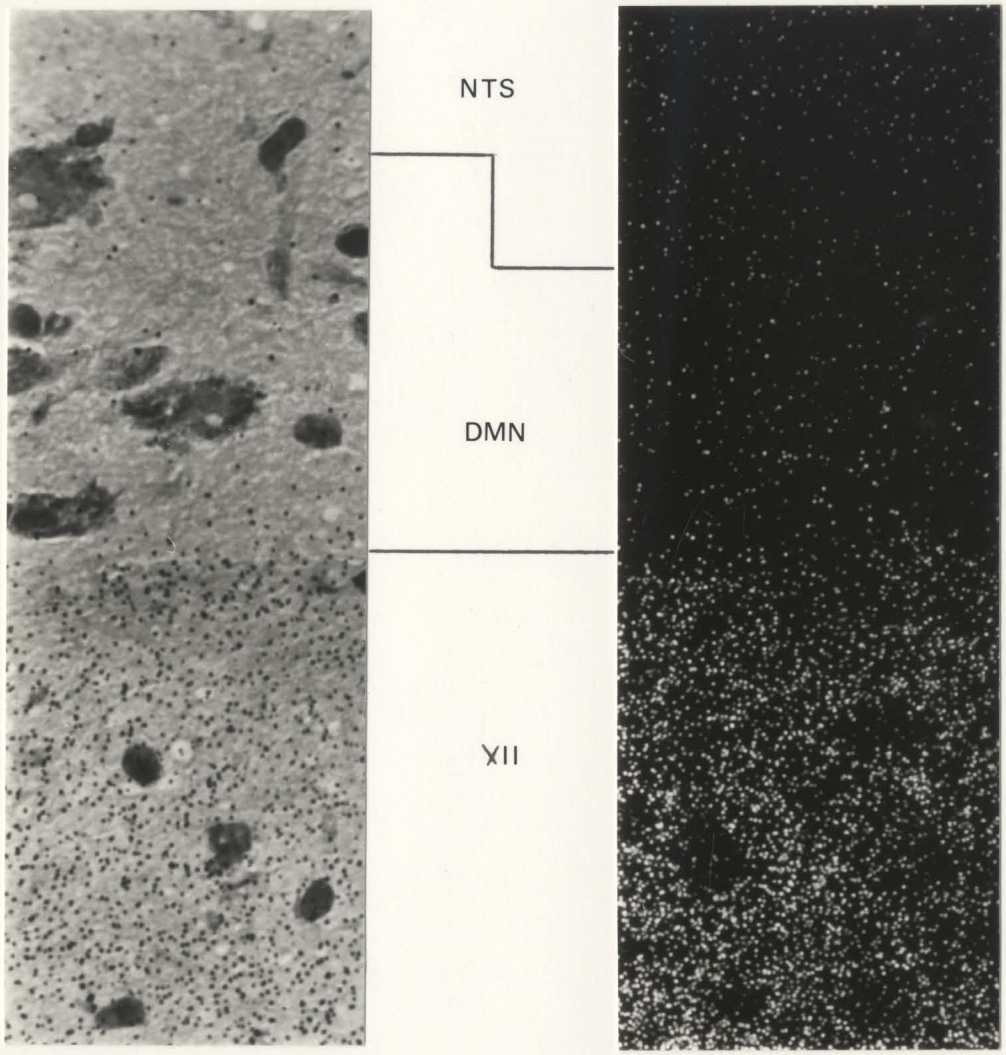
NTS
DMN
XII
A
B

Figure 13 A,B: Darkfield photographs of the rootlets of XII to demonstrate uptake of ^{3}H-2DG into fibre tracts. (x334).

A

B

2.3.2. Animals of 2 weeks

Differences in uptake of ^{3}H-2DG into the various regions of the brainstems of 2 week rats were not as pronounced as they were in the older animals. Uptake was more generalized in the 2 week animals so that specific nuclei did not stand out in the autoradiograms, either because of a higher silver grain density such as XII or because of a lower silver grain density such as the NTS. Thus the border between XII and NTS/DMN formed by the silver grains was not as evident as it was in the older animals.

Localized ^{3}H-2DG uptake by fibre tracts was not observed in the 2 week animals. As in the older animals, uptake of ^{3}H-2DG into cell perikarya was not observed to be higher than into the surrounding neuropil.

2.3.3. Artifacts

Experimental slides displayed the same types of artifact silver grain accumulation as did the blank controls where no isotope was present (see previous section). The density of grains at the edges of the experimental sections was, by visual assessment, the same as that in the blank controls.

2.4. Development of metabolic requirements in the "cardiovascular" NTS

Figures 14 and 15 illustrate typical autoradiograms of the NC and NM in a 2 week WKY and a 2 week SHR. Autoradiograms of the two subnuclei were similar at all ages studied. ^{3}H-2DG uptake was quantified in the NC and NM of WKYs and SHRs at 2, 4, 8, and 12 weeks of age. Data are plotted in figures 16 and 17.

2.4.1. NC

In the WKYs, ^{3}H-2DG uptake decreased between 2 and 4 weeks (144 ± 25 to 41 ± 11). At 8 weeks, ^{3}H-2DG uptake increased to a level similar to that at 2 weeks (155 ± 56). By 12 weeks, the uptake had once again decreased to a level similar to that at 4 weeks (52 ± 29).

Uptake of ^{3}H-2DG into the NC of SHRs generally followed the same trends as the WKYs did. That is, a decrease from 2 to 4 weeks was followed by an increase at 8 weeks and a decrease at 12 weeks. At 2 and 4 weeks, however, the ^{3}H-2DG uptake was significantly higher in the SHR compared with the WKY. At 8 and 12 weeks, uptake in the SHR was not significantly different from that in the WKY (two-tailed t test).

2.4.2. NM

As in the NC, ^{3}H-2DG in the NM of the WKYs decreased between 2 and 4 weeks (154 ± 32 to 37 ± 25). At 8 weeks,

Fig. 14 A,B: Typical autoradiograms from the nucleus commissuralis of a 2 week WKY (A) and a 2 week SHR (B). Localization of ^{3}H-2DG is demonstrated by the presence of black silver grains. Cresyl fast violet, x334

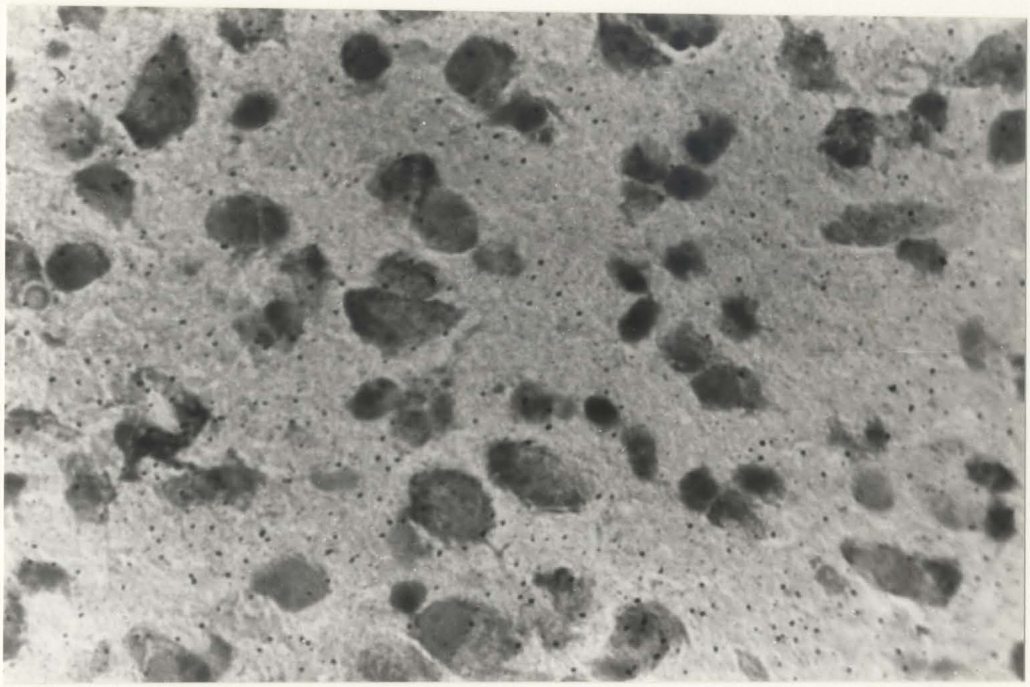

A

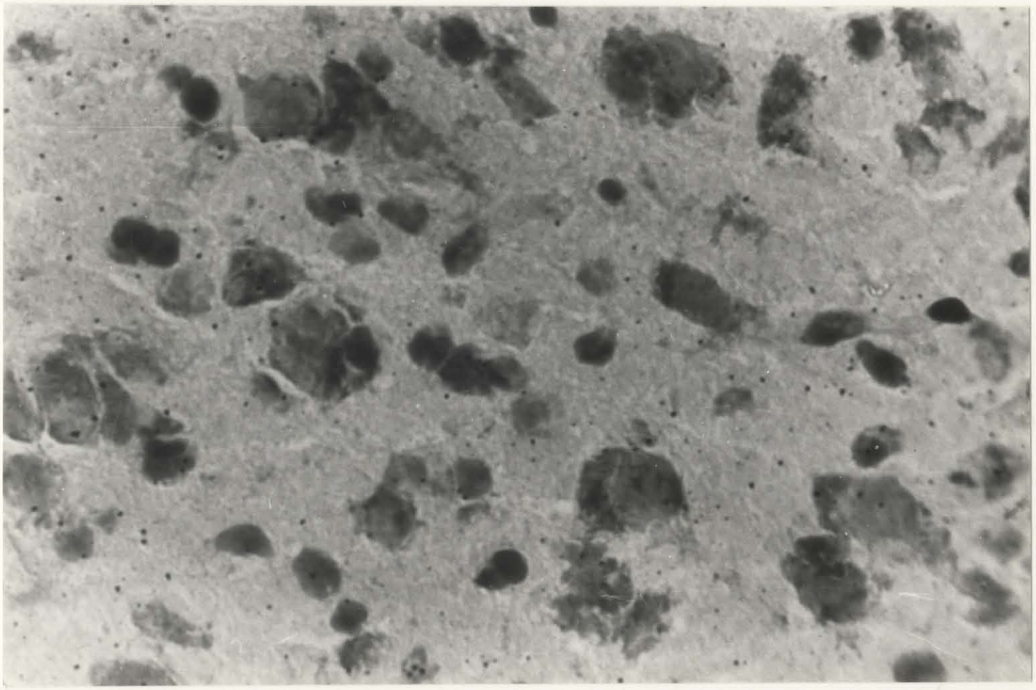

B

Fig. 15 A,B: Typical autoradiograms from the nucleus medialis of a 2 week WKY (A) and a 2 week SHR (B). Localization of ^{3}H-2DG is demonstrated by the presence of black silver grains. Cresyl fast violet, x334

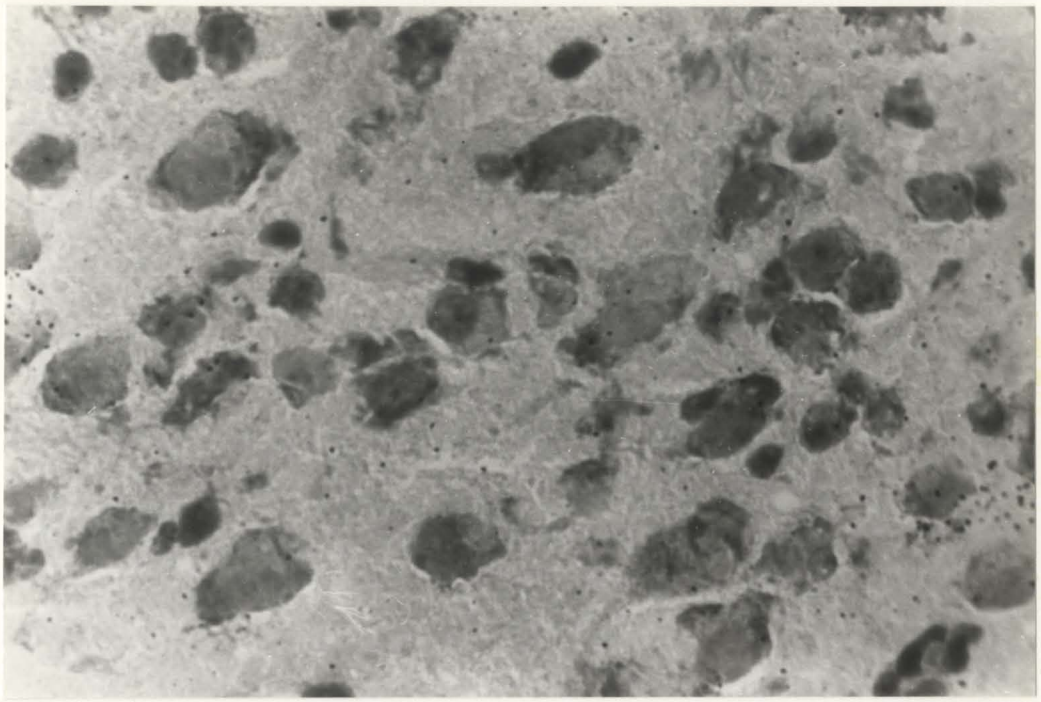

A

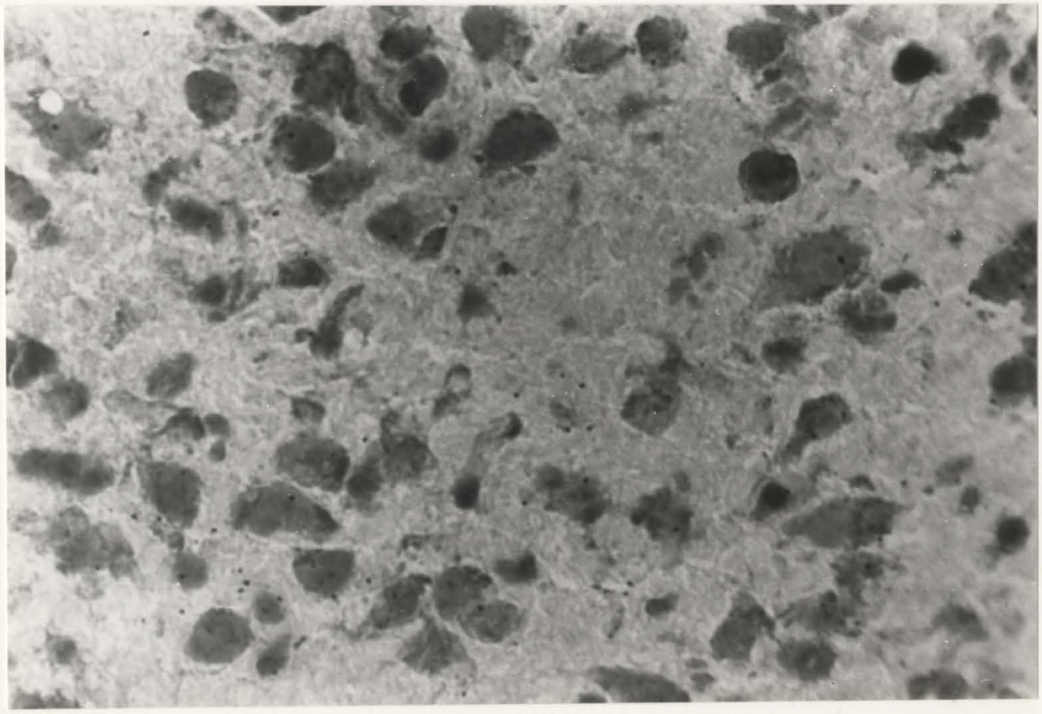

B

Figure 16: Relative metabolic activity in the nucleus commissuralis (NC) in WKYs (white bars) and SHRs (stippled bars) at 2, 4, 8, and 12 weeks of age. (xx = significant difference; $p < 0.05$, two-tailed t test).

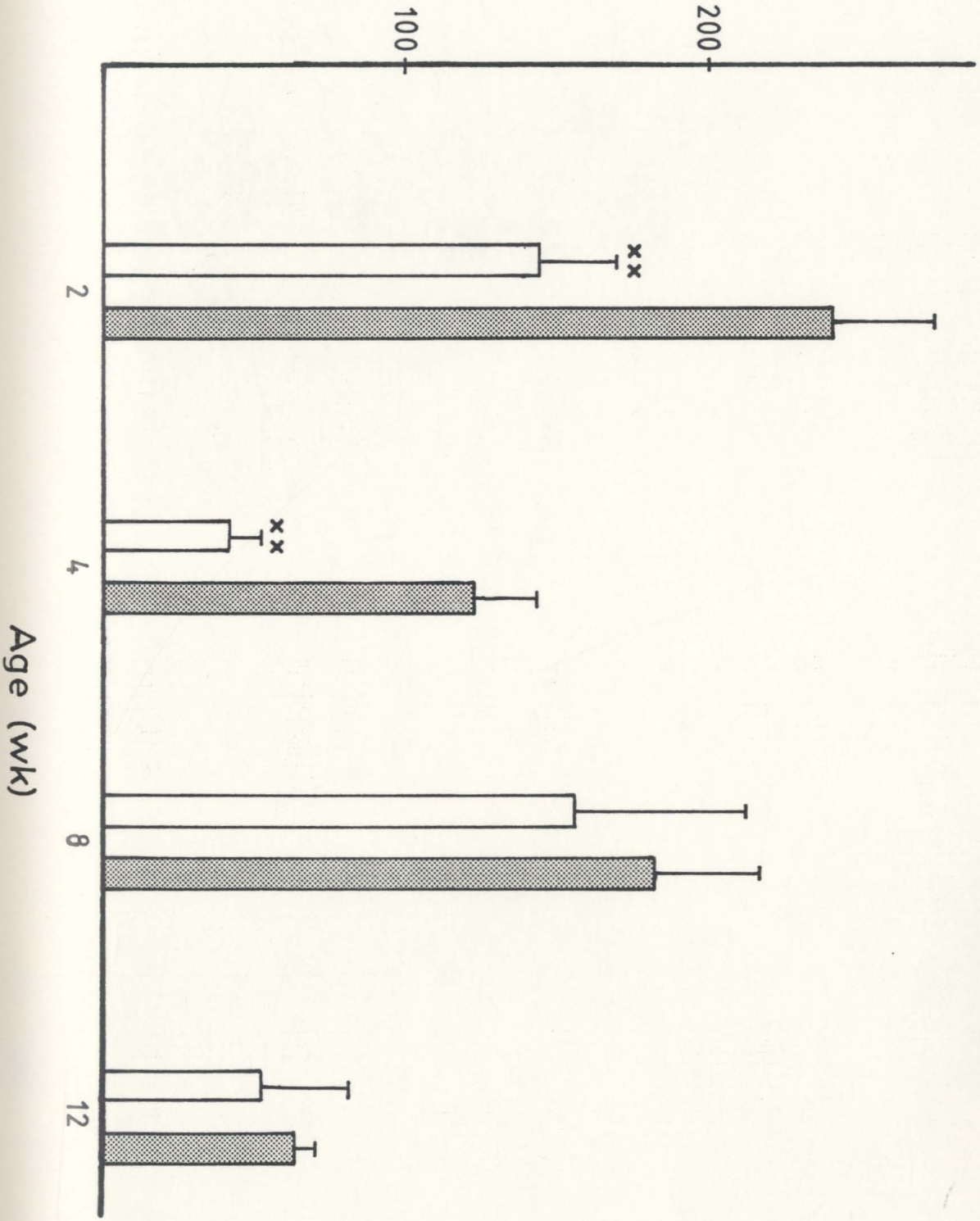
Relative Metabolic Activity
in NC
100
200
2
4
8
12
Age (wk)
xx
xx

Figure 17: Relative metabolic activity in the nucleus medialis (NM) in WKYs (white bars) and SHRs (stippled bars) at 2, 4, 8, and 12 weeks of age.

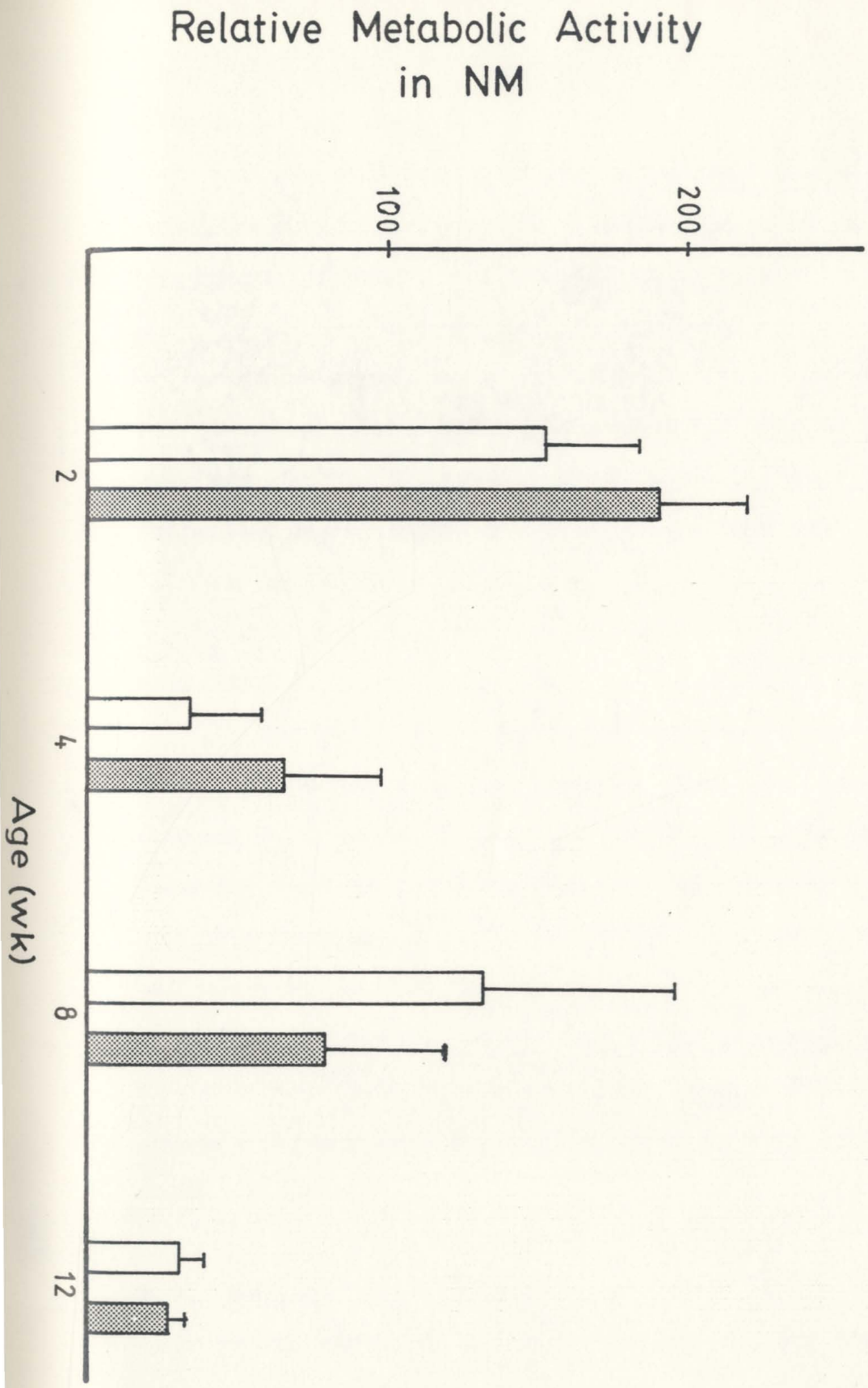
Relative Metabolic Activity
in NM
100
200
2
4
8
12
Age (wk)

uptake increased (133 ± 64) and at 12 weeks, it decreased once again (32 ± 9).

Uptake of ^{3}H-2DG into the NM of SHRs was not significantly different from that of the WKYs at any of the age groups studied (two-tailed t test).

3. Neuronal Densities

Neuronal densities were measured in the NC and NM of WKYs and SHRs at 2, 4, 8, and 12 weeks of age. Data were expressed as "n" neurons/3.6 x 10^3 μm^2 and are plotted in figures 18 and 19.

3.1. NC

In the WKYs, the density of neurons in the NC decreased as the animals matured. From 13.02 ± 0.76 neurons at 2 weeks of age, the density of neurons decreased linearly to 9.11 ± 0.95 neurons at 12 weeks of age.

The neuronal density in the NC of 2 and 4 weeks SHRs was the same as that of the WKYs at the corresponding ages. However, at 8 and 12 weeks of age the neuronal densities in the SHRs were significantly higher than in the WKYs. The density of neurons in the NC of SHRs did not change after 4 weeks of age.

3.2. NM

In the WKYs, as was the case for the NC, the neuronal density in the NM decreased as the animals matured. From

Figure 18: Density of neurons in the nucleus commissuralis (NC) in WKYs (white bars) and SHRs (stippled bars) at 2, 4, 8, and 12 weeks of age. (xxx = significant difference; $p < 0.005$, two-tailed t test).

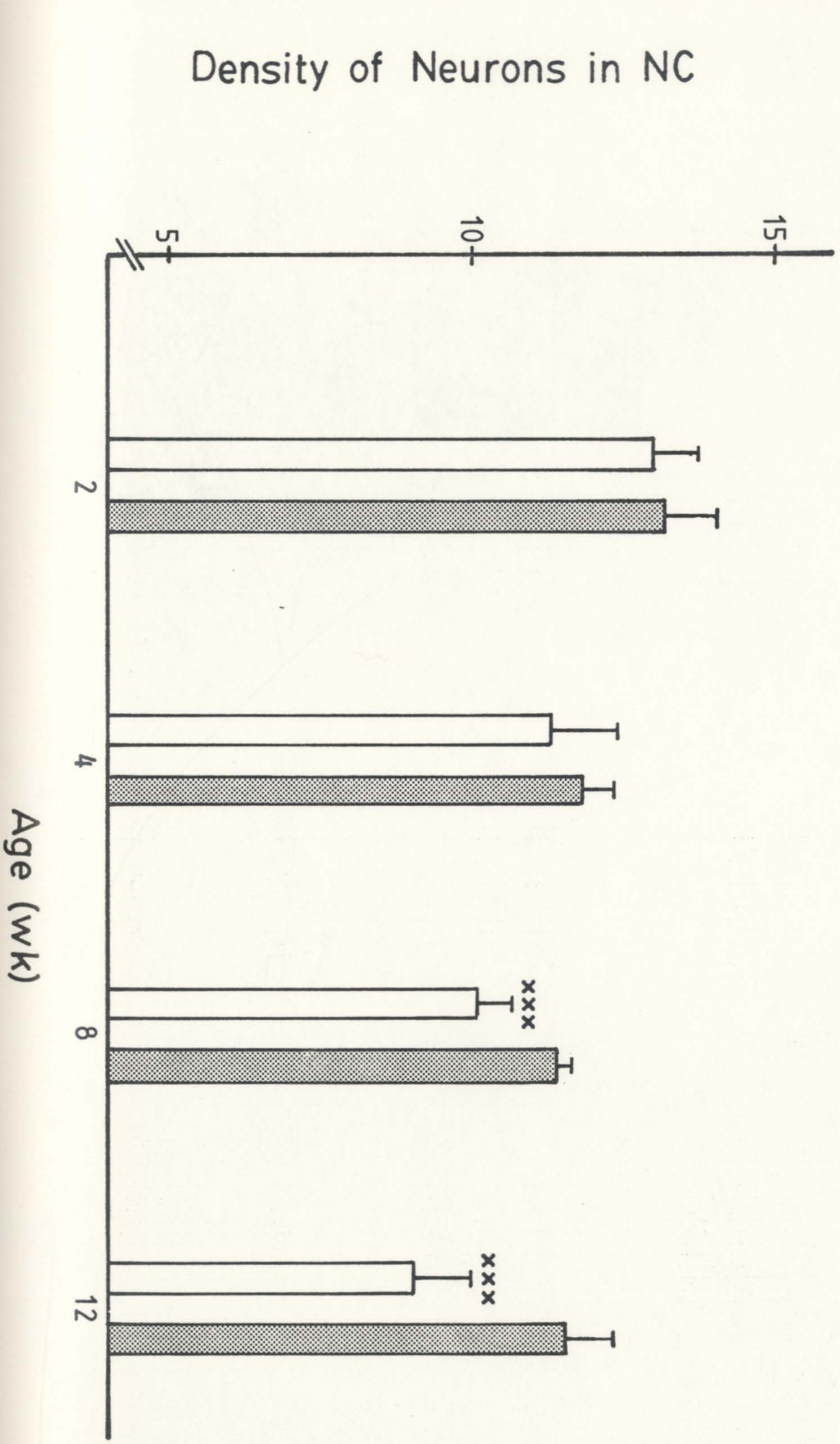
Density of Neurons in NC
5
10
15
2
4
8
12
Age (wk)
×××
×××

Figure 19: Density of neurons in the nucleus medialis (NM) in WKYs (white bars) and SHRs (stippled bars) at 2, 4, 8, and 12 weeks of age. (x, xx = significant difference; x: $p < 0.05$; xx: $p < 0.025$).

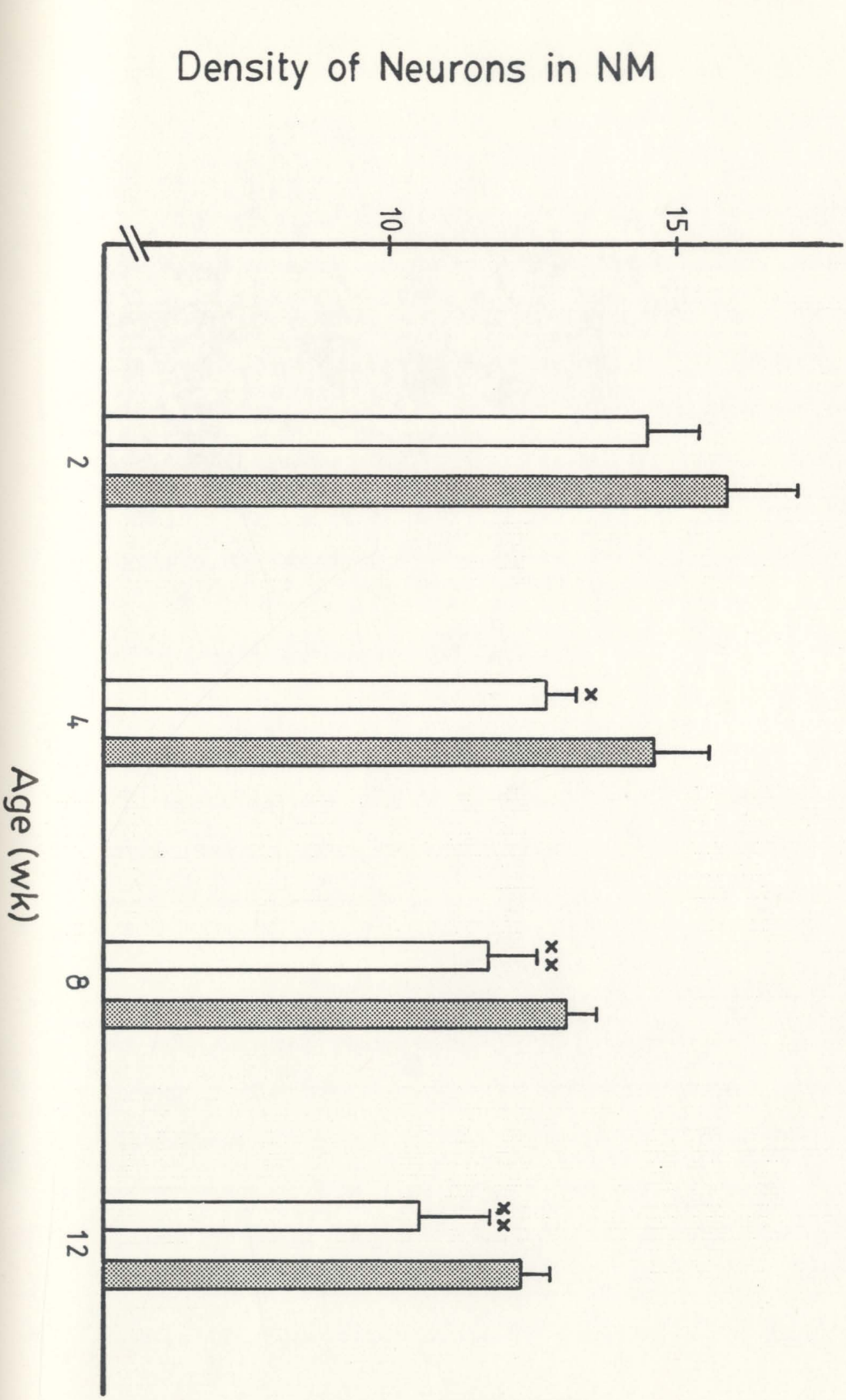
Density of Neurons in NM
10
15
2
4
8
12
Age (wk)
x
xx
xx

14.49 ± 0.77 neurons at 2 weeks of age, the neuronal density decreased to 10.54 ± 1.22 neurons at 12 weeks of age.

The density of neurons in the NM of 2 week SHRs was not significantly different from that of 2 week WKYs. At 4, 8, and 12 weeks, however, the neuronal densities in the SHRs were significantly higher than in the WKYs at the corresponding ages. As in the WKYs, the neuronal density in the NM of the SHRs decreased as the animals matured. From 15.86 ± 1.26 neurons at 2 weeks of age, the density of neurons in the SHRs decreased to 12.31 ± 0.53 neurons.

4. Blood vessel quantification

The number of exchange vessels in the NC and NM of 4 and 12 week male WKYs and SHRs was quantified. Counts for all sections are tabled in appendix 3. A photograph demonstrating the quantification of the exchange vessels is also shown in appendix 3. Grouped data are shown in table 2.

In each group of animals it was found that there was no significant difference between counts made from any level of the two subnuclei studied (Student's t test). Therefore, the data from all levels in all animals within a group were pooled ("NC and NM" column in table 2). At both 4 and 12 weeks of age, there was no significant difference between the number of exchange vessels in the WKYs and SHRs. To determine whether the number of vessels at 12

Table 2: Numbers of exchange vessels in the nucleus commissuralis (NC) and nucleus medialis (NM) of four- and twelve-week WKYs and SHRs

Age (weeks)	Strain	NC	NM	NC and NM	Total
4	WKY	28 ± 3 (n = 7)	27 ± 4 (n = 6)	27 ± 4	
	SHR	30 ± 3 (n = 8)	30 ± 5 (n = 7)	30 ± 4	29 ± 4
12	WKY	33 ± 3 (n = 8)	35 ± 4 (n = 8)	34 ± 4	
	SHR	32 ± 6 (n = 8)	33 ± 5 (n = 8)	32 ± 5	33 ± 5

weeks was different from that at 4 weeks, the data from both strains at each age were combined ("total" column in table 2). Although the number of vessels at 12 weeks (33 ± 5) tends to be greater than at 4 weeks of age (29 ± 4), the difference does not reach a level of significance (5%).

DISCUSSION

The results of this investigation have demonstrated that the metabolic requirements in the NTS subnuclei, NC and NM, are not constant in the rat between 2 and 12 weeks of age. A high level of metabolic activity was found at 2 and 8 weeks; a lower level was found at 4 and 12 weeks. The same trends of metabolic requirements were found in the spontaneously hypertensive rat (SHR); however, the relative metabolic activity in the NC of 2 and 4 week SHRs was significantly higher than in the normotensive rats. The differences in metabolic requirements in the young SHRs were not related to differences in neuronal densities or exchange vessel capacities at the ages in question. The significance of the above results will be discussed. In addition, an evaluation of the techniques used to obtain these results will be presented.

1. Route of administration of the ^{3}H-2DG

1.1. Intraperitoneal versus intravenous administration

Until recently, the i.v. route of administration of labelled 2DG was used exclusively. The restraining and cannulation procedures necessary for i.v. administration, however, restricted the use of the 2DG technique to certain types of studies. In 1980, Meibach et al. (131) conclusively demonstrated that i.p. injection of labelled 2DG yielded results identical to those after i.v.

injection. These findings were subsequently confirmed (158). Thus, conscious, unrestrained animals under normal physiological conditions could now be given a pulse of labelled 2DG without the restraints made necessary by i.v. administration.

1.2. Anesthetic effects

Most barbiturates, including pentobarbital, lower glucose and oxygen consumption in the brain (22, 73, 143, 157, 163, 202, 218). It has been demonstrated that cerebral cortical glucose utilization is depressed to a level 44% below the normal rate when cerebral pentobarbital levels exceed 50 mg/kg of tissue (42). Such an effect would likely reduce or mask possible differences which were of interest in the developmental metabolic study of the present investigation.

A control study was carried out to determine whether the 2DG has an effect on blood pressure. A blood pressure change did occur after 45 minutes, during which the rats were anesthetized with pentobarbital. Therefore a sham control study was carried out; it demonstrated that the blood pressure change occurred even in the absence of 2DG. A decrease in blood pressure during pentobarbital anesthesia has been reported in the literature (27, 73, 142, 197). Since other variables had not been introduced into these control studies, it was concluded that the observed shift in blood pressure was caused by the

pentobarbital anesthesia. Since one of the major objectives of the present study was to determine whether metabolic development in the NTS was altered during the development of hypertension, an anesthesia-induced change in blood pressure was considered to be best avoided.

1.3. Summary

Because of the ease of administration, and especially to avoid the depressant effects that anesthesia has on glucose utilization in the brain and on blood pressure, the intraperitoneal route of ^{3}H-2DG administration, where animals would be conscious and unrestrained, was used in the present study.

2. The thaw-mount technique

The thaw-mount technique employed in the present study has been widely used for ^{3}H-2DG autoradiography. Besides being less tedious than freeze-drying methods, the thaw-mount procedure ensures more even contact between the tissue section and emulsion. It has been demonstrated (122, 204) that frozen sections thaw-mounted onto emulsion-coated slides can be air-dried at room temperature without out loss of resolution quality due to movement of ^{3}H-2DG-6-phosphate during the drying process. In the present study, the drying time of the sections on the emulsion was substantially less than in previous studies using this technique and was achieved by using a small fan

which directed room air over the sections. This shorter drying time, then, gave even greater assurance that localization of the water-soluble H-2DG-6-phosphate, formed as a result of metabolic activity, would be preserved.

Two criteria were used to determine whether the ^{3}H-2DG-6-phosphate had diffused from its site of formation (63). First, edges of sections were studied to determine whether grain densities might be changed as a result of diffusion of the ^{3}H-2DG-6-phosphate out of the section. The grain density at the periphery of experimental sections was not different than that at the periphery of control sections where no isotope was present. Therefore, it was concluded that the ^{3}H-2-DG-6-phosphate had not diffused out of the sections. Second, it was found that, within the sections themselves, boundaries between areas of high and low grain densities were sharp. For example, a sharp border formed by silver grains was always seen between XII and NTS/DMN. One would not expect to find these distinct borders if diffusion of the ^{3}H-2-DG-6-phosphate had occurred since movement of this compound from an area of high concentration to one of lower concentration would obliterate the sharpness. Therefore, it was concluded that the ^{3}H-2DG-6-phosphate had not undergone diffusion within the sections.

3. Autoradiographical artifacts

Stress forces are the most commonly encountered causes of the formation of artifact silver grains in autoradiography (168). Blank control sections, in which no isotope was present, were used in the present study to assess the influence of these and other factors on the autoradiograms. In general, artifact grains were present along edges of the sections where the tissue would undergo the greatest stress during the drying process (eg. along the periphery of the sections, in tears formed during sectioning, and in the central canal when it was present). Artifact grains also formed where adhesion was poor, areas where, presumably, stress forces would also be high.

In the blank controls, four sections were mounted on each slide. It was consistently found that the highest density of artifact grains was found in the two sections which were mounted first and thus would have had their drying stream of air interrupted two or three times as new sections were mounted on the same slide. The section with least silver grains was the section which was mounted last and would thus have had no interruptions in its drying process. That is, of the four sections, the one mounted last would have had the shortest drying time. Artifact grains in the latter section were limited only to edges and tears in the section. Therefore, in order to minimize the formation of artifact silver grains in the subsequent

experimental slides and to restrict them to areas which were not of interest in the present study (ie. edges and tears), no more than one section was mounted per slide. This procedure ensured the shortest drying time for that section.

4. General metabolic requirements

4.4.1. Cellular localization

Cellular localization of ^{3}H-2DG-6-phosphate in neurons was not observed to occur in the present study. This finding is in agreement with the information in the literature which suggests that such localization would not be expected to occur when specific external stimulation is not applied. For example, it has been estimated that nearly half of the brain's energy requirement is used for the maintenance and restoration of ionic gradients and membrane potentials in neuronal processes (219), and that therefore, electrical activity is the physical process which is most involved with functional activity (201, 223). It has also been suggested that alterations in the metabolic activity of synaptic terminals are responsible for the changes in brain glucose utilization which occur in response to altered functional activity (60, 184-186, 201, 220). In addition, the contribution of glial tissue should not be excluded from the consideration of energy requirements by nervous tissue. Glial cells are known to be involved in such energy-dependent functions as the

synthesis and transport of proteins into axons (71, 117) and the accumulation of extracellular potassium that is released during neural activity (81, 86).

Differential labelling of neuronal perikarya has been demonstrated after intense external stimulation. Bassinger et al. (13) demonstrated label over bipolar neurons in the goldfish retina after a stimulus of flashing lights. Also using the visual system, Wagner et al. (211) demonstrated cellular localization of ^{3}H-2DG over the neurons of specific layers of the cat visual cortex after intense visual stimulation.

The above studies suggest that in the normal state of functional maintenance in the brain, glucose uptake is as active in the neuropil as in the neuronal perikarya. In special systems such as the visual system, and under specific stimulation, however, it appears that the glucose requirements of neuronal perikarya may exceed that of the surrounding neuropil.

Recently, Pilgrim & Wagner (158) demonstrated cellular localization of silver grains over neurons from unstimulated brain using the thaw-mount technique. They were unable to find localization from the same type of tissue which had been resin-embedded. Whether the cellular localization seen is a result of true ^{3}H-2DG-6-phosphate localization or is merely artifact is questionable. In the unlabelled controls of the present study described previously, artifact grains were formed over larger

neuronal perikarya (eg. XII) when the drying time was extended. These neurons, therefore, appear to be susceptible to the stress forces which cause artifact grains to be formed. It is possible, therefore, that the cellular localization described by Pilgrim & Wagner (158) is, in fact, the accumulation of artifact grains due to stress forces. Presumably, their technique of thaw-mounting and refreezing of sections would generate considerable stress forces in the tissue. In support of this is their finding that the "2DG-accumulating cells" were found predominantly in periventricular areas (ie. along edges), the same types of areas which demonstrated the greatest number of artifact grains in the control sections of the present study. In addition, in resin-embedded sections, where stress forces are at a minimum, cellular localization of silver grains was not found.

4.2. Fibre tracts

Some fibre tracts, in particular the rootlets of XII and the internal arcuate fibres, demonstrated clear uptake of ^{3}H-2DG in the present study. That this localization was not autoradiographic artifact was proven with the unlabelled control sections in which accumulation of artifact silver grains over fibre tracts was never seen. Uptake of ^{3}H-2DG into fibre tracts of nervous tissue has not been addressed to any extent in the literature.

However, it has been reported (58) that such uptake is localized primarily over the myelin sheath and not over the axon proper. This finding once again suggests, as was stated previously, that the energy requirements of glial tissue should not be overlooked.

4.3. NTS versus other areas

The uptake of ^{3}H-2DG into the NTS and DMN was consistently lower (to varying extents) than into surrounding areas such as XII. Several reports in the literature have demonstrated the same pattern of relative uptake into the NTS. For example, using ^{14}C-2DG, Singer & Mehler (194) showed autoradiograms which clearly demonstrate a lower density of silver grains in the NTS relative to XII. The same phenomenon has been demonstrated with ^{3}H-2DG (63). In a series of studies by Savaki et al. (179-180), the uptake of ^{14}C-2DG into the NTS was slightly less than or equal to the uptake into adjacent areas. Only one study has reported a greater uptake of ^{14}C-2DG into NTS than into the adjacent XII (84). Data were expressed as rates of glucose utilization, but no autoradiograms were shown from which direct conclusions about relative ^{14}C-2DG uptake could be made.

Therefore, the present study is in agreement with most of the previous studies which suggest that the metabolic requirements of the NTS are lower than or equal to those of adjacent areas.

4.4. Ontogeny of metabolic requirements in the rat brainstem

Metabolic development in the brainstem had not been studied with the H-2DG technique prior to the present investigation. In general, the pattern of ^{3}H-2DG uptake into the brainstem at the levels studied did not change after 8 weeks. Uptake appeared to be more localized into specific nuclei and fibre tracts than in younger animals. The uptake of ^{3}H-2DG into the brainstems of 4 week animals differed from the older animals only in the localization of ^{3}H-2DG in fibre tracts. Although this localization was present, it was not as prominent in the 4 week animals as in the older animals. The uptake of ^{3}H-2DG into the brainstems of 2 week animals was more uniform than in older animals; specific nuclei and fibre tracts were not delineated by silver grains.

The differences in ^{3}H-2DG uptake which occurred as the rats matured suggests that energy requirements in the brainstem change as development occurs. For example, myelination in the rat is not complete until after 3 to 4 weeks (161, 164). The lack of ^{3}H-2DG uptake into fibre tracts at 2 weeks and the beginning of this phenomenon at 4 weeks found in the present study lends support to the suggestion that myelin sheaths have greater energy demands than the axons which they surround (58). In addition, the more uniform uptake of ^{3}H-2DG into the brainstems of the 2

week rats may suggest that a high proportion of the total energy requirement at this phase in development is used in the processes of growth of the brainstem. In the older animals where maturation is near or at completion, on the other hand, the greater proportion of the energy requirement may be used for functional purposes as is suggested by the more localized uptake of ^{3}H-2DG into nuclei and fibre tracts.

5. Metabolic development in the NC and NM

5.1. The use of the hypoglossal nucleus as an internal standard

Inherent to the technique of autoradiography are variations such as differences in emulsion thickness, development time, etc., which, if not corrected for, can introduce error when quantification of silver grains is required. In order to eliminate this error from the present investigation, an internal standard for each section was used against which the grain counts from the NC and NM of the NTS were corrected.

The hypoglossal nucleus was chosen as the internal standard for four reasons. First, this nucleus is not likely to be involved in cardiovascular control. Thus, changes in blood pressure, either in the WKYs or the SHRs, would not be expected to have any effect on the uptake of ^{3}H-2DG into the hypoglossal nucleus. Second, since the hypoglosal nucleus is located very near to the NTS,

conditions of autoradiography would likely be very similar for the two nuclei, in contrast to a nucleus located near the edge of the section, for instance, where stress forces would be different from those near the centre. Third, the hypoglossal nucleus is present at all levels of the NTS which were of interest in the present study. Finally, it has been shown (84) that the metabolic activity in the hypoglossal nucleus of 4 week WKYs is the same as that in SHRs of the same age. Thus, after consideration of the above factors, the hypoglossal nucleus was deemed to be the best choice for an internal standard.

There is one disadvantage in using an internal standard from the developing brainstem: one cannot be certain that the metabolic requirements of the internal standard remain in a steady state throughout the entire period under study. Thus an alteration in the metabolic activity of the standard could be a possible source of error in the final interpretation of results.

5.2. Relative metabolic activity

Developmentally, the relative metabolic activity in the NC and NM followed the same trends in the WKYs and SHRs. A decrease from 2 to 4 weeks was followed by an increase at 8 weeks and a decrease at 12 weeks. The two phases of metabolic activity in the NC and NM (2 and 4 weeks versus 8 and 12 weeks) may, as was suggested earlier, reflect different energy requirements in the brain stem as

development occurs. The first phase may result from decreasing requirements which may occur as developmental changes occur less frequently. The second phase, where development is virtually complete, may more closely represent functional metabolic requirements in the NC and NM. The reason for the increase in energy requirements which occurred between 4 and 8 weeks of age in both strains is not clear but may, as was pointed out in the previous section, be a reflection of an altered state of metabolic activity in the internal standard. It is possible that the weaning process which occurred just after 4 weeks of age had an effect on the metabolic activity of XII between 4 and 8 weeks of age. Such a change could then be partly responsible for the apparent increase in metabolic activity within the NC and NM between 4 and 8 weeks of age.

The NTS, in particular the subnuclei NC and NM, plays an inhibitory role in the regulation of blood pressure; in the rat, electrical stimulation in the caudal two-thirds of the NTS results in hypotension and lesions result in hypertension (31, 165). Thus, it might have been anticipated that an increase in blood pressure such as that which occurs between 8 and 12 weeks of age would result in an increased rate of glucose utilization in the NTS. However, since the energy demands of neuronal excitation and inhibition are not well defined at the present time, alteration in glucose utilization during an increase in blood pressure should not be assigned to a particular

energy-requiring process "a priori". It has been suggested (179) that the increase in glucose utilization which occurs during hypotension may reflect decreased inhibitory input from the baroreceptors and consequent increased activity of disinhibited neurons. Again, the corroboration of this suggestion must await resolution of energy requirements which result from inhibition and excitation.

6. Neuronal densities in the NC and NM

The neuronal densities in the NC and NM of WKYs and SHRs were quantified. In general, the density of neurons in the NM was found to be higher than in the NC in both strains at all ages studied.

The neuronal densities in the NC and NM of WKYs decreased linearly as the rats matured from 2 to 12 weeks of age. Neurons do not divide after they have been formed during embryonic development (192). Therefore, the apparent decrease in density which occurred as age increased was not unexpected since the same (or smaller) number of neurons would be present in an ever-increasing volume of nervous tissue as the size of the brain increased with development.

In the SHRs, the neuronal densities in both the NC and NM differed developmentally from those in the WKYs. In the case of the NC the neuronal densities decreased from 2 to 4 weeks of age and were not significantly different from those of the NC in the WKYs at the corresponding ages.

Whereas the density of neurons in the WKYs continued to decrease with age, the density in the NC of SHRs remained unchanged from 4 to 12 weeks of age. Thus, the neuronal densities in the NC of SHRs at 8 and 12 weeks of age were significantly higher than those in the WKYs.

The neuronal density in the NM of the SHRs decreased with development in the same way as in the WKYs. However, at 4, 8, and 12 weeks, the densities of neurons in the SHRs were significantly higher than those in the WKYs.

It has recently been shown that the brains of WKYs are larger than the brains of SHRs at 12 weeks (141) and at 8 months of age (120). In the former study entire brains rostral to the medullospinal junction were measured; it was found that the SHR brain volume and brain weight were 11.8% and 10.6% below that of the WKY brain. In the latter study, measurements in millimeters were made in different dimensions at various locations on the surface of 8-month-old WKY and SHR brains. The authors concluded that SHRs have smaller mesencephalons and diencephalons than WKYs, but larger metencephalons. However, a closer look at the results reveals that the metencephalon of the SHRs was larger than that of the WKYs only in a ventro-dorsal direction at the mid-pons level. In addition, the measurement included the cerebellum. Thus the results of Lehr et al. (120) disclose nothing about the size of the more caudal brainstem of SHRs relative to WKYs.

A general decrease in the size of the SHR brain could

explain the differences seen in the neuronal densities of NMs in WKYs and SHRs. That is, if the absolute number of neurons in this area is not different in WKYs and SHRs, the relative decrease in volume available for the same number of neurons in the SHR would cause the neuronal densities to be higher in these animals. The lack of a significant difference in the neuronal density of the very young animals (2 weeks of age) may imply that differences in brain size between WKYs and SHRs do not begin to appear until a later point in development (4 weeks of age or older).

The same explanation may apply in part to the NC of WKYs and SHRs. That is, the difference in brain size of the SHRs may again explain the significant differences in the neuronal densities between the NC of the WKYs and SHRs at 8 and 12 weeks of age. However, since the density of neurons in the NC of the SHRs did not decrease with development as would be expected as brain size increased, other factors may be involved. There are numerous examples in the literature which demonstrate a correlation between morphometric changes in the CNS and functional activity of specific brain areas (15, 16, 82, 136, 139, 141, 156). These changes include densities of cells, somal cross-sectional areas, nucleoli numbers, and dendritic orientation. Therefore it is possible that the observed differences in the neuronal densities of the NCs between SHRs and WKYs at 8 and 12 weeks of age may underlie or

result from the cardiovascular abnormalities associated with spontaneous hypertension in rats.

7. Exchange vessels in the NC and NM

The technique for quantifying exchange vessels in the present study has previously been employed to study capillary numbers in central nervous tissue (113) and myocardium (147). In the present study, the number of exchange vessels within 5.4×10^4 μm^2 was counted in the NC and NM of 4 and 12 week WKYs and SHRs. It was found that there was no difference in exchange vessel density in the NC and NM in animals within a group, between strains, or between the two age groups.

Since no difference in exchange vessel density was found between 4 and 12 week rats within either strain it appears that the adult level of maximum exchange capacity in the NC and NM of the NTS in WKYs and SHRs is reached by 4 weeks of age. Developmentally, the nervous system of a 4 week rat is similar to that of a 12 week rat except for relative numbers of specific components (96). Therefore the finding of a similar density of exchange vessels at these ages is not unexpected.

Exchange vessel density in the NC and NM was not significantly different between normotensive and hypertensive rats at either 4 or 12 weeks. This finding is in agreement with a previous study (113) in which no difference was found in the capillary density between

3-month WKY and SHR cerebral cortex. These findings suggest that the state of elevated blood pressure in SHRs does not cause exchange vessel density in the brain to increase or decrease.

8. General discussion

In the NC, but not in the NM, the relative metabolic activity of 2 and 4 week SHRs was found to be significantly higher than that in the normotensive WKYs. In the older animals (8 and 12 week) no difference was found between the relative metabolic activity in the NC (or NM) of WKYs and SHRs. It is possible that the differences which were found between the NC of young WKYs and SHRs were also present in the NM but were not distinguishable using the method of ^{3}H-2DG quantification which was used for that subnucleus. In contrast to the NC, where a larger area was studied and representative counts were made, all of the silver grains within a much smaller area of the NM were counted. Because of the smaller area of the NM and the resulting smaller counts, final results were more greatly affected by variations in counts. Thus the standard deviations in the NM counts were greater than in the NC counts and real differences in the metabolic activity of the NM between young WKYs and SHRs may have been hidden.

To date, only one other study has addressed the question of differences in glucose utilization in SHR brains compared to WKY controls (86). As in the present

study, Hiyashi and Nakamura (86) found that 2DG uptake into the NC of 4 weeks SHRs was significantly higher than in WKYs; in the more rostral NTS, no difference was found. The same findings were made in 20 week rats. The latter finding suggests a descrepancy with the results obtained for the older animals in the present study. However, a careful analysis of the paper by Hiyashi & Nakamura (84) suggests that the results which they reported must be questioned. For example, because of the lack of histological verification it was not possible to assess which part of the NC was studied. In addition, in the large number of structures studied in their investigation glucose utilization was found to be unchanged or of an increased magnitude. One must question why no structures demonstrated a decrease in glucose utilization, a phenomenon which would be expected in at least a small number of areas studied and which would be due to increased inhibition of those areas. Finally, the complete lack of autoradiograms in the publication make any kind of visual assessment of ^{14}C-2DG uptake into the nervous tissue impossible.

It is important to consider the possible cause(s) of the differences in metabolic rates in the NC of young WKYs and SHRs. Since the cell densities in the NC of 2 and 4 week WKYs and SHRs were found to be the same, the different energy requirements in the NC of the two strains cannot be explained by greater energy demands of a higher density of

cells. In the same way, since the maximum exchange vessel capacity was found to be the same in the NC of 4 week WKYs and SHRs, the different rates of metabolic activity cannot be explained by an altered capacity of blood supply in the SHRs.

If the first phase of metabolic activity found in the present study (2 to 4 weeks) does reflect developmental metabolic needs, as was suggested earlier, the difference in relative metabolic activity found in the young rats may indicate a developmental defect in the NC of SHRs. Such a defect could conceivably play an important role in the subsequent development of hypertension in SHRs. For example, it has been found that the NC is the area of the NTS which contains axo-axonic contacts, the sites where regulation of baroreceptor reflexes are thought to occur through presynaptic inhibition (33). Developmental alterations in the numbers or structure of these contacts might trigger or allow the development of hypertension in SHRs.

If developmental metabolic requirements are not responsible for the differences in metabolic activity in young SHRs, different rates of functional activities (eg. transmission, maintenance, etc.) must be considered. Since the relative rates of metabolism in the NTS of SHRs were no longer different at 8 and 12 weeks of age, the differences in functional activities which may be present in the 2 and 4 weeks SHRs must no longer be present from 8 weeks

onwards.

Both of the above arguments lend support to the neurogenic hypothesis for the development of spontaneous hypertension (98-100, 222). According to the hypothesis, increases in blood pressure in SHRs occur because of increased vasomotor tone in young SHRs at the initial stage of hypertension. The altered tone is hypothesized to be caused by an abnormality which exists somewhere within the central nervous system and which triggers the development of hypertension but which may no longer be present in the established phase of hypertension. The increased neural tone may then enhance the metabolism of noncollagenous protein. This increase leads to medial hypertrophy in the vasculature. The hypertension itself enhances collagenous protein metabolism so that changes in the vasculature finally increase the nonneural component of peripheral vascular resistance and maintain the blood pressure in its elevated state. That the hypothesized abnormality exists in the NC of the NTS of SHRs cannot be concluded from the present study. However, regardless of the exact location or nature of the abnormality, it can be concluded that it is, at the very least, expressed in the NC by virtue of the extensive connections between the NC and other CNS structures which are involved in the regulation of blood pressure.

SUMMARY AND CONCLUSIONS

1. The ontogeny of metabolic requirements was studied in two subnuclei of the rat NTS, the nucleus commissuralis (NC) and nucleus medialis (NM), using the ^{3}H-2-deoxy-D-glucose (^{3}H-2DG) technique whereby the uptake of ^{3}H-2DG was quantified with autoradiography. The metabolic activity in the NC and NM was not constant between 2 and 12 weeks of age. A high level of metabolic activity at 2 and 8 weeks and a lower level of activity at 4 and 12 weeks were found. The two phases of metabolic requirements suggest that energy requirements in the NC and NM change as development occurs.

2. The ontogeny of metabolic requirements in the NC and NM was studied in the SHR to determine whether energy requirements in these subnuclei were altered during the development of hypertension. The same trends of metabolic requirements seen in the normotensive rats were found in the SHRs; however the relative metabolic activity in the NC of 2 and 4 week SHRs was significantly higher than in the normotensive WKYs.

3. The differences in metabolic requirements in the young SHRs were not related to differences in neuronal densities or exchange vessel capacities. These findings suggest that a deviation from the normal, either developmental or functional, occurs in the brains of young, prehypertensive SHRs. This alteration may serve to trigger

the onset of hypertension development but may not necessarily be present to maintain the conditions in older animals.

4. In both WKYs and SHRs, ^{3}H-2DG uptake was more generalized in the brainstems of 2 week animals than in older animals. At 4 weeks and older, uptake of ^{3}H-2DG was more localized, once again suggesting that energy requirements in the brainstem change as development occurs. A higher proportion of the total energy requirements in the brainstems of very young rats may be used in the processes of growth, whereas in the older rats, a higher proportion may be used for functional purposes.

5. Developmentally, no difference was found in exchange vessel densities in NC and NM between 4- and 12-week-old rats, between the NC and NM at either age, or between WKYs and SHRs.

6. A quantification of neuronal densities in the NC and NM of WKYs and SHRs revealed that the density of neurons in the NM is generally higher than in the NC. As expected, the densities in the WKYs decreased linearly as the rats matured. The same finding was made in the NM of SHRs but not in the NC where the neuronal density did not decrease. This difference may underlie or result from the cardiovascular abnormalities associated with spontaneous hypertension in rats.

References

1. Aars, H.; Myhre, L.; Haswell, B.A. (1978). The function of baroreceptor C-fibres in the rabbit's aortic nerve. Acta Physiol. Scand. 102: 84-

2. Albus, K. (1979). ^{14}C-deoxyglucose mapping of orientation subunits in the cat's visual cortical areas. Exp. Brain Res. 37: 190-194

3. Alexander, G.M.; Schwartzman, R.J.; Bell, J.Y.; Renthal, A. (1981). Quantitative measurement of local cerebral metabolic rate for glucose utilizing 2-deoxyglucose. Brain Res. 223: 59-67

4. Alexander, L. & Putman, T.J. (1938). Pathological alterations of cerebral vascular patterns. I. Introduction, with discussion of the technique. Assoc. Res. Nerv. Dis. 18: 471-543

5. Allen, T.O.; Adler, N.T.; Greenberg, J.H.; Reivich, M. (1981). Vaginocervical stimulation selectively increases metabolic activity in the rat brain. Science 211: 1070-1072

6. Allen, W.F. (1923). Origin and distribution of the tractus solitarius in the guinea pig. J. Comp. Neurol. 35: 171-204

7. Altman, J. & Bayer, S.A. (1980). Development of the brainstem in the rat. I. Thymidine-radiographic study of the time of origin of neurons of the lower medulla. J. Comp. Neurol. 194: 1-35

8. Angell-James, J.E. & Daly, M. deB. (1970). Comparison of the reflex vasomotor responses to separate and combined stimulation of the carotid sinus and aortic arch baroreceptors by pulsatile and non-pulsatile pressures in the dog. J. Physiol. 209: 257-293

9. Arndt, J.O.; Dorrenhaus, A.; Wiechen, H. (1975). The aortic arch baroreceptor response to static and dynamic stretches in an isolated aorta-depressor nerve preparation of cats "in vitro". J. Physiol. 252: 559-578

10. Astic, L. & Saucier, D. (1981). Ontogenesis of the functional activity of rat olfactory bulb: autoradiographic study with the 2-deoxyglucose method. Dev. Brain Res. 2: 243-256

11. Astrom, K.E. (1953). On the central course of afferent fibres in the trigeminal, facial, glossopharyngeal, and vagus nerves and their nuclei in the mouse. Acta Physiol. Scand., suppl. 106: 209-224

12. Basbaum, A.I.; Clanton, C.H.; Fields, H.L. (1978). Three bulbospinal pathways from the rostral medulla of the cat: an autoradiographic study of pain modulating systems. J. Comp. Neurol. 178: 209-224

13. Bassinger, S.F.; Gordon, W.C.; Lam, D.M.K. (1979). Differential labelling of retinal neurons by ^{3}H-2-deoxyglucose. Nature 280: 682-684

14. Beckstead, R.M. & Norgren, R. (1979). An autoradiographic examination of the central distribution of the trigeminal, glossopharyngeal, and vagal nerves in the monkey. J. Comp. Neurol. 184: 455-472

15. Bereiter, D.A. & Jeanrenaud, B. (1979). Altered neuroanatomical organization in the central nervous system of the genetically obese (ob/ob) mouse. Brain Res. 165: 249-260

16. Bereiter, D.A. & Jeanrenaud, B. (1980). Altered dendritic orientation of hypothalamic neurons from genetically obese (ob/ob) mice. Brain Res. 202: 201-206

17. Betz, A.L. & Gilboe, D.D. (1974). Kinetics of cerebral glucose transport "in vivo": inhibition by 3-o-methylglucose. Brain Res. 65: 368-372

18. Biscoe, T.J. & Sampson, S.R. (1970). Field potentials evoked in the brainstem of the cat by stimulation of the carotid sinus, glossopharyngeal, aortic and superior laryngeal nerves. J. Physiol. 209: 341-358

19. Blessing, W.W.; Goodchild, A.K.; Dampney, R.A.L.; Chalmers, J.P. (1981). Cell groups in the lower brainstem of the rabbit projecting to the spinal cord with special reference to catecholamine-containing neurons. Brain Res. 221: 35-55

20. Bolter, C.P. & Ledsome, J.R. (1980). Influence of cervical sympathetic nerve stimulation on carotid sinus baroreceptor afferents. Experientia 36: 1301-1302

21. Bolwig, T.G.; Rafaelsen, O.J.; Hertz, M.M.; Paulson, O.B.; Spotoft, H. (1977). The permeability of the blood-brain barrier during electrically induced seizures in man. Eur. J. Clin. Invest. 7: 87-93

22. Bolwig, T.G.; Hertz, M.M.; Holm-Jensen, J. (1977). Blood-brain barrier permeability during electroshock seizures in the rat. Eur. J. Clin. Invest. 7: 95-100

23. Brodal, A.; Szabo, T.; Torvik, A. (1956). Corticofugal fibres to sensory trigeminal nuclei of the solitary tract. An experimental study in the cat. J. Comp. Neurol. 106: 527-556

24. Buschiazzo, P.M.; Terrell, E.B.; Regen, D.M. (1970). Sugar transport across the blood-brain barrier. Am. J. Physiol. 219: 1505-1513

25. Calaresu, F.R. & Henry, J.R. (1970). The mechanism of the cardioacceleration elicited by electrical stimulation of the parahypoglossal area in the cat. J. Physiol. 210: 107-120

26. Carey, R.M.; Dacey, R.G.; Jane, J.A.; Winn, H.R.; Ayers, C.R.; Tyson, G.W. (1979). Production of sustained hypertension by lesions in the nucleus tractus solitarius of the American foxhound. Hypertension 1: 246-254

27. Carvalho, J.S. & Cherkes, J.K. (1982). Renin release by pentobarbital anesthesia in the rat: a role for vascular mechanisms. Life Sci. 30: 887-897

28. Cedarbaum, J.M. & Aghajanian, G.K. (1978). Afferent projections to the rat locus coeruleus as determined by a retrograde tracing technique. J. Comp. Neurol. 178: 1-16

29. Chai, C.Y. & Wang, S.C. (1962). Localization of central cardiovascular control mechanisms in lower brainstem of the cat. Am. J. Physiol. 202: 25-30

30. Chalmers, J.P. (1975). Brain amines and models of experimental hypertension. Circ. Res. 36: 469-480

31. Chalmers, J.P.; Blessing, W.W.; West, M.J.; Howe, P.R.C.; Costa, M.; Furness, J.B. (1981). Importance of new catecholamine pathways in control of blood pressure. Clin. Exp. Hypertension 3: 393-416

32. Chiba, T. & Doba, N. (1975). The synaptic structure of catecholaminergic varicosities in the dorsomedial portion of the nucleus tractus solitarius of the cat: possible roles in the regulation of cardiovacular reflexes. Brain Res. 84: 31-46

33. Chiba, T. & Doba, N. (1976). Catecholaminergic axo-axonic synapses in the nucleus tractus solitarius (pars commissuralis) of the cat: possible relation to presynaptic regulation of baroreceptor reflexes. Brain Res. 102: 255-265

34. Chiba, T. & Kato, M. (1978). Synaptic structures and quantification of catecholaminergic axons in the

nucleus tractus solitarius of the rat: possible modulatory roles of catecholamines in baroreceptor reflexes. Brain Res. 151: 323-338

35. Chu, N.-S. & Bloom, F.E. (1974). The catecholamine-containing neurons in the cat dorsolateral pontine tegmentum: distribution of the cell bodies and some axonal projections. Brain Res. 66: 1-22

36. Ciriello, J. & Calaresu, F.R. (1980a). Autoradiographic study of ascending projections from cardiovascular sites in the nucleus tractus solitarii in the cat. Brain Res. 186: 448-453

37. Ciriello, J. & Calaresu, F.R. (1980b). Monosynaptic pathway from cardiovascular neurons in the nucleus tractus solitarii to the paraventricular nucleus in the cat. Brain Res. 193: 529-533

38. Coleridge, H.M.; Coleridge, J.C.G.; Howe, A. (1967). A search for pulmonary arterial chemoreceptors in the cat, with a comparison of the blood supply of the aortic bodies in the new-born and the adult animal. J. Physiol. 191: 353-374

39. Coleridge, H.M.; Coleridge, J.C.G.; Howe, A. (1970). Thoracic chemoreceptors in the dog: a histological and electrophysiological study of the location, innervation and blood supply of the aortic bodies. Circ. Res. 26: 235-247

40. Cottle, M.K.W. (1964). Degeneration studies of primary afferents of the IXth and Xth cranial nerves in the cat. J. Comp. Neurol. 122: 329-345

41. Cottle, M.K.W. & Calaresu, F.R. (1980). Some terminal regions of secondary visceral afferents. Can. J. Physiol. 4: 173

42. Crane, P.D.; Braun, L.D.; Cornford, E.M.; Cremer, J. E.; Glass, J.M.; Oldendorf, W.H. (1978). Dose dependent reduction of glucose utilization by pentobarbital in rat brain. Stroke 9: 12-18

43. Crawley, J.N.; Maas, J.W.; Roth, R.H. (1980). Evidence against specificity of electrical stimulation of the nucleus locus coeruleus in activating the sympathetic nervous system in the rat. Brain Res. 183: 301-311

44. Crone, C. (1960). The diffusion of some organic non-electrolytes from blood to brain tissue. Acta Physiol. Scand. 50 (suppl. 175): 33-34

45. Crone, C. (1965). Facilitated transfer of glucose

from blood into brain tissue. J. Physiol. 181: 103-113

46. Crone, C. & Thompson, A.M. (1973). Comparative studies of capillary permeability in brain and muscle. Acta Physiol. Scand. 87: 252-260

47. Czachurski, J.; Lackner, K.J.; Ockert, D.; Seller, H. (1982). Localization of neurons with baroreceptor input in the medial solitary nucleus by means of intracellular application of HRP in the cat. Neurosci. Lett. 28: 133-137

48. Dahlstrom, A. & Fuxe, K. (1965). Evidence for the existence of monoamine neurons in the central nervous system. II. Experimentally induced changes in the intraneuronal amine levels of bulbospinal neuron systems. Acta Physiol. Scand. 64 (suppl 247): 1-36

49. Daly, M. de B.; Hazzeldine, J.L.; Howe, A. (1965). Reflex respiratory and peripheral vascular responses to stimulation of the isolated perfused aortic arch chemoreceptors in the dog. J. Physiol. 177: 300-322

50. Daly, M. de B. & Unger, A. (1966). Comparison of the reflex respoonses elicited by stimulation of separately perfused carotid and aortic body chemo-receptors in the dog. J. Physiol. 182: 379-403

51. Dampney, R.A.L. (1981). Brainstem mechanisms in the control of arterial pressure. Clin. Exp. Hyper-tension 3: 379-391

52. Dampney, R.A.L.; Kumada, M.; Reis, D.J. (1979). Central neural mechanisms of the cerebral ischemic response. Circ. Res. 45: 48-62

53. Dampney, R.A.L. & Moon, E.A. (1980). Role of ventro-lateral medulla in vasomotor response to cerebral ischemia. Am. J. Physiol. 239: H349-H358

54. DeJong, W. & Palkovits, M. (1976). Hypertension after localized transection of brain stem fibres. Life Sci. 18: 61-64

55. DeJong, W.; Wijkamp, F.P.; Bohus, B. (1975). Role of noradrenaline and serotonin in the central control of blood pressure in normotensive and spontaneously hypertensive rats. Arch. Int. Pharmacodyn. 213: 272-284

56. DeJong, W.; Zandberg, P.; Palkovits, M.; Bohus, B. (1977). Acute and chronic hypertension after lesions and transections in the rat brain stem.

Prog. Brain Res. 47: 189-197

57. Des Rosiers, M.H. & Descarries, L. (1978). Adaptation de la methode au desoxyglucose a l'echelle cellulaire: Preparation histologique du systeme nerveux central en vue de la radioautographie a haute resolution. C.R. Acad. Aci. (D) (Paris) 287: 153-156

58. Des Rosiers, M.H. & Descarries, L. (1979). In: Ninety-Second Session of the American Assoc. of Anatomists

59. Des Rosiers, M.H.; Sakurada, O.; Jehle, J.; Shinohara, M.; Kennedy, C.; Sokoloff, L. (1978). Functional plasticity in the immature striate cortex of the monkey shown by the ^{14}C-deoxyglucose method. Science 260: 447-449

60. Diamond, I. & Fishman, R.A. (1973). High-affinity transport and phosphorylation of 2-deoxy-D-glucose in synaptosomes. J. Neurochem. 20: 1533-1542

61. Diamond, J. & Howe, A. (1956). Chemoreceptor activity in the aortic bodies of the cat. J. Physiol. 134: 319-326

62. Doba, N. & Reis, D.J. (1976). Acute fulminating neurogenic hypertension produced by brainstem lesions in the cat. Circ. Res. 32: 584-593

63. Durham, D.; Woolsey, T.A.; Kruger, L. (1981). Cellular localization of 2-^{3}H-deoxy-D-glucose from paraffin-embedded brains. J. Neurosci. 1: 519-526

64. Euler, C. von; Hayward, J.N.; Marttila, I.; Wyman, R.J. (1973a). Respiratory neurones of the ventrolateral nucleus of the nucleus of the solitary tract of the cat: vagal input, special connections and morphological identification. Brain Res. 61: 1-22

65. Euler, C. von; Hayward, J.N.; Marttila, I.; Wyman, R.J. (1973b). The spinal connections of the inspiratory neurones of the ventrolateral nucleus of the cat's tractus solitarius. Brain Res. 61: 23-33

66. Falk, G.J. & King, R.D. (1963). Radioautographic efficiency for tritium as a function of section thickness. Radiat. Res. 20: 466-470

67. Faraco-Cantin, F.; Courville, J.; Lund, J.P. (1980). Methods for ^{3}H-2-deoxyglucose autoradiography on film and fine-grain emulsions. Stain Technol. 55: 247-252

68. Fidone, S.J. & Sato, A. (1969). A study of chemo-receptor and baroreceptor A- and C-fibres in the cat carotid nerve. J. Physiol. 205: 527-548

69. Finch, L.; Haeusler, G.; Thoenen, H. (1972). Failure to induce experimental hypertension in rats after intraventricular injection of 6-hydroxydopamine. Br. J. Pharmacol. 44: 356-357

70. Foley, J.O. & DuBois, F.S. (1934). An experimental study of the rootlets of the vagus nerve in the cat. J. Comp. Neurol. 60: 137-156

71. Gainer, H.; Tasaki, I.; Lasek, R.J. (1977). Evidence for the glia-neuron protein transfer hypothesis from intracellular perfusion studies of squid giant axons. J. Cell Biol. 74: 524-530

72. Gebber, G.L.; Taylor, D.G.; Weaver, L.C. (1973). Electrophysiological studies on organization of central vasopressor pathways. Am. J. Physiol. 224: 470-481

73. Gjedde, A. & Rasmussen, M. (1980). Pentobarbital anesthesia reduces blood-brain glucose transfer in the rat. J. Neurochem. 35: 1382-1387

74. Gold, B.I. & Kyle, J.T. (1981). (^{3}H)-2-deoxyglucose transport by slices of cerebral cortex: apparent dependence upon mitochondrial energy. Neurochem. Res. 6: 939-948

75. Goldberg, L.; Courville, J.; Lund, J.P.; Kauer, J.S. (1980). Increased uptake of ^{3}H-deoxyglucose and ^{14}C-deoxyglucose in localized regions of the brain during stimulation of the motor cortex. Can. J. Physiol. Pharmacol. 58: 1086-1091

76. Goldman, H. & Sapirstein, L.A. (1973). Brain blood flow in the conscious and anesthetized rat. Am. J. Physiol. 224: 122-126

77. Goodchild, A.K. & Dampney, R.A.L. (1980). Afferent and efferent connections of the ventrolateral pressor area in the medulla oblongata of the rabbit. Proc. Aust. Physiol. Pharmacol. Soc. 11: 33P

78. Guertzenstein, P.G. & Silver, A. (1974). Fall in blood pressure produced from discrete regions of the ventral surface of the medulla by glycine and lesions. J. Physiol. 242: 489-503

79. Guyton, A.C. (1971). Basic Human Physiology: Normal Function and Mechanisms of Disease. W.B. Saunders Co., Toronto

80. Haeusler, G. (1976). Central adrenergic neurons in experimental hypertension. In: Regulation of Blood Pressure by the Central Nervous System. Eds.: Onesti, G.; Fernandes, M.; Kim, K.E. Grune & Stratton, N.Y.; pp. 53-75

81. Haljamaie, H. & Hamberger, A. (1971). Potassium accumulation by bulk prepared neuronal and glial cells. J. Neurochem. 18: 1903-1921

82. Hatton, G.I. & Walters, J.K. (1973). Induced multiple nucleoli, nucleolar margination, and cell size changes in supraoptic neurons during dehydration and rehydration in the rat. Brain Res. 59: 137-154

83. Hawkins, R.A.; Miller, A.L.; Cremer, J.E.; Veech, R.L. (1974). Measurement of the rate of glucose utilization by rat brain "in vivo". J. Neurochem. 23: 917-923

84. Hayashi, T. & Nakamura, K. (1981). Cerebral neuronal activity in spontaneously hypertensive rats as demonstrated by the ^{14}C-deoxyglucose method. Naunym-Schmied. Arch. Pharmacol. 316: 331-339

85. Healy, D.P.; Jew, J.Y.; Black, A.C.; Williams, T. (1981). Bradycardia following injection of 6-hydroxydopamine into the intermediate portion of nucleus tractus solitarius medialis. Brain Res. 206: 415-420

86. Henn, F.A.; Haljamae, H.; Hamberger, A. (1972). Glial cell function: active control of extracellular potassium concentration. Brain Res. 43: 437-443

87. Henry, J.L. & Calaresu, F.R. (1974). Excitatory and inhibitory inputs from medullary nuclei projecting to spinal cardioacceleratory neurons in the cat. Exp. Brain Res. 20: 485-504

88. Heyman, C. & Neil, E. (1958). Reflexogenic Areas of the Cardiovascular System. Churchill, London

89. Hilton, S.M. (1963). Inhibition of baroreceptor

reflexes on hypothalamic stimulation. J. Physiol. 165: 56P-57P

90. Hilton, S.M. (1975). Ways of viewing the central nervous control of the circulation--old and new. Brain Res. 87: 213-219

91. Hilton, S.M. & Spyer, K.M. (1971). Participation of the anterior hypothalamus in the baroreceptor reflex. J. Physiol. 218: 271-293

92. Himwich, H.E. (1951). Brain Metabolism and Cerebral Disorders. Williams & Wilkins, Baltimore

93. Hopkins, D.A. & Holstege, G. (1978). Amygdaloid projections to the mesencephalon, pons and medulla oblongata in the cat. Exp. Brain Res. 32: 529-547

94. Humphrey, D.R. (1967). Neuronal activity in the medulla oblongata of cat evoked by stimulation of the carotid sinus nerve. In: Baroreceptors and Hypertension. Ed.: Kedzi, P. Pergammon Press, Toronto; pp. 131-168

95. Ingvar, D.H. & Lassen, N.A. (Eds.) (1976). Alfred Benzon Symp. VIII Brain Work. Munksgaard, Copenhagan

96. Jacobson, M. (1978). Developmental Neurobiology. Plennum Press, N.Y.; 2nd ed.

97. Jourdan, F.; Duveau, A.; Astic, L.; Holley, A. (1980). Spatial distribution of ^{14}C-2-deoxyglucose uptake in the olfactory bulbs of rats stimulated with two different odours. Brain Res. 188: 139-154

98. Judy, W.V. & Farrell, S.K. (1979). Arterial baroreceptor reflex control of sympathetic nervous activity in the SHR. Hypertension 1: 605-614

99. Judy, W.V.; Watanabe, A.M.; Henry, D.P.; Besch, H.R.; Murphy, W.R.; Hockel, G.M. (1976). Role in regulation of blood pressure in the spontaneously hypertensive rat. Circ. Res. 38 (suppl. 2): 21-29

100. Judy, W.V.; Watanabe, A.M.; Murphy, W.R.; Aprison, B.S.; Yu, P.-L. (1979). Sympathetic nervous activity and blood pressure in normotensive backcross rats genetically related to the spontaneously hypertensive rat. Hypertension 1: 598-604

101. Kadekaro, M.; Savaki, H.; Sokoloff, L. (1980). Metabolic mapping of neural pathways involved in gastrosecretory response to insulin hypoglycemia in the rat. J. Physiol. 300: 393-407

102. Kalia, M. & Mesulam, M.-M. (1980a). Brainstem projections of sensory and motor components of the vagus complex in the cat. I. The cervical vagus and nodose ganglion. J. Comp. Neurol. 193: 435-465

103. Kalia, M. & Mesulam, M.-M. (1980b). Brainstem projections of sensory and motor components of the vagus complex in the cat. II. Laryngeal, tracheobronchial, pulmonary, cardiac and gastrointestinal branches. J. Comp. Neurol. 193: 467-508

104. Kawamura, H.; Gunn, C.G.; Frohlich, E.D. (1975). Altered cardiovascular modulation by locus coeruleus in spontaneously hypertensive rat (SHR). Circ. Res. 52 (suppl. 2): 122

105. Kawamura, H.; Gunn, C.G.; Frohlich, E.D. (1976). Modified cardiovascular responses by nuclei tractus solitarius and locus loeruleus in spontaneously hypertensive rat (SHR). Circ. Res. 54 (suppl. 2): 143

106. Kawamura, H.; Gunn, C.G.; Frohlich, E.D. (1978). Cardiovascular alteration by nucleus locus coeruleus in spontaneously hypertensive rats. Brain Res. 140: 137-147

107. Kennedy, C.; Des Rosiers, M.H.; Jehle, J.W.; Reivich, M.; Sharpe, F.; Sokoloff, L. (1975). Mapping of functional neural pathways by autoradiographic survey of local metabolic rate with ^{14}C-deoxyglucose. Science 187: 850-853

108. Kennedy, C.; Des Rosiers, M.H.; Sakurada, O.; Shinohara, M.; Reivich, M.; Jehle, J.W.; Sokoloff, L. (1976). Metabolic mapping of the primary visual system of the monkey by means of the autoradiographic ^{14}C-deoxyglucose technique. Proc. Natl. Acad. Sci. USA 73: 4230-4234

109. Kerr, F.W.L. (1962). Facial, vagal, and glossopharyngeal nerves in the cat. Afferent connections. Arch. Neurol. (Chic.) 6: 164-281

110. Kerr, F.W.L. (1969). Preserved vagal visceromotor function following destruction of the dorsal motor nucleus. J. Physiol. 202: 755-769

111. King, G.W. (1980). Brain stem blood vessels and the organization of the lateral reticular formation in the medulla oblongata. Brain Res. 191: 253-259

112. Kneisley, L.W.; Biber, M.P.; LaVail, J.H. (1978). A study of the origin of brainstem projections to

monkey spinal cord using the retrograde transport method. Exp. Neurol. 60: 116-139

113. Knox, C.A. & Oliveira, A. (1980). Brain aging in normotensive and hypertensive strains of rats. Acta Neuropath. 52: 17-25

114. Korner, P.I. (1980). Operation of the central nervous system in reflex circulatory control. Fed. Proc. 39: 2504-2512

115. Korner, P.I. (1981). The central nervous system and its operation in cardiovascular control. Clin. Exp. Hypertension 3: 343-368

116. Kunze, D.L. (1972). Reflex discharge patterns of cardiac vagal efferent fibres. J. Physiol. 222: 1-16

117. Lasek, R.J.; Gainer, H.; Barker, J.L. (1977). Cell-to-cell transfer of glial proteins to the squid giant axon. The glia-neuron transfer hypothesis. J. Cell Biol. 74: 501-523

118. Lassen, N.A.; Trap-Jensen, J.; Alexander, S.C.; Oleson, J.; Paulson, O.B. (1971). Blood-brain barrier studies in man using a double-indicator method. Am. J. Physiol. 220: 1627-1633

119. LeFevre, P.G. & Peters, A.A. (1966). Evidence of mediated transfer of monosaccharides from blood to brain in rodents. J. Neurochem. 43: 35-46

120. Lehr, R.P.; Browning, R.A.; Hurley Myers, J. (1980). Gross morphological brain differences between Wistar-Kyoto and spontaneously hypertensive rats. Clin. Exp. Hypertension 2: 123-127

121. Leslie, R.A.; Gwyn, D.G.; Hopkins, D.A. (1982). The ultrastructure of the subnucleus gelatinosus of the nucleus tractus solitarius in the cat. J. Comp. Neurol. 206: 109-118

122. Lippe, W.R.; Steward, O.; Rubel, E.W. (1980). The effect of unilateral basilar papilla removal upon nuclei laminaris and magnocellularis of the chick examined with ^{3}H-2-deoxy-D-glucose autoradiography. Brain Res. 196: 43-58

123. Loewy, A.D. & Burton, H. (1978). Nuclei of the solitary tract: efferent projections to the lower brain stem and spinal cord of the cat. J. Comp. Neurol. 181: 421-450

124. Loizou, L.A. (1969). Projections of the nucleus

locus coeruleus in the albino rat. Brain Res. 15: 563-566

125. Lund-Andersen, H. (1979). Transport of glucose from blood to brain. Physiol. Rev. 59: 305-352

126. Lund-Andersen, H. & Kjeldsen, C.S. (1977). Uptake of glucose analogues by rat brain cortex slices: membrane transport versus metabolism of 2-deoxy-D-glucose. J. Neurochem. 29: 205-211

127. Mata, M.; Fink, D.J.; Gainer, H.; Smith, C.B.; Davidson, L.; Savaki, H.; Schwartz, W.J.; Sokoloff, F. (1980). Activity-dependent energy metabolism in rat posterior pituitary reflects sodium pump activity. J. Neurochem. 34: 213-215

128. Matsunami, K.; Kageyama, T.; Kubota, K. (1981). Radioactive 2-deoxy-D-glucose incorporation into the prefrontal and premotor cortex of the monkey performing a forelimb movement. Neurosci. Lett. 26: 37-41

129. McAllen, R.M. (1976). Inhibition of the baroreceptor input to the medulla by stimulation of the hypothalamic defence area. J. Physiol. 257: 45P

130. McIlwain, H.H. (1966). Biochemistry and the Central Nervous System. Churchill, London

131. Meibach, R.C.; Glick, S.D.; Ross, D.A.; Cox, R.D.; Maayani, S. (1980). Intraperitoneal administration and other modifications of the 2-deoxy-D-glucose technique. Brain Res. 195: 167-176

132. Miller, A.L. et al. (1982). Cerebral metabolic responses to electroconvulsive shock and their modification by hypercapnia. J. Neurochem. 38: 916-924

133. Miura, M. & Reis, D.J. (1968). Electrophysiological evidence that carotid sinus nerve fibres terminate in the bulbar reticular formation. Brain Res. 9: 394--397

134. Miura, M. & Reis, D.J. (1969). Termination and secondary projections of carotid sinus nerve in the cat brain stem. J. Physiol. 217: 142-153

135. Mogenson, G.J. & Calaresu, F.R. (1973). Cardiovascular responses to electrical stimulation of the amygdala in the rat. Exp. Neurol. 39: 166-180

136. Mohishita, H.; Kawamoto, M.; Masuda, Y.; Higuchi, R.; Nagamachi, N.; Mitani, H.; Ozasa, T.; Adachi, H. (1974). Quantitative histological changes in the

hypothalamic nuclei in the prepuberal, puberal and postpuberal female rat. Brain Res. 76: 41-47

137. Monmaur, P.; Orsini, J.-C.; Delacour, J. (1982). Radioautographic analysis of (^{14}C)2-deoxyglucose uptake in hippocampal formation of the rat during physostigmine-induced theta. Neurosci. Lett. 28: 229-234

138. Morest, D.K. (1967). Experimental study of the projections of the nucleus of the tractus solitarius and the area postrema in the cat. J. Comp. Neurol. 130: 277-293

139. Morris, J.R. & Dyball, R.E.J. (1974). A quantitative study of the ultastructural changes in the hypothalamo-neurohypophyseal system during and after experimentally induced hypersecretion. Cell Tiss. Res. 36: 415-416

140. Nathan, M.A. & Reis, D.J. (1975). Fulminating arterial hypertension with pulmonary edema from release of adrenomedullary catecholamines after lesions of the anterior hypothalamus in the rat. Circ. Res. 37: 226-235

141. Nelson, D.O. & Boulant, J.A. (1981). Altered CNS neuroanatomical organization of spontaneously hypertensive (SHR) rats. Brain Res. 226: 119-130

142. Nemoto, E.M.; Stezoski, S.W.; MacMurdo, D. (1978). Glucose transport across the rat blood-brain barrier during anesthesia. Anesthesiology 49: 170-176

143. Nilsson, L. & Siesjo, B.K. (1975). The effect of phenobarbitone anaesthesia on blood flow and oxygen consumption in the rat brain. Acta Anaesth. Scand. (suppl. 57): 18:24

144. Norberg, K. & Siesjo, B.K. (1974). Quantitative measurement of blood flow and oxygen consumption in the rat brain. Acta Physiol. Scand. 91: 154-164

145. Nornes, H.O. & Morita, M. (1979). Time of origin of the neurons in the caudal brainstem of rat. Dev. Neurosci. 2: 101-114

146. Oberg, B.; Kendrick, E.; Thoren, P.; Wennergren, G. (1981). Reflex cardiovascular responses to graded stimulation of low- and high-threshold afferents in the carotid sinus and aortic nerves in the cat. Acta Physiol. Scand. 113: 129-137

147. Odek-Ogunde, M. (1982). Myocardial capillary density in hypertensive rats. Lab. Invest. 46: 54-60

148. Okamoto, K. (1969). Spontaneous hypertension in rats. Int. Rev. Exp. Pathol. 7: 227

149. Okamoto, K. & Akai, K. (1963). Development of a strain of spontaneously hypertensive rats. Jap. Circ. J. 27: 282-293

150. Okamoto, K.; Yamori, Y.; Ooshima, A.; Park, C.; Harbara, H.; Matsumoto, M.; Tanaka, T.; Okuda, T.; Hazama, F.; Kyogoku, M. (1971). Establishment of the inbred strain of the spontaneously hypertensive rat and genetic factors involved in hypertension. In: Spontaneous Hypertension. Its Pathogenesis and Complications. Ed.: Okamoto, K. Springer-Verlag, Berlin, Heidelberg, N.Y.; pp. 1-8

151. Palkovits, M. & Zaborsky, L. (1977). Neuroanatomy of central cardiovascular control. Nucleus tractus solitarii: afferent and efferent neuronal connections in relation to the baroreceptor reflex arc. Prog. Brain Res. 47: 9-34

152. Pardridge, W.M. & Oldendorf, W.H. (1975). Kinetics of blood-brain barrier transport of hexoses. Biochim. Biophys. Acta 382: 377-392

153. Passmore, R. & Robson, J.S. (Eds.) (1976). A Companion to Medical Studies, Vol. 1. J.B. Lippincott, Co.; Toronto

154. Peiss, C.N. (1965). Concepts of cardiovascular regulation: past, present, and future. In: Nervous Control of the Heart. Ed.: W.C. Randall; Williams & Wilkins Co., Baltimore; pp. 154-197

155. Pelletier, C.L.; Clement, D.L.; Shepherd, J.T. (1972). Comparison of afferent activity of canine aortic and sinus nerves. Circ. Res. 31: 557-568

156. Pfaff, D.W. (1966). Morphological changes in the brains of adult male rats after neonatal castration. J. Endocrinology 36: 415-416

157. Pierce, E.C.; Lambertsen, C.J.; Deutsch, S.; Chase, P.E.; Linde, H.W.; Dripps, R.D.; Price, H.L. (1962). Cerebral circulation and metabolism during thiopental anesthesia and hyperventilation in man. J. Clin. Invest. 41: 1664-1671

158. Pilgrim, Ch. & Wagner, H.-J. (1981). Improving the resolution of the 2-deoxy-D-glucose method. J. Histochem. Cytochem. 29: 190-194

159. Prasannan, K.G. & Subrahmanyam, K. (1968). Effect of insulin on the synthesis of glycogen in cerebral cortical slices of alloxan diabetic rats. Endocrinology 82: 1-6

160. Price, J.L. & Amaral, D.G. (1981). An autoradiographic study of the projections of the central nucleus of the monkey amygdala. J. Neurosci. 1: 1242-1259

161. Privat, A. & Fulcrand, J. (1977). Neuroglia--from the subventricular precursor to the mature cell. In: Cell, Tissue, and Organ Cultures in Neurobiology. Eds.: Fedoroff, S. & Hertz, L. Academic Press, N.Y.; pp. 11-38

162. Przuntek, H. & Philippu, A. (1973). Reduced pressor responses to stimulation of the locus coeruleus after lesion of the posterior hypothalamus. Naunym-Schmied. Arch. Pharmacol. 276: 119-122

163. Rafalowska, U.; Erecinska, M.; Wilson, D.F. (1980). Energy metabolism in rat brain synaptosomes from Nembutal-anesthetized and nonanesthetized animals. J. Neurochem. 34: 380-1386

164. Raine, C.S. (1977). Morphological aspects of myelin and myelin formation. In: Myelin. Ed.: Morell, P. Plenum Press, N.Y.; London

165. Reis, D.J.; Doba, N.; Nathan, M.A. (1976). Neurogenic arterial hypertension produced by brain stem lesions. In: Regulation of Blood Pressure by the Central Nervous System. Eds.: Onesti, G.; Fernandes, M.; Kim, K.E. Grune & Stratton, N.Y.; pp. 35-52

166. Rhoton, A.L.; O'Leary, J.L.; Ferguson, J.P. (1966). The trigeminal, facial, vagal, and glossopharyngeal nerves in the monkey. Arch. Neurol. (Chic.) 14: 530-540

167. Ricardo, J.A. & Koh, E.T. (1978). Anatomical evidence of direct projections from the nucleus of the solitary tract to the hypothalamus, amygdala, and other forebrain structures in the rat. Brain Res. 153: 1-26

168. Rogers, A.W. (1975). Techniques of Autoradiography. Elsevier, Amsterdam.

169. Ross, C.A.; Ruggiero, D.A.; Reis, D.J. (1981). Afferent projections to the cardiovascular portion of the nucleus tractus solitarius in the rat. Brain Res. 223: 402-408

170. Ross, C.A.; Glick, S.D.; Meibach, R.C. (1982). Sexually dimorphic cerebral asymmetries in 2-deoxy-D-glucose uptake during postnatal development of the rat: correlation with age and relative brain activity. Dev. Brain Res. 3: 341-347

171. Sagar, S.M. & Snodgrass, S.R. (1980). Effects of substantia nigra lesions on forebrain 2-deoxy-glucose retention in the rat. Brain Res. 185: 335-348

172. Sakai, K.; Touret, M.; Salvert, D.; Leger, L.; Jouvet, M. (1977). Afferent projections to the cat locus coeruleus as visualized by the horseradish peroxidase technique. Brain Res. 119: 21-41

173. Sakumoto, T.; Tohyama, M.; Satoh, K.; Kimoto, Y.; Kinugasa, T.; Tanizawa, O.; Kurachi, K.; Shimizu, N. (1978). Afferent fiber connections from lower brain stem to hypothalamus studied by the horseradish peroxidase method with special reference to noradrenaline innervation. Exp. Brain Res. 31: 81-94

174. Saper, C.B.; Loewy, A.D.; Swanson, L.W.; Cowan, W.M. (1976). Direct hypothalamo-autonomic connections. Brain Res. 117: 305-312

175. Sapru, H.N.; Gonzalez, E.; Krieger, A.J. (1981). Aortic nerve stimulation in the rat: cardiovascular and respiratory responses. Brain Res. Bull. 6: 393-398

176. Satoh, K.; Tohyama, M.; Yamamoto, K.; Sakumoto, T.; Shimizu, N. (1977). Noradrenaline innervation of the spinal cord studied by the horseradish peroxidase method combined with monoamine staining. Exp. Brain Res. 30: 175-186

177. Saunders, R.L. & Bell, M.A. (1971). X-ray microscopy and histochemistry of the human cerebral blood vessels. J. Neurosurg. 35: 128-140

178. Savaki, H.E.; Macpherson, H.; McCulloch, J. (1982). Alterations in local cerebral glucose utilization during hemorrhagic hypotension in the rat. Circ. Res. 50: 633-644

179. Savaki, H.E.; McCulloch, J.; Kadekaro, M.; Sokoloff, L. (1982). Influence of α-receptor blocking agents

upon metabolic activity in nuclei involved in central control of blood pressure. Brain Res. 233: 347-358

180. Savaki, H.E.; Kadekaro, M.; McCulloch, J.; Sokoloff, L. (1982). The central noradrenergic system in the rat: metabolic mapping with α-adrenergic blocking agents. Brain Res. 234: 65-79

181. Schoppman, A. & Struyker, M.P. (1981). Physiological evidence that the 2-deoxyglucose method reveals orientation columns in cat visual cortex. Nature 293: 574-576

182. Schwaber, J.S.; Kapp, B.S.; Higgins, G. (1980). The origin and extent of direct amygdala projections to the region of the dorsal motor nucleus of the vagus and the nucleus of the solitary tract. Neurosci. Lett. 20: 15-20

183. Schwartz, W.J. (1978). A role for the dopaminergic nigrostriatal bundle in the pathogenesis of altered brain glucose consumption after lateral hypothalamic lesions. Evidence using the ^{14}C-labelled deoxyglucose technique. Brain Res. 158: 129-147

184. Schwartz, W.J.; Sharp, F.R.; Gunn, R.H.; Evarts, E.V. (1976). Lesions of ascending dopaminergic pathways decrease forebrain glucose uptake. Nature 261: 155-157

185. Schwartz, W.J.; Smith, C.B.; Davidsen, L.; Savaki, H.; Sokoloff, L.; Mata, M.; Fink, D.J.; Gainer, H. (1979). Metabolic mapping of functional activity in the hypothalamo-neurohypophysial system of the rat. Science 205: 723-725

186. Sejnowski, T.J.; Reingold, S.C.; Kelley, D.B.; Gelperin, A. (1980). Localization of ^{3}H-2-deoxy-glucose in single molluscan neurones. Nature 287: 449-451

187. Share, L. & Levy, M.N. (1962). Cardiovascular receptors and blood titer of antidiuretic hormone. Am. J. Physiol. 203: 425-428

188. Share, L. & Levy, M.N. (1966). Effect of carotid chemoreceptor stimulation on plasma antidiuretic hormone titer. Am. J. Physiol. 210: 157-161

189. Sharp, F.R. (1976). Rotation induced increases of glucose uptake in rat vestibular nuclei and vestibulocerebellum. Brain Res. 110: 141-151

190. Sharp, F.R.; Kauer, J.S.; Shepherd, G.M. (1975). Local sites of activity-related metabolism in rat olfactory bulb during olfactory stimulation. Brain Res. 98: 596-600

191. Sharp, F.R. & Kilduff, T.S. (1981). The 2-deoxy-glucose neuroanatomical mapping technique. TINS 4: 144-148

192. Sidman, R.L.; Miale, I.L.; Feder, N. (1959). Cell proliferation and migration in the primitive ependymal zone: an autoradiographic study of histo-genesis in the nervous system. Exp. Neurol. 1: 322-333

193. Siesjo, B.K. (1978). Brain Energy Metabolism. Wiley, N.Y.

194. Singer, P. & Mehler, L. (1980). 2-deoxy(^{14}C)glucose uptake in rat hypoglossal nucleus after nerve transection. Exp. Neurol. 69: 617-626

195. Skeen, L.C. (1977). Odor-induced patterns of deoxy-glucose consumption in the olfactory bulb of the tree shrew. Brain Res. 124: 147-153

196. Smith, O.A., Jr. (1965). Anatomy of central neural pathways mediating cardiovascular functions. In: Nervous Control of the Heart. Ed.: Randall, W.C.; Willians & Wilkins, Baltimore; pp. 34-52

197. Smith, T.L. & Hutchins, P.M. (1980). Anesthetic effects on hemodynamics of spontaneously hyper-tensive rats and Wistar-Kyoto rats. Am. J. Physiol. 238: H539-H544

198. Sokoloff, L. (1977). Relation between physiological function and energy metabolism in the central nervous system. J. Neurochem. 29: 13-26

199. Sokoloff, L. (1979). The ^{14}C-deoxyglucose method: four years later. Acta Neurol. Scand. 60 (suppl. 72): 639-649

200. Sokoloff, L. (1979). Mapping of local cerebral function activity by measurement of local cerebral glucose utilization with ^{14}C-deoxyglucose. Brain 102: 653-668

201. Sokoloff, L. (1981). The relationship between function and energy metabolism: its use in the localization of functional activity in the nervous system. Neurosci. 19: 159-210

202. Sokoloff, L.; Reivich, M.; Kennedy, C.; Des Rosier,

M.H.; Patlek, C.S.; Pettigrew, K.D.; Sakurada, O.; Shinohara, M. (1977). The ^{14}C-deoxyglucose method for the measurement of local cerebral glucose utilization: theory, procedure, and normal values in the conscious and anesthetized albino rat. J. Neurochem. 28: 897-916

203. Spyer, K.M. (1975). Organization of baroreceptor pathways in the brainstem. Brain Res. 87: 221-226

204. Steward, O. & Smith, L.K. (1980). Metabolic changes accompanying denervation and reinnervation of the dentate gyrus of the rat measured by ^{3}H-2-deoxy-glucose autoradiography. Exp. Neurol. 69: 513-527

205. Struyker Boudier, H.A.J.; Smeets, G.W.M.; Brouwer, G.M.; van Rossum, J.M. (1974). Hypothalamic alpha adrenergic receptors in cardiovascular regulation. Neuropharmacol. 13: 837-846

206. Tanase, H.; Suzuki, Y.; Ooshima, A.; Yamori, Y.; Okamoto, K. (1971). Further genetic analysis of blood pressure in spontaneously hypertensive rats. In: Spontaneous Hypertension. Its Pathogenesis and Complications. Ed.: Okamoto, K. Springer-Verlag, Berlin, Heidelberg, N.Y.; pp. 9-11

207. Thomas, M.R. & Calaresu, F.R. (1974). Responses of single units in the medial hypothalamus to electrical stimulation of the carotid sinus nerve in the cat. Brain Res. 44: 49-62

208. Torvik, A. (1956). Afferent connections to the sensory trigeminal nuclei, the nucleus of the solitary tract and adjacent structures. An experimental study in the cat. J. Comp. Neurol. 106: 51-141

209. Truex, R.C. & Carpenter, M.B. (Eds.) (1969). Human Neuroanatomy. Willians & Wilkins Co., Baltimore; 6th Ed.

210. Ungerstedt, U. (1971). Stereotaxic mapping of the monoamine pathways in the rat brain. Acta Physiol. Scand. 82 (suppl. 376): 1-48

211. Wagner, H.-J.; Hoffman, K.-P.; Zwerger, H. (1981). Layer-specific labelling of cat visual cortex after stimulation with visual noise: a (^{3}H)2-deoxy-D-glucose study. Brain Res. 224: 31-43

212. Wang, S.C. & Ranson, S.W. (1939). Descending pathways from the hypothalamus to the medulla and spinal cord. Observations of blood pressure and bladder responses. J. Comp. Neurol. 71: 457-472

213. Wang, S.C. & Ranson, S.W. (1841). The role of the hypothalamus and preoptic region in the regulation of heart rate. Am. J. Physiol. 132: 5-8

214. Ward, D.G. & Gunn, C.G. (1976a). Locus coeruleus complex: elicitation of a pressor response and a brain stem region necessary for its occurrence. Brain Res. 107: 401-406

215. Ward, D.G. & Gunn, C.G. (1976b). Locus coeruleus complex: differential modulation of depressor mechanisms. Brain Res. 107: 407-411

216. Ward, D.G. et al. (1975). Activation of solitary nucleus neurons from the locus coeruleus and vicinity. Neurosci. Abstr. 1: 424

217. Warren Cottle, M.K. & Calaresu, F.R. (1975). Projections from the nucleus and tractus solitarius in the cat. J. Comp. Neurol. 161: 143-158

218. Wechsler, R.L.; Dripps, R.D.; Kety, S.S. (1951). Blood flow and oxygen consumption in the human brain during anesthesia produced by thiopental. Anesthesiology 12: 308

219. Whittam, R. (1962). The dependence of the respiration of brain cortex on active cation transport. Biochem. J. 82: 205-212

220. Wieraszki, A. (1982). Changes in the hippocampal slices energy metabolism following stimulation and long-term potentiation of Schaffer collaterals--pyramidal cell synapses tested with the 2-deoxy-glucose technique. Brain Res. 237: 449-457

221. Witkovsky, P. & Yang, Ch.-Y. (1982). Uptake and localization of ^{3}H-2-deoxy-D-glucose by retinal photoreceptors. J. Comp. Neurol. 204: 105-116

222. Yamori, Y. (1976). Neurogenic mechanisms of spontaneous hypertension. In: Regulation of Blood Pressure by the Central Nervous System. Eds.: Onesti, G.; Fernandes, M.; Kim, K.E. Grune & Stratton, N.Y.

223. Yarowsky, P.J.; Jehle, J.; Ingvar, D.H.; Sokoloff, L. (1979). Relationship between functional activity and glucose utilization in the rat superior cervical ganglion "in vivo". In: Neurosci. Abstracts, Vol. V; p. 421

224. Yudilevich, D.L. & deRose, N. (1971). Blood-brain transfer of glucose and other molecules measured by

rapid indicator dilution. Am. J. Physiol. 220: 841-846

225. Zeman, W. & Innes, J.R.M. (Eds.) (1963). Craigie's Neuroanatomy of the Rat. Academic Press, N.Y.; London

APPENDICES

1. 2-deoxyglucose and ^{3}H-2-deoxyglucose dosages

1.1. 2DG

Maximum dosage of ^{14}C-2DG (130) = 150 μCi/kg

= 0.150 mCi/kg

Molecular weight of 2DG = 164.2 gm

^{14}C-2DG is purchased at a specific activity of 50 mCi/mmol.

Therefore, $\frac{0.150 \text{ mCi/kg}}{50 \text{ mCi/mmol}}$ = 0.003 mmol/kg

0.003 mmol/kg x 0.1642 gm/mmol = 0.0004926 gm/kg

= 0.5 mg/kg

Therefore, the concentration of the 2DG must be less than 0.5 mg/kg body weight in order to be present in trace amounts.

1.2. ^{3}H-2DG

^{14}C-2DG is purchased at a specific activity of 50 mCi/mmol and ^{3}H-2DG is purchased at a specific activity of 50 Ci/mmol. Since ^{3}H-2DG has approximately 1000x more activity than ^{14}C-2DG, greater activity can be administered to the experimental animals without exceeding the maximum allowable dosage of the 2DG itself. A dosage of 200 μCi/100 gm body weight of ^{3}H-2DG is well under the maximum dosage.

2. Processing for Thin Sections

2.1. Half-strength Karnovsky fixative

i. Add 20 ml of distilled water to 2 gm paraformaldehyde and heat to 60^{o}C.

ii. Use a few drops of concentrated NaOH to clear the solution. Cool.

iii. Add 10 ml of 25% glutaraldehyde and make up to 60 ml with distilled water.

iv. Bring to 100 ml with 0.2M sodium cacodylate buffer. The pH should be 7.2.

Note: Sodium cacodylate buffer may be replaced by phosphate buffer when thin sections are required.

2.2. Embedding

i. Fix in half-strength Karnovsky fixative for 1 to 2 hours.

ii. Wash in 5.4% sucrose buffer for 30 min. Tissue can be stored in the buffer under refrigeration.

iii. Postfix in osmium tetroxide : sodium cacodylate buffer (1:1) for one hour. Use 2% osmium tetroxide and a 0.2M stock solution of sodium cacodylate buffer.

iv. Wash in 0.1M sodium cacodylate buffer for 30 min.

v. Stain en bloc with uranyl acetate (saturated solution in 50% alcohol) for one hour.

vi. Dehydrate by passing the tissue through graded alcohols (50%, 70%, 90%, 100%), 30 min each.

vii. Clear in 100% acetone for 15 to 20 min.

viii. Soak in Araldite/acetone (1:1) for 24 hours.

ix. Infiltrate with Araldite for about 6 hours.

x. Embed in capsule. Place the capsule into a 60°C oven overnight or longer.

2.3. 0.2M Sodium Cacodylate Buffer

i. Dissolve 4.28 gm of sodium cacodylate in 70 ml distilled water.

ii. Buffer with 0.5% HCl so that the pH is between 7.4 and 7.6; dilute to 100 ml with distilled water. The pH should decrease slightly.

iii. Add NaOH (1.0 N) to obtain the desired pH.

2.4. 5.4% Sucrose in 0.1M Buffer

50 ml of 0.2M sodium cacodylate buffer

50 ml distilled water

5.4 gm sucrose

Dissolve the sucrose in the 0.1M buffer.

2.5. Araldite Preparation

Epoxy resin (Araldite CY212)	10.0 parts by weight
DDSA (2,4,6-tri(dimethylaminomethyl) phenol)	10.0 parts by weight
Dibutyl Phthalate	1.0 part by weight
DMP-30 (Dodecenylsuccinic anhydride)	0.4 part by weight

Polymerization: 60° - 24 hours

37^{0} - 2 to 3 days

3. Quantification of Exchange Vessels

Figure 20 (A and B) is an example of the semi-thin sections used to quantitate the exchange vessels in the NC. The rectangle within which vessels were counted represents an area of 5.4×10^{4} μm^{2}.

Tables 3 and 4 contain the counts of exchange vessels for all sections studied from WKYs and SHRs of 4 and 12 weeks of age.

Figure 20 A,B: Photographs of semi-thin sections to demonstrate the quantification of exchange vessels in the NC. Toluidine blue.

A. Low-power micrograph (x100) to demonstrate the general appearance of the semi-thin section.

B. Micrograph of the NC medial to the tractus solitarius with rectangular border within which exchange vessels were counted. (x334).

A

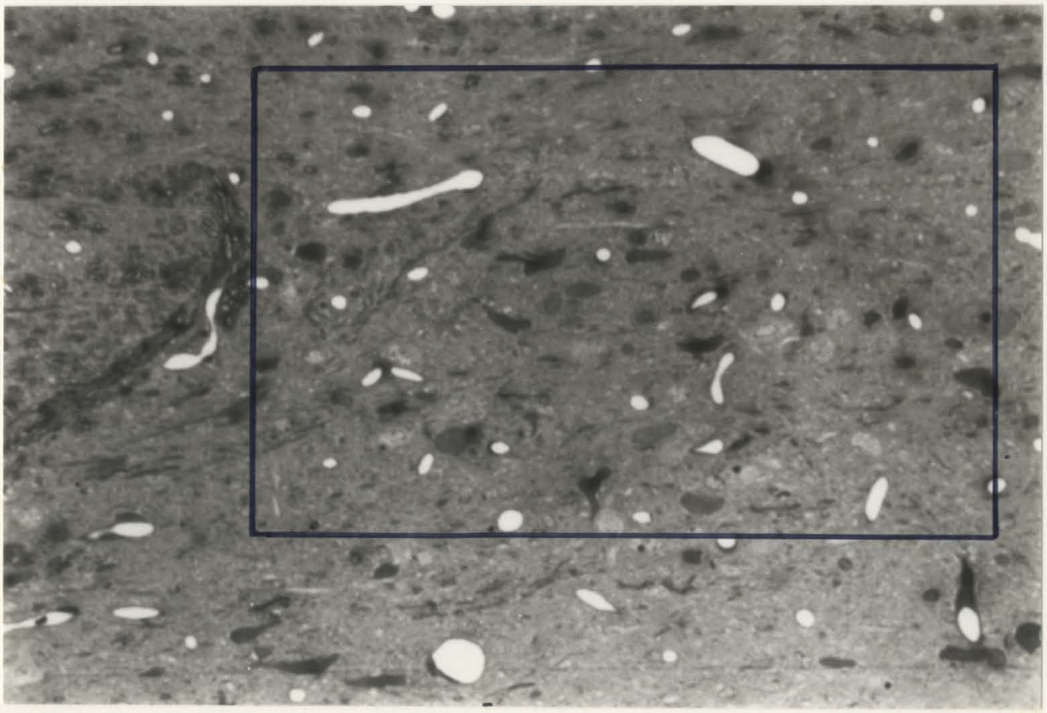

B

Table 3: Numbers of exchange vessels in the nucleus commissuralis (NC) and nucleus medialis (NM) of four-week WKYs and SHRs

Strain	Number	NC	NM	Strain	Number	NC	NM
	1	24	25		1	31	32
		27	22			28	29
	2	26	22		2	32	
WKY	3	30	31	SHR		34	35
		30			3	28	35
	4	31	26			32	30
		25	32		4	27	33
						26	23
Means ± S.D.		28	27			30	30
		±3	±4			±3	±5

Table 4: Numbers of exchange vessels in the nucleus commissuralis (NC) and nucleus medialis (NM) of twelve-week WKYs and SHRs

Strain	Number	NC	NM	Strain	Number	NC	NM
	1	36	34		1	32	38
		31	38			28	28
	2	34	36		2	34	29
WKY		38	32	SHR		28	40
	3	30	41		3	29	25
		32	37			35	36
	4	35	28		4	43	34
		29	34			25	33
Means ± S.D.		33	35			32	33
		±3	±4			±6	±5